

Development of a Packed-bed Reactor
Containing Supported Sol-gel Immobilized
Lipase for Transesterification

by

Sarah M. Meunier

A thesis
presented to the University of Waterloo
in fulfillment of the
thesis requirement for the degree of
Doctor of Philosophy
in
Chemical Engineering

Waterloo, Ontario, Canada, 2012
© Sarah M. Meunier 2012

I hereby declare that I am the sole author of this thesis. This is a true copy of the thesis, including any required final revisions, as accepted by my examiners.

I understand that my thesis may be made electronically available to the public.

ABSTRACT

The objective of this work was to develop a novel enzyme immobilization scheme for supported lipase sol-gels and to evaluate the potential of the immobilized biocatalyst for the production of biodiesel in a packed bed reactor. Two sources of lipase (EC 3.1.1.3 triacylglycerol hydrolase) were used in this study and the transesterification of methanol and triolein to produce glycerol and methyl oleate was used as a model reaction of biodiesel production. A commercially available form of immobilized lipase, Novozym[®] 435, was used as a basis for comparison to the literature.

Upon establishing a lipase sol-gel formulation technique, the experimental methodology for the transesterification reaction using Novozyme[®] 435 was developed. Subsequently, a series of inert materials were considered based on their suitability as supports for immobilized lipase sol-gels and the synthesis of methyl oleate. The value of a supported lipase sol-gel is to improve the activity and stability of the enzyme and develop an immobilized biocatalyst that is practical for use under packed bed reactor conditions. Of the six support materials considered (6-12 mesh silica gel, Celite[®] R633, Celite[®] R632, Celite[®] R647, anion exchange resin, and Quartzel[®] felt), the diatomaceous earth supports (Celite[®] R633, R632 and R647) exhibited high enzymatic activity, were thermally stable, and possessed high sol-gel adhesion.

From the three types of diatomaceous earth considered, Celite[®] R632 supported lipase sol-gels were identified as the most promising supported lipase sol-gels for methyl oleate production via transesterification. Upon further evaluation, the Celite[®] R632 lipase sol-gels were found to achieve high methyl oleate percent conversions, glycerol-water absorption was only significant at glycerol levels higher than 75%, and the immobilized lipase had high stability upon storage at 4°C for 1.5 years.

To determine the effects of methanol and glycerol inhibition as well as temperature on the reaction kinetics, a ping-pong bi-bi kinetic model was developed and validated over a range of methanol concentrations and temperatures. The optimal methanol concentration for the conditions tested was in the range of 1.3 M to 2.0 M, and increased with increasing temperature. The model developed was consistent with the experimental data and confirmed that glycerol inhibition and the presence of products had significant effects on the reaction kinetics.

The methyl oleate production capabilities of the Celite® supported lipase sol-gel were investigated using a packed bed reactor and compared with Novozym® 435 under similar operating conditions. A kinetic and mass transfer based model was developed for the reactor system using a novel efficiency correlation to account for the effect of glycerol on the enzymatic activity. Increasing the flow rate (1.4 mL/min to 20 mL/min) increased the reaction rate, presumably due to the reduction of the glycerol inhibition effect on the immobilized biocatalyst. The Celite® supported lipase sol-gel was found to have superior performance over Novozym® 435 both under batch stirred tank reaction conditions and in a packed bed reactor (83% conversion for Celite® sol-gel vs. 59% conversion for Novozym® 435 at 20 mL/min in the packed bed reactor).

Based on the results obtained, Celite® supported lipase sol-gels exhibited good performance for the transesterification of triolein with methanol to produce methyl oleate in both batch and packed bed reactors, and warrant further exploration for the enzymatic production of biodiesel.

ACKNOWLEDGEMENTS

There are so many people who have made this journey possible – I'd like to thank you all. In particular, I would like to extend my sincere gratitude to the following people:

To my supervisor, Raymond Legge, thank you for giving me the opportunity to do my PhD and for all the support, guidance, and advice you have provided along the way.

Thank you to my PhD examination committee members, Dr. Amarjeet Bassi, Dr. Christine Moresoli, Dr. Eric Croiset, and Dr. Kesen Ma, for your valuable input on my research and thesis.

To Trevor Williams and Amin Rajabzadeh, thank you for collaborating with me and providing valuable insight on the research completed in Chapters 7 and 8. Trevor helped collect the experimental data used in Chapters 7 and 8, and Amin contributed to the development of the kinetic and mass transfer models used in Chapters 7 and 8.

Thank you to the Faculty and Staff in the Department of Chemical Engineering at the University of Waterloo for the many ways you have helped make my PhD a success. Special thanks to Ralph Dickhout whose analytical expertise has saved me so much frustration, Ron Neill who built the apparatus for the packed bed, and Bert Habicher who helped make all the pieces fit together.

Thank you to the Natural Sciences and Engineering Research Council for the financial support provided by a NSERC Doctoral Postgraduate Scholarship; to the University of Waterloo for the financial support provided by President's Graduate Scholarships, a University of Waterloo Graduate Scholarship, and a Provost Doctoral Entrance Award for Women; and to the Ontario Student Assistance Program for the financial support provide by an Ontario Graduate Scholarship.

To all those who have reviewed my thesis partially or completely, including the reviewers of my published work, thank you for your insight, it has improved my thesis tremendously.

Thank you to my friends and colleagues who were always around to give me the expertise and support I needed. Special thanks to Rachel Campbell for being by my side through all the phases of this journey.

Finally, thank you to my family, the Meuniers and the Mercers, for having unlimited faith in me.

Dedicated to Marc, Félix, Théodore and Nicolas

You are my world.

Contents

| | |
|---|-------|
| AUTHOR'S DECLARATION | ii |
| ABSTRACT | iii |
| ACKNOWLEDGEMENTS | v |
| DEDICATION | vi |
| List of Figures | xi |
| List of Tables | xv |
| List of Abbreviations | xvii |
| Nomenclature | xviii |
| Chapter 1 Introduction | 1 |
| 1.1 Objectives | 1 |
| 1.2 Thesis Organization | 2 |
| Chapter 2 Literature Review | 3 |
| 2.1 Biodiesel | 3 |
| 2.2 Lipase | 5 |
| 2.3 Sol-gel entrapment | 6 |
| 2.4 Immobilization of sol-gels on support materials | 9 |
| 2.5 Biodiesel production | 10 |
| 2.5.1 Enzyme screening | 12 |
| 2.5.2 Optimization | 13 |
| 2.5.3 Glycerol removal | 16 |
| 2.5.4 Alcohol deactivation | 16 |
| 2.5.5 Kinetics and reaction mechanism | 17 |
| 2.6 Reactor design | 21 |
| 2.6.1 Packed bed reactors | 21 |
| 2.6.2 Modelling | 23 |
| Chapter 3 Experimental Background | 26 |
| 3.1 Lipase entrapment in a sol-gel matrix | 26 |
| 3.2 Thermal properties of sol-gel entrapped lipase | 28 |

| | | |
|-----------|---|----|
| 3.3 | Methyl oleate synthesis with Novozym® 435 | 30 |
| 3.4 | Sol-gel methyl oleate formation | 34 |
| Chapter 4 | Study of Support Materials for Sol-gel Immobilized Lipase | 37 |
| 4.1 | Introduction | 38 |
| 4.2 | Experimental | 39 |
| 4.2.1 | Materials | 39 |
| 4.2.2 | Methods | 40 |
| 4.3 | Results and discussion | 42 |
| 4.3.1 | Surface coating | 42 |
| 4.3.2 | Coating properties | 44 |
| 4.3.3 | Enzymatic properties | 46 |
| 4.4 | Conclusions | 48 |
| 4.5 | Acknowledgements | 49 |
| Chapter 5 | Evaluation of Diatomaceous Earth as a Support for Sol-gel Immobilized Lipase for Transesterification | 50 |
| 5.1 | Introduction | 51 |
| 5.2 | Experimental | 52 |
| 5.2.1 | Materials | 52 |
| 5.2.2 | Methods | 53 |
| 5.3 | Results and discussion | 55 |
| 5.3.1 | Surface morphology | 55 |
| 5.3.2 | Physical properties | 57 |
| 5.3.3 | Enzymatic properties | 57 |
| 5.4 | Conclusions | 59 |
| 5.5 | Acknowledgements | 61 |
| Chapter 6 | Evaluation of Diatomaceous Earth Supported Lipase Sol-gels as a Medium for Enzymatic Transesterification to Produce Biodiesel | 62 |
| 6.1 | Introduction | 63 |
| 6.2 | Experimental | 64 |
| 6.2.1 | Materials | 64 |
| 6.2.2 | Methods | 65 |
| 6.3 | Results and discussion | 67 |

| | | |
|--|---|-----|
| 6.3.1 | Physical properties | 67 |
| 6.3.2 | Enzymatic properties | 69 |
| 6.3.3 | Adsorptive properties | 72 |
| 6.4 | Conclusions | 75 |
| 6.5 | Acknowledgements | 76 |
| Chapter 7 Kinetic Modelling of the Production of Methyl Oleate by Celite® Supported Lipase Sol-gels 77 | | |
| 7.1 | Introduction | 78 |
| 7.2 | Experimental | 80 |
| 7.2.1 | Materials | 80 |
| 7.2.2 | Methods | 80 |
| 7.3 | Results and discussion | 82 |
| 7.3.1 | Comparison of lipase immobilization schemes | 82 |
| 7.3.2 | Kinetic model – initial reaction rate | 83 |
| 7.3.3 | Kinetic model – time-dependent reaction rate | 85 |
| 7.3.4 | Methyl oleate concentration profile | 85 |
| 7.3.5 | Kinetic model predictions for transesterification | 89 |
| 7.4 | Conclusions | 90 |
| 7.5 | Acknowledgements | 90 |
| 7.6 | Nomenclature | 90 |
| Chapter 8 Kinetic and Mass Transfer Modelling of Methyl Oleate Production in an Immobilized Lipase Packed Bed Reactor 93 | | |
| 8.1 | Introduction | 94 |
| 8.2 | Experimental | 96 |
| 8.2.1 | Materials | 96 |
| 8.2.2 | Methods | 96 |
| 8.3 | Modelling | 99 |
| 8.3.1 | Kinetic model | 99 |
| 8.3.2 | Packed bed reactor model | 99 |
| 8.3.3 | Physical properties | 100 |
| 8.3.4 | Packed bed efficiency correlation | 101 |
| 8.4 | Results and discussion | 102 |
| 8.4.1 | Batch kinetics | 102 |

| | | |
|------------|--|-----|
| 8.4.2 | Experimental and modelling results _____ | 102 |
| 8.4.3 | Comparison of Celite® supported sol-gel to Novozym® 435 _____ | 105 |
| 8.4.4 | Model predictions _____ | 106 |
| 8.4.5 | Catalyst reusability _____ | 106 |
| 8.5 | Conclusions _____ | 107 |
| 8.6 | Acknowledgements _____ | 108 |
| 8.7 | Nomenclature _____ | 108 |
| Chapter 9 | Conclusions and Recommendations _____ | 111 |
| 9.1 | Most significant contributions _____ | 111 |
| 9.1.1 | Objective A – Experimental Background _____ | 111 |
| 9.1.2 | Objective B – Study of Support Materials for Sol-gel Immobilized Lipase _____ | 111 |
| 9.1.3 | Objective C – Evaluation of Diatomaceous Earth as a Support for Sol-gel Immobilized Lipase for Transesterification _____ | 112 |
| 9.1.4 | Objective D – Evaluation of Diatomaceous Earth Supported Sol-gels as a Medium for Enzymatic Transesterification to Produce Biodiesel _____ | 112 |
| 9.1.5 | Objective E – Kinetic Modelling of the Production of Methyl Oleate by Celite® Supported Lipase Sol-gels _____ | 113 |
| 9.1.6 | Objective F – Kinetic and Mass Transfer Modelling of Methyl Oleate Production in an Immobilized Lipase Packed Bed Reactor _____ | 113 |
| 9.2 | Recommendations for Future Work _____ | 114 |
| References | _____ | 115 |
| Appendix A | List of Publications _____ | 129 |
| Appendix B | Lipase Source Change _____ | 130 |
| Appendix C | Sample Calculations _____ | 133 |

List of Figures

| | |
|--|----|
| Figure 2.1: Transesterification of a triglyceride with an alcohol to produce fatty acid alkyl esters and glycerol | 3 |
| Figure 2.2: Lipase structure with the α -helical loop circled: (a) closed-lid and (b) open-lid. Adapted from Krebs and Gerstein (2000). | 5 |
| Figure 2.3: Sol-gel formation scheme adapted from Jin and Brennan (2002). | 8 |
| Figure 2.4: Intermediate reactions for the transesterification of triglycerides with alcohol to produce fatty acid alkyl esters and glycerol: (a) triglycerides to diglycerides, (b) diglycerides to monoglycerides, and (c) monoglycerides to glycerol. | 19 |
| Figure 2.5: Schematic representation of the ping-pong bi-bi kinetic mechanism for the transesterification of triglycerides to produce biodiesel. Adapted from Cheirsilp <i>et al.</i> (2008). | 19 |
| Figure 3.1: Linoleic acid activity of the lipase sol-gel based on 91, 104 and 146 days of storage at 4°C. The error bars represent the standard error with n=2-6. | 28 |
| Figure 3.2: Relative activity of the sol-gel entrapped lipase after incubation at 70°C. The error bars represent the standard error with n=2-6. | 29 |
| Figure 3.3: Linoleic acid concentration profile as a function of time for sol-gel immobilized lipase at 70°C and 30°C for 12 h. The slopes of the lines represent the initial reaction rates. | 29 |
| Figure 3.4: Normalized final methyl oleate concentration at various methanol molar ratios for 6 h at 40°C (normalized to the Novozym® 435 batch maximum). The error bars represent the standard deviation with n=2-5. | 31 |
| Figure 3.5: Percent conversion of methanol to methyl oleate as a function of reaction temperature after 6 h for both solvent-free and solvent-based (50% hexane) reaction media with a methanol to triolein molar ratio of 1:1. | 31 |
| Figure 3.6: Percent conversion of methanol to methyl oleate at a methanol to triolein molar ratio of 1:1 in solvent-free and solvent-based (50% hexane) reaction media at 40°C. Error bars represent the standard error with n=3-4. | 33 |
| Figure 3.7: Percent conversion of methanol to methyl oleate at a methanol to triolein molar ratio of 1.5:1 in solvent-free and solvent-based (50% hexane) reaction media at 40°C. | 33 |
| Figure 3.8: Percent conversion of methanol to methanol oleate at a methanol to triolein molar ratio of 1:1 for solvent-free and solvent-based (50% hexane) systems with and without the addition of 3% water. | 35 |
| Figure 3.9: Methanol to methyl oleate conversion using immobilized lipase from Novozym® 435, 80% PTMS sol-gel and 20% PTMS sol-gel with a molar ratio of triolein to methanol of 1.5:1 at 40°C. Error bars represent the standard error with n=2. | 35 |

Figure 4.1: SEM images at 3000x (a) unsupported lipase sol-gel; silica gel (b) without and (c) with sol-gel immobilized on the surface; Celite® R633 (d) without and (e) with sol-gel immobilized on the surface; anion exchange resin (f) without and (g) with sol-gel immobilized on the surface; and Quartzel® felt (h) without and (i) with sol-gel immobilized on the surface. _____ 43

Figure 4.2: Adhesion of sol-gel (mg sol-gel/g material) and protein loading (μg lipase/g material) for each support material. Supports: SG (silica gel), R633 (Celite® R633), R632 (Celite® R632), R647 (Celite® R647), AE (anion exchange resin), and QF (Quartzel® felt). Due to the low density of QF, data are presented on a per cm^2 basis rather than a per gram basis. _____ 45

Figure 4.3: Final weight percent of the supports with and without sol-gel based on TGA. Supports: SG (silica gel), R633 (Celite® R633), R632 (Celite® R632), R647 (Celite® R647), AE (anion exchange resin), and QF (Quartzel® felt). Error bars represent a 90% confidence interval. _____ 45

Figure 4.4: Kinetic profile for a typical lipid transesterification reaction with Celite® R632 as the support. _____ 47

Figure 5.1: SEM images at 3000x magnification of (a) uncoated Celite R633®, (b) uncoated Celite R632®, (c) uncoated Celite R647®, (d) Celite R633® coated with lipase sol-gel, (e) Celite R632® coated with lipase sol-gel, and (f) Celite R647® coated with lipase sol-gel. Arrows identify some clusters of sol-gel on the surfaces of the Celite®. _____ 55

Figure 5.2: Percent sol-gel coverage on the surface of Celite® as determined by SEM image analysis. The error bars represent the 95% confidence intervals of the sample mean based on $n = 45$. _____ 56

Figure 5.3: Adhesion of sol-gel on the support for each type of Celite® considered. The error bars represent the 95% confidence intervals of the sample mean based on $n = 3$. _____ 58

Figure 5.4: Loading of protein per gram for each support: A) the amount of protein per gram of material, and B) the amount of protein per gram of sol-gel. The error bars represent the 95% confidence interval of the sample mean based on $n = 3$. _____ 58

Figure 5.5: Percent methanol conversion per gram of material after 6 h for each sol-gel formulation. The error bars represent the 95% confidence interval of the sample mean based on $n = 9$. _____ 60

Figure 5.6: Initial lipase activity for each sol-gel formulation measured by the initial amount of methyl oleate produced per minute per gram of protein. The error bars represent the 95% confidence interval of the sample mean based on $n = 9$. _____ 60

Figure 6.1: Protein content and degree of protein immobilization for four sol-gel formulations. Error bars represent a 95% confidence interval. _____ 68

Figure 6.2: Percent conversion of methanol to methyl oleate based on a 6 h batch reaction for each sol-gel formulation without and with a drying step prior to the enzymatic assay. Error bars represent a 95% confidence interval. _____ 70

Figure 6.3: The enzymatic activity on a per gram of material basis for each sol-gel formulation as determined from the conversion of methyl oleate and the protein content of the gels. Both the sol-gel formations without and with a drying step prior to the reaction were considered. Errors bars represent a 95% confidence interval. 70

Figure 6.4: Average percent conversion of methanol to methyl oleate for sol-gels after storage at 4°C for unsupported (Δ) and Celite® R632 supported sol-gels (o). The lines represent the lines of best fit for the unsupported sol-gel (broken) and the Celite® R632 supported sol-gel (solid). Error bars represent a 95% confidence interval. _____ 71

Figure 6.5: Typical TGA profile including the sample weight (solid) and the derivative weight (broken). The peak desorption point and the total mass loss are indicated on the graph. The sample shown is Celite® R632 sol-gel (C-SG-4) at 50% glycerol equilibrating solution. _____ 73

Figure 6.6: Peak desorption rates for Celite® R632 sol-gels (Δ) and plain Celite® R632 (o) based on different levels of glycerol in the equilibrating solution. Error bars represent a 95% confidence interval. _____ 73

Figure 6.7: Total percentage mass loss for Celite® R632 sol-gels (Δ) and plain Celite® R632 (o) based on different levels of glycerol in the equilibrating solution. Error bars represent a 95% confidence interval. _____ 74

Figure 6.8: Peak desorption temperatures for Celite® R632 (Δ) sol-gels and plain Celite® R632 (o) based on different levels of glycerol in the equilibrating solution. Error bars represent a 95% confidence interval. _____ 75

Figure 7.1: Initial reaction rate as a function of methanol concentration at three temperatures (40°C, 50°C, and 60°C). The lines represent the predictions from the model provided by Equation 7.2 and the symbols represent the experimental data. _____ 83

Figure 7.2: Methyl oleate concentration at 6 h with respect to the initial methanol concentration at three temperatures (40°C, 50°C, and 60°C). The lines represent the model predictions and the symbols represent the experimental data. The main plot represents the results from Equation 7.3 while the inset plot (upper left) represents the results from Equation 7.2. _____ 84

Figure 7.3: Correlation between the predicted and experimental methyl oleate concentration values using the kinetic model described by Equation 7.3. _____ 86

Figure 7.4: Comparison of model predictions (lines) and experimental data (symbols) for four methanol concentrations (0.3 M, 0.6 M, 0.9 M, and 1.8 M) and three temperatures (40°C, 50°C, and 60°C). Plot a) T = 40°C, b) T = 50°C, c) T = 60°C, d) [A]°=1.8 M. _____ 88

Figure 7.5: Surface plot of the kinetic model (Equation 7.3) predictions for the methyl oleate concentration after 6 h at different initial methanol concentrations (0-4 M) and temperatures (30-70°C). _____ 89

Figure 8.1: Schematic of the packed bed reactor apparatus. _____ 98

Figure 8.2: Packed bed results with the experimental (symbols) and model (lines) methyl oleate concentrations as a function of contact time in the reactor with Celite® supported sol-gels at 4 flow rates (1.4 mL/min, 5 mL/min, 12.5 mL/min and 20 mL/min). The confidence intervals shown are estimated from a pooled variance of 16 samples in triplicate. _____ 103

- Figure 8.3: Packed bed results with the experimental (symbols) and modelling (lines) methyl oleate concentrations as a function of contact time in the reactor for Novozym® 435 at flow rates of 5 mL/min and 20 mL/min. The confidence intervals shown are estimated from a pooled variance of 16 samples in triplicate. _____ 105
- Figure 8.4: Contour map for model predictions for methyl oleate concentration with respect to the flow rate and contact time based on kinetics and mass transfer. _____ 106
- Figure 8.5: Reusability runs in the packed bed reactor over 5 days at $T = 40^{\circ}\text{C}$, substrate ratio 1:1, and flow rate = 5 mL/min. A new substrate mixture (triolein and methanol) was supplied to the existing CSG bed at the beginning of each day. _____ 107

List of Tables

| | |
|---|-----|
| Table 2.1: Results of lipase screening studies for enzymatic biodiesel production. | 11 |
| Table 2.2: Enzymatic biodiesel production reaction optimization literature results. | 13 |
| Table 3.1: Reported and measured activities for Novozym 435®, 80% PTMS sol-gel and 20% PTMS sol-gel. | 36 |
| Table 4.1 Properties of the lipase sol-gel support materials. Pore diameter and particle size are as provided by the suppliers. Initial sol-gel capacity is defined as the amount of liquid sol-gel required to fully wet the support without excess material. | 40 |
| Table 4.2: Enzymatic properties of the supported lipase sol-gels: percent conversion of methanol to methyl oleate (MO) after 6 h of reaction, initial reaction rate, and enzymatic activity. For Quartzel® felt, the conversion and reaction rate are presented in terms of cm ² rather than g due to the low density of the felt material. All error ranges are based on the 90% confidence interval of replicated experiments. | 47 |
| Table 5.1: Particle size and pore diameter for each type of Celite® based on the manufacturer's specifications, and surface areas of Celite® without lipase sol-gel (support) and with lipase sol-gel (coated). The confidence limits indicated represent the 95% confidence interval of the mean based on n ≥ 6. | 56 |
| Table 5.2: Quantification of the sol-gel clusters found on each of the Celite® samples. 45 images for each type of Celite® were used for this determination. | 56 |
| Table 5.3: Effect of the presence of silica and Celite® on methyl oleate production with Novozym® 435 and unsupported sol-gel containing lipase. | 59 |
| Table 6.1: Description of the lipase preparations used for analysis in terms of the support material, sol-gel formulation, and lipase solution concentration. | 66 |
| Table 7.1: Comparison of Novozym® 435 (N435), free lipase (Free), unsupported sol-gel (US), and Celite® supported sol-gel (CSG) in terms of their final percent conversion, initial reaction rate, and initial activity at 40°C and methanol to triolein molar ratio of 1.5:1. *For N435, the initial activity is based on the weight of N435 rather than the weight of lipase since the amount of lipase in the enzyme preparation is unknown. | 82 |
| Table 7.2: Kinetic parameter estimation for the models presented in Equations 7.2 and 7.3. | 84 |
| Table 7.3: Comparison of the performance of the two proposed models (Equations 7.2 and 7.3) in terms of their SSE, R ² , and RMSE for the 6 h methyl oleate concentration. | 86 |
| Table 8.1: Kinetic constants determined by fitting the results of the batch experiments to Equation 8.1 for the Celite® sol-gel (CSG) and the Novozym® 435 (N435) immobilized enzyme preparations. Ethanolysis kinetic constants from the literature using N435 are included for comparison (Chesterfield <i>et al.</i> , 2012). | 101 |
| Table 8.2: Parameters used to model the experimental packed bed reactor results for each of the immobilized biocatalysts. | 103 |

Table 8.3: Summary of some of the parameters calculated from the modelling of the packed bed reactor experiments. _____ 104

Table 8.4: Comparison of solvent-free biodiesel packed bed reactor performance using immobilized lipase. ____ 104

List of Abbreviations

| | |
|----------------|---|
| AE | Anion exchange resin |
| BCA | Bicinchoninic acid |
| BET | Brunauer, Emmett and Teller method |
| BSA | Bovine serum albumin |
| BSTFA | N,O-Bis(trimethylsilyl)trifluoroacetamide |
| CSG | Celite® supported lipase sol-gel |
| DOI | Degree of immobilization |
| FAME | Fatty acid methyl ester |
| Free | Free lipase |
| GC-MS | Gas chromatography–mass spectrometry |
| HDA-ME | heptadecanoic acid methyl ester |
| HPLC | High-performance liquid chromatography |
| LA | Linoleic acid |
| MO | Methyl oleate |
| N435 | Novozym® 435 |
| PDA | Pentadecanoic acid |
| PTMS | Propyltrimethoxysilane |
| QF | Quartzel® felt |
| R ² | Coefficient of determination |
| R632 | Celite® R632 |
| R633 | Celite® R633 |
| R647 | Celite® R647 |
| RMSE | Root mean squared error |
| SAA | Surface area analyzer |
| SEM | Scanning electron microscopy |
| SG | Silica gel |
| SSE | Sum of squared errors |
| TGA | Thermogravimetric analysis |
| TMOS | Tetramethoxysilane |
| TMS | Trimethylsilyl |
| US | Unsupported lipase sol-gel |
| UV | Ultra violet |

Nomenclature

| | |
|----------|---|
| A | Reactor cross-sectional area (m^2) |
| C_A | Bulk concentration of substrate A (mol/m^3) |
| C_A^S | Concentration of A at the catalytic surface (mol/m^3) |
| D_{AB} | Diffusion of solute A in solvent B (m^2/s) |
| D_{MT} | Diffusion of methanol in triolein (m^2/s) |
| d_P | Particle diameter (m) |
| d_R | Reactor diameter (m) |
| K_a | Temperature constant (dimensionless) |
| k_C | Mass transfer coefficient (m/min) |
| K_{eq} | Equilibrium constant (dimensionless) |
| K_{IX} | Inhibition constant for component X |
| | Batch reaction (M). Continuous reaction (mol/m^3) |
| K_{mX} | Michaelis constant for component X |
| | Batch reaction (M). Continuous reaction (mol/m^3) |
| M_X | Molar mass of component X (g/mol) |
| Q | Volumetric flow rate (m^3/min) |
| r_A | Reaction rate with respect to substrate A ($\text{mol}/\text{m}^3\text{min}$) |
| Re | Reynolds number of the reactor (dimensionless) |
| Re_P | Reynolds number of the particle (dimensionless) |
| S_B | External surface area of the catalyst (m^2/m^3) |
| Sc | Schmidt number (dimensionless) |
| Sh | Sherwood number (dimensionless) |
| Su | Catalyst surface area (m^2/kg) |

| | |
|------------|---|
| t | Time (min) |
| T | Temperature (K) |
| U | Superficial molar velocity (m/min) |
| v | Reaction velocity (M/min) |
| v_A | Molal volume A (m^3/mol) |
| v_i | Initial reaction velocity (M/min) |
| V_{max} | Maximum initial reaction velocity Batch reaction (M/min). Continuous reaction ($\text{mol}/\text{m}^3\text{min}$) |
| V_{maxF} | Maximum velocity of the forward reaction (M/min) |
| V_{maxR} | Maximum velocity of the reverse reaction (M/min) |
| W_P | Protein weight in the reactor (kg) |
| $[X]$ | Concentration of component X , where: A is alcohol, T is triolein, M is methyl oleate, G is glycerol and E is enzyme Batch reaction (M). Continuous reaction (mol/m^3) |
| z | Position along the length of the reactor (m) |

Greek Letters

| | |
|---------------|--|
| α | Efficiency correlation (dimensionless) |
| α_X | Constants for the efficiency correlation ($X=1, 2, 3, 4, \text{ or } 5$) (dimensionless) |
| ε | Reactor bed void fraction (dimensionless) |
| μ | Dynamic viscosity (Pa s) |
| ν | Kinematic viscosity (cSt) |
| ρ | Density of the liquid (g/cm^3) |
| ρ_B | Bulk catalyst density (kg/m^3) |
| ρ_X | Density of component X (kg/m^3) |
| φ | Dissociation factor for the solvent (dimensionless) |

Chapter 1

Introduction

The research described in this thesis focuses on the immobilization of lipase in supported sol-gels and the evaluation of the immobilization scheme based on the ability of the supported biocatalyst to produce methyl oleate through the transesterification of triolein and methanol. The main focus was the investigation of the support material developed and the potential effects of the support material on the production of fatty acid methyl esters.

1.1 Objectives

The main objective of the research was to develop a lipase immobilization scheme for use as a catalyst packing material in a packed bed reactor for the production of methyl oleate from triolein and methanol. Six sub-objectives were identified to achieve this main objective:

- A. To entrap lipase in sol-gels and to evaluate the enzymatic activity and stability of the immobilized lipase, as well as to evaluate their potential to produce methyl oleate via enzymatic transesterification.
- B. To evaluate a variety of inert supports for the sol-gel entrapped lipase for use ultimately in a packed bed reactor.
- C. To fully characterize the most promising support materials in terms of the efficacy to produce methyl oleate via enzymatic transesterification.
- D. To evaluate the potential of the optimal support material and to determine any evident shortcomings for the enzymatic production of methyl oleate.
- E. To model the transesterification kinetics of the supported lipase sol-gel in a batch reactor with the primary variables being temperature and methanol concentration.
- F. To develop, model, and optimize a packed bed reactor containing supported lipase sol-gel and to compare the methyl oleate production capabilities of the supported lipase sol-gel with respect to a commercially immobilized lipase.

1.2 Thesis Organization

This thesis contains four main parts: the literature review, the experimental background, a series of five chapters addressing the research objectives, and the overall conclusions with recommendations for future work.

The literature review (Chapter 2) is a comprehensive review of the work that has been published with respect to lipase, sol-gel entrapment, supported sol-gels, biodiesel production, and reactor design and modelling.

The experimental background (Chapter 3) lays the foundation for immobilizing lipase in sol-gels, assessing their activity and stability, producing methyl oleate via the enzymatic transesterification of triolein with the commercially immobilized lipase Novozym® 435, and determining whether lipase sol-gels have potential for the production of methyl oleate.

The main results chapters encompass a series of self-contained studies, each with a unique introduction, materials and methods, results and discussion, conclusions, and references. Chapter 4 is an evaluation of a series of lipase sol-gel support materials to determine the optimal material for the production of methyl oleate via enzymatic transesterification. Chapter 5 is an evaluation of three types of diatomaceous earth and with a detailed comparison to elucidate the best support material for lipase sol-gels. Chapter 6 is an investigation of Celite® R632 supported sol-gels with an evaluation of the effect of protein loading and drying on the methyl oleate production capacity. It also evaluates the potential effect of glycerol and the stability of the immobilized enzyme. Chapter 7 focuses on the development of a kinetic model for the Celite® supported sol-gels with attention on the effects of temperature, methanol concentration, and glycerol inhibition. Chapter 8 describes the performance of the Celite® supported sol-gel in a packed bed reactor in comparison to the commercially immobilized lipase Novozym® 435 through experimental data and modelling.

Chapter 9 presents the overall conclusions of the thesis and recommends additional areas of research that would complement the research described.

Chapter 2

Literature Review

The following sections provide a review of the current state of knowledge in the areas of lipase, sol-gel-based enzyme entrapment, immobilization of sol-gels on support materials, enzymatic biodiesel production, reactor design, and modelling as it is relevant to the research presented in this thesis.

2.1 Biodiesel

Biodiesel is a mixture of fatty acid alkyl esters that can be produced via the transesterification of triglycerides. Transesterification is a catalytic reaction that converts triglycerides into fatty acid alkyl esters and glycerol in the presence of an alcohol as shown in Figure 2.1. Biodiesel is an environmentally-friendly fuel that emits low exhaust emissions and can be used either on its own or blended with petroleum diesel for use in unmodified engines (Tan *et al.*, 2010). Since biodiesel can be produced entirely from vegetable oils or animal fats, it is both renewable and biodegradable (Vasudevan and Briggs, 2008), and it is considered an alternative energy source (Jaeger and Eggert, 2002). The majority of biodiesel is produced using alkaline catalysts (sodium or potassium hydroxide) due to the short reaction time required, but this process is energy intensive, glycerol recovery is difficult, the catalyst is complicated to remove from the product, wastewater is produced which must be treated, and free fatty acids and water inhibit the reaction (Fukuda *et al.*, 2001; Meher *et al.*, 2006; Ranganathan *et al.*, 2008; Vasudevan and Briggs, 2008). Acid catalysts (sulfuric, hydrochloric, or sulfonic acid) are also used to produce biodiesel, but these reactions typically have a low reaction rates, the acidic environment is a challenge for reactor design, and high alcohol to oil ratios are necessary (Vasudevan and Briggs, 2008).

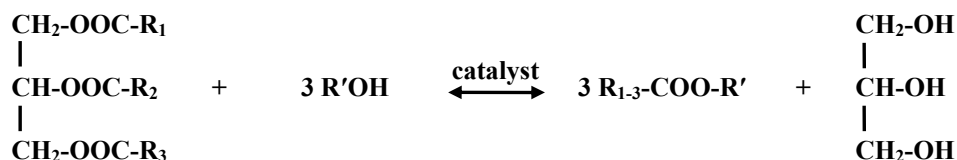


Figure 2.1: Transesterification of a triglyceride with an alcohol to produce fatty acid alkyl esters and glycerol

Therefore, alternative catalysts that overcome the disadvantages of acidic and alkaline catalysts are desirable. Transesterification can also be catalyzed by the enzyme, lipase, so there is significant interest in the enzymatic production of biodiesel. Some of the benefits of enzymatic biodiesel production over chemically catalyzed biodiesel production are that it is less energy intensive and more efficient, it produces less waste and by-products, it involves milder operating conditions (temperature and pH), enzyme and product recovery are less complicated, and there is no soap (fatty acid salt) formation (Akoh *et al.*, 2007; Fjerbaek *et al.*, 2009; Fukuda *et al.*, 2001; Marchetti *et al.*, 2007; Vasudevan and Briggs, 2008).

The challenges of lipase catalyzed biodiesel production include the potential for product and substrate inactivation of the enzyme and the high cost of enzymes (Akoh *et al.*, 2007; Fukuda *et al.*, 2001; Ganesan *et al.*, 2009; Marchetti *et al.*, 2007; Robles-Medina *et al.*, 2009; Vasudevan and Briggs, 2008). There is currently considerable interest in immobilizing lipase for biodiesel production because immobilization improves the biocatalyst thermal and chemical stability, and facilitates recovery and reuse of the enzyme which in turn decreases the costs associated with the enzyme (Akoh *et al.*, 2007; Bajaj *et al.*, 2010; Fukuda *et al.*, 2001; Jaeger and Eggert, 2002; Macario *et al.*, 2009; Vasudevan and Briggs, 2008). Biodiesel production using immobilized lipase is known to be less costly than that using free lipase, and the costs associated with enzymatic biodiesel production are expected to be competitive with those of alkaline biodiesel production if the immobilized lipase is recovered and reused more than five times or the cost associated with the enzyme is reduced significantly (Jegannathan *et al.*, 2011).

Sol-gels, as immobilization supports for enzymes, have been shown to improve the thermal and chemical stability as well as the activity of lipase (Aucoin *et al.*, 2004; Pirozzi *et al.*, 2009; Reetz *et al.*, 1996; Reetz, 1997). In addition, lipase entrapped sol-gels have the potential to be immobilized on inert supports or carriers which could be used in enzymatic bioreactors. By immobilizing sol-gel entrapped lipase on as a thin film on an inert support, the diffusion limitations that are common for sol-gel immobilized systems can be overcome (Brányik *et al.*, 2000; Orçaire *et al.*, 2006; Pogorilyi *et al.*, 2007) while at the same time facilitating the reuse of the enzyme (Orçaire *et al.*, 2006).

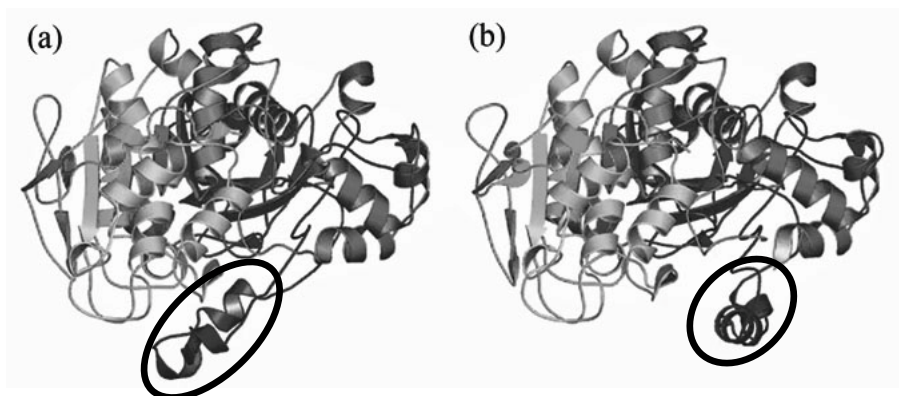


Figure 2.2: Lipase structure with the α -helical loop circled: (a) closed-lid and (b) open-lid. Adapted from Krebs and Gerstein (2000).

2.2 Lipase

Lipase (E.C. 3.1.1.3) is a triacylglycerol hydrolase which catalyzes the hydrolysis of ester bonds of triglycerides at lipid/water interfaces such as the reaction shown in Figure 2.1. Some of the biotechnological applications for lipases are for the production of biopolymeric substances and biodiesel, for triglyceride and blood cholesterol determination in enzyme-catalyzed biosensors, for the synthesis of therapeutics to aid digestion, and for the production of herbicides, cosmetic lotions and oils, and perfumes containing menthol (Hasan *et al.*, 2006; Jaeger and Eggert, 2002). In addition, they are also used in the pulp and paper industry for wastepaper deinking, in the textile industry for desizing (removing size lubricants) and enzyme wash treatments (stone washing), in household and industrial detergents to remove oils, and in the food processing industry to modify oils, improve flavour, and remove fats from meats (Hasan *et al.*, 2006).

At hydrophobic interfaces, lipase undergoes a conformational change called interfacial activation. Prior to contact with a hydrophobic interface, the enzyme has limited catalytic activity; at hydrophobic interfaces, the movement of an α -helical loop (or lid) uncovers the enzyme's active site and the enzymatic activity is dramatically increased (Sarda and Desnuelle, 1958). The closed- and open-lid structures are shown in Figure 2.2 where (a) represents the closed-lid configuration and (b) represents the open-lid configuration and the α -helical loop is circled.

Due to the interfacial activation phenomenon exhibited by lipases, it is crucial to maintain a hydrophobic interface during lipase catalyzed reactions. The presence of water during enzymatic transesterification and interesterification reactions is necessary due to the formation of a liquid-liquid interface involving

water and the oily substrate where the enzymatic reaction occurs. The addition of a small amount of a water-miscible solvent, such as ethanol or methanol, may also provide the interface necessary for the reaction in addition to acting as a reaction substrate. However, as the concentration of the water/solvent is increased sufficiently there is an inhibitory effect on the enzymatic activity since water hinders the interaction between the enzyme and substrate (Al-Zuhair, 2005; Fukuda *et al.*, 2001; Hsu *et al.*, 2001a; Robles-Medina *et al.*, 2009; Samukawa *et al.*, 2000; Shimada *et al.*, 2002; Watanabe *et al.*, 2001). Therefore, the activity of lipase is strongly influenced by the nature of the interface, the interfacial properties, and the interfacial area (Akoh *et al.*, 2007).

2.3 Sol-gel entrapment

Immobilization facilitates enzyme recovery and reuse thereby decreasing the cost associated with the enzyme, and in some cases also improves the thermal stability, chemical stability and activity of the enzyme (Akoh *et al.*, 2007; Bajaj *et al.*, 2010; Fukuda *et al.*, 2001; Jaeger and Eggert, 2002; Macario *et al.*, 2009; Vasudevan and Briggs, 2008). There are a variety of methods for enzyme immobilization which can be classified as immobilization by either binding or physical retention (Hartmeier, 1988). Immobilization by binding, which is subdivided into binding to carriers and cross-linking, tends to lead to a more stable immobilized biocatalyst with lower activity due to the bond between the enzyme and the carrier (Hartmeier, 1988). Alternatively, immobilization by physical retention, which is further subdivided into matrix entrapment and membrane enclosure, does not involve a bond between the enzyme and the carrier so the enzyme can be immobilized without significantly altering the enzyme and therefore maintaining the enzymatic activity (Hartmeier, 1988). However, mass transfer limitations are often a concern when immobilization by physical retention is considered (Hartmeier, 1988). Therefore, for any type of enzyme immobilization, a balance between activity and stability is desired. Although there is a broad spectrum of methods for immobilizing enzymes, including covalent attachment and adsorption, enzyme entrapment in polymers is the most desirable as it provides a stable enzyme support with stronger bonds than those that are attainable via adsorption, and it does not require complex chemical preparation as in covalent attachment (Reetz *et al.*, 1996).

The immobilization of enzymes in polymers, such as sol-gels, diminishes the inhibition of lipase in the presence of alcohols (Hsu *et al.*, 2001a). In addition to water-miscible solvent sensitivity, lipases are also sensitive to high temperatures and pressures which can cause irreversible enzyme

denaturation (Noel and Combes, 2003). According to Reetz *et al.*, sol-gel entrapped lipases are chemically and thermally stable and have very high activities – up to 88-fold enhanced esterification activity (Reetz *et al.*, 1996; Reetz, 1997). In addition to improving thermal and chemical stability, and enzymatic activity and selectivity, the immobilization of enzymes is also beneficial due to the ease of enzyme reuse, continuous process control, product separation, and minimal effluent and materials handling challenges (Gupta, 1993).

Some of the key challenges of enzyme entrapment according to Jin and Brennan (2002) are:

- Ensuring that the protein itself and the protein's active site are accessible to the substrate.
- Preventing the protein from becoming denatured during the immobilization process by temperature, pH, or non-aqueous conditions.
- Maintaining the polymer matrix pore size so that the substrate can easily diffuse into the polymer, the hydrolysis products can diffuse out of the matrix, and the enzyme remains entrapped within the polymer.
- Tuning the material properties of the immobilization material to maximize the activity of the entrapped enzyme and the diffusion of analytes.
- Developing a material that is straight-forward and reproducible to fabricate in a variety of forms based on the desired function.

In addition, the nature of the protein, precursors, and additives used to form the sol-gel may affect the homogeneity, orientation, aggregation, and interaction of the enzyme with the sol-gel. The substrate and product interactions with the sol-gel matrix such as electrostatic, hydrogen bonding, and hydrophobic interactions which affect the accessibility of the enzyme to the substrates may also be important (Jin and Brennan, 2002).

During the past two decades, sol-gel entrapment of enzymes has seen significant advances and has been the subject of a variety of reviews (Avnir *et al.*, 1994; Gill and Ballesteros, 2000; Jin and Brennan, 2002; Livage *et al.*, 2001; Pierre, 2004; Reetz, 1997). Sol-gels are formed through the hydrolysis and subsequent condensation of silica-precursors as shown in Figure 2.3. The first step, precursor hydrolysis, forms a colloidal suspension (sol) which, under the appropriate conditions, can be cross-linked upon gelation (condensation). Finally, the sol-gel is strengthened and conditioned with a series of aging, drying, crushing, and washing steps.

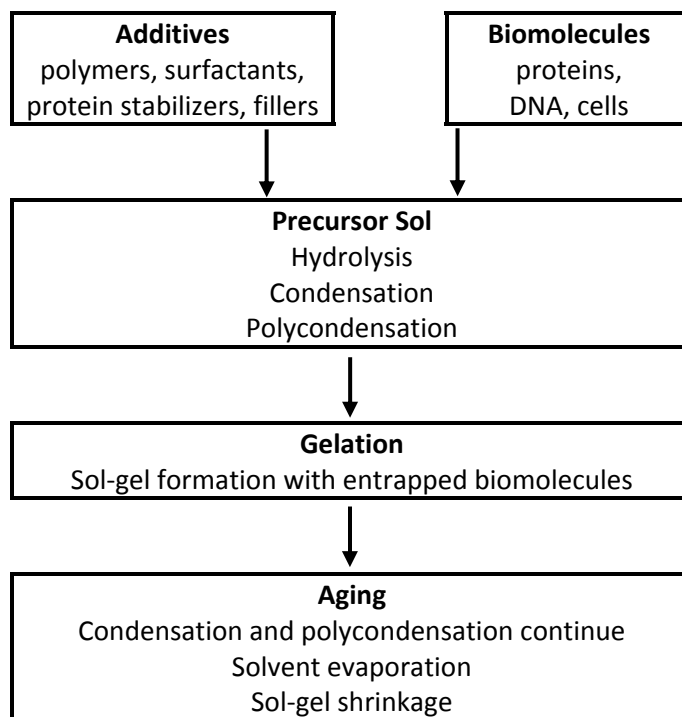


Figure 2.3: Sol-gel formation scheme adapted from Jin and Brennan (2002).

In order for an enzyme to be entrapped within the polymer matrix, it must be added between the hydrolysis and condensation stages since the acidic conditions necessary for hydrolysis will denature the enzyme and the sol-gel matrix must develop around the enzyme. Some of the parameters that can be adjusted to achieve the desired entrapment properties are the water-silane ratio, solvent, precursor and catalyst properties, agitation conditions, and enzyme entrapment time (Pierre, 2004).

Hydrophobic interfaces, such as micelles of substrates and immiscible organic solvents, stimulate the α -helical loop conformation of lipases which permits substrate accessibility to the active site (Bastida *et al.*, 1998; Galarneau *et al.*, 2006). Therefore, sol-gel materials with high hydrophobicity provide excellent supports for lipase immobilization – if the lipase is located at the hydrophobic/hydrophilic interface upon gelation it is possible to immobilize the enzyme in its active conformation (Reetz *et al.*, 1996).

A variety of applications have been developed for sol-gel immobilized enzymes, including selective coatings for biosensors (optical and electrochemical), affinity chromatography stationary phases, immunoabsorbent and solid-phase extraction materials, solid phase biocatalysts, controlled release agents (as in drug delivery), biophysical study matrices, fine organic chemical synthesis, and biocompatible prostheses (Jin and Brennan, 2002; Pierre, 2004; Soares *et al.*, 2006).

2.4 Immobilization of sol-gels on support materials

Several groups have studied the immobilization of sol-gels on support materials. Orçaire *et al.* considered lipase immobilized in silica aerogels reinforced with silica quartz fiber felts (Nasreddine *et al.*, 2008; Orçaire *et al.*, 2006). The gels were most active when composed of 40% methyltrimethoxysilane and 60% tetramethoxysilane due to the increase in hydrophobic groups. The enzymatic activity was comparable to the commercially immobilized lipase, Novozym® 435, for biodiesel production in the presence of an organic solvent; however, in the absence of solvent the diffusion limitations in the silica aerogels resulted in a less active preparation (Orçaire *et al.*, 2006).

Similarly, Li *et al.* considered the immobilization of papain on cotton fabric using tetraethylorthosilicate sol-gels (Li *et al.*, 2007). In this case, the fabric was immersed in the sol and enzyme solution which was subsequently dried onto the fabric. The residual enzymatic activity after six continuous uses for the sol-gel immobilized papain was 30% – a significant improvement over the adsorption immobilization scheme which had less than 20% residual activity after two consecutive uses. The thermostability of the enzyme was not affected by the immobilization procedure and the immobilized lipase was less sensitive to pH than the native papain (Li *et al.*, 2007).

To prepare highly stable and active biocatalysts for commercial use, Pogorilyi *et al.* developed a double immobilization technique where urease was immobilized using the sol-gel procedure on a silica gel (Pogorilyi *et al.*, 2007). In this case, a polysiloxane layer containing the enzyme was formed on the inorganic support. The activity increased when hydrophobic groups and polyvinyl alcohol were used in the sol-gel preparation, and the activity also increased as the thickness of the polysiloxane layer decreased (Pogorilyi *et al.*, 2007). The enzyme was more accessible to the substrate in films and, therefore, it can be inferred that diffusion limitations in the xerogels resulted in lower activity (Pogorilyi *et al.*, 2007).

Comparing sol-gels with polyurethane foam and ceramic foam in packed bed and fluidized bed reactors, tetraethoxysilane sol-gels with whole cell enzymes performed inferiorly for phenol degradation in comparison to both ceramic and polyurethane foams due to their mass transfer limitations (Brányik *et al.*, 2000).

Enzyme entrapped sol-gels have enhanced enzymatic properties when diatomaceous earth is used as a support material (Furukawa *et al.*, 2000; Furukawa *et al.*, 2002a; Furukawa *et al.*, 2002b; Furukawa and

Kawakami, 1998; Kawakami, 1996; Kawakami and Yoshida, 1996; Kawakami *et al.*, 2003; Koszelewski *et al.*, 2010). In one such study, ω -transaminases entrapped in Celite[®] sol-gels demonstrated enhanced activity despite high pH levels and high temperatures which are typically detrimental to enzymatic activity (Koszelewski *et al.*, 2010). In addition, this immobilization scheme allowed the catalyst material to be recycled eight times without causing an adverse effect on the achievable conversion (Koszelewski *et al.*, 2010). When lipase was supported on Celite[®] 545, higher activity, thermal stability, and reusability were exhibited in comparison to both free lipase and lipase supported on Amberlite[®] IRA-938 (Sağiroğlu and Telefoncu, 2004; Sağiroğlu, 2008; Sağiroğlu *et al.*, 2004). Comparing lipase sol-gels immobilized on Celite[®] 545 with lipase bound directly to Celite[®] 545, the sol-gel entrapment scheme had improved activity and thermostability (Kawakami, 1996; Kawakami and Yoshida, 1996).

Although sol-gel immobilized enzymes are promising for stability and reuse, there are many hurdles to overcome before they see practical application. Mass transfer limitations are common occurrences in sol-gel immobilized systems (Bajaj *et al.*, 2010; Brányik *et al.*, 2000; McDuffie 1991; Orçaire *et al.*, 2006; Pogorilyi *et al.*, 2007). Preparing enzymes in small particle sizes or on outer layers of carrier matrices are common methods to improve reactor performance (McDuffie, 1991). Therefore, immobilization of sol-gels as films on inorganic supports appears to be a reasonable solution to overcome this challenge.

2.5 Biodiesel production

Biodiesel production is a very active area of research with numerous reviews recently published (Abbaszaadeh *et al.*, 2012; Atadashi *et al.*, 2012; Chouhan and Sarma, 2011; Fan *et al.*, 2012; Gog *et al.*, 2012; Semwal *et al.*, 2011; Shahid and Jamal, 2011; Tan *et al.*, 2010; Yusuf *et al.*, 2011; Zhang *et al.*, 2012). The production of biodiesel using lipase has advantages over chemically (acid/base) catalyzed processes because it is less energy intensive, more efficient, and highly selective; in addition, enzymatic biodiesel production involves mild operating conditions, has little downstream processing, produces less waste and by-products, and does not involve soap formation (Akoh *et al.*, 2007; Marchetti *et al.*, 2007; Vasudevan and Briggs, 2008). However, some challenges associated with enzymatic biodiesel production are the potential for enzyme inhibition by the alcohol substrate, inhibition by the glycerol product, and the high cost of enzymes (Akoh *et al.*, 2007; Fukuda *et al.*, 2001; Vasudevan and Briggs, 2008). Immobilized enzymes are undergoing significant research for biodiesel production, and have the

potential to be competitive with chemical catalysts for commercial biodiesel production (Zhang *et al.*, 2012).

Table 2.1: Results of lipase screening studies for enzymatic biodiesel production.

| Lipases Considered | Results | Reference |
|--|--|------------------------------------|
| Lipozyme [®] TL IM and Novozym [®] 435 | Novozym [®] 435 was the most robust catalyst. | (Hernández-Martín and Otero, 2008) |
| Novozym [®] 435 and Lipozyme [®] TM IM | Novozym [®] 435 achieved the highest conversions, but a mixture of 60% Novozym [®] 435 and 40% Lipozyme [®] TM IM was optimal. | (Huang <i>et al.</i> , 2010) |
| <i>C. antarctica</i> , <i>P. cepacia</i> , and <i>T. lanuginosus</i> (immobilized) | <i>P. cepacia</i> and <i>T. lanuginosus</i> had the highest reaction rates in alkane solvents | (Gagnon and Vasudevan, 2011) |
| <i>P. fluorescens</i> , <i>P. cepacia</i> , <i>M. javanicus</i> , <i>C. rugosa</i> and <i>R. niveus</i> (free and immobilized) | <i>P. fluorescens</i> had the highest activity. Immobilized enzymes had improved activity over free enzymes. | (Iso <i>et al.</i> , 2001) |
| <i>C. rugosa</i> , <i>P. camembertii</i> , <i>P. roqueforti</i> , <i>P. cepacia</i> , <i>P. fluorescens</i> , <i>C. lypolytica</i> and <i>K. oxytoca</i> . | <i>C. rugosa</i> , <i>P. fluorescens</i> and <i>P. cepacia</i> had high catalytic activity. <i>P. cepacia</i> was the most methanol resistant and was less dependent on the amount of water present. | (Kaieda <i>et al.</i> , 2001) |
| Novozym [®] 435 and Lipozyme [®] IM 60 | Novozym [®] 435 was most active. | (Lai <i>et al.</i> , 2005) |
| <i>T. lanuginosus</i> , <i>P. fluorescens</i> , <i>B. cepacia</i> , <i>P. camembertii</i> , and porcine pancreatic lipase | <i>P. fluorescens</i> had the highest activity. | (Moreira <i>et al.</i> , 2007) |
| Novozym [®] 435, Lipozyme [®] RM IM, PS-C and PS-D | PS-D (immobilized on diatomaceous earth) was the most active for biodiesel production. | (Salis <i>et al.</i> , 2005) |
| <i>C. viscosum</i> (free and immobilized), <i>C. rugosa</i> and porcine pancreatic lipase | <i>C. viscosum</i> was the only lipase to have appreciable biodiesel yield. Immobilizing <i>C. viscosum</i> increased the yield by 10%. | (Shah <i>et al.</i> , 2004) |
| <i>R. delemar</i> , <i>A. niger</i> , <i>F. heterosporum</i> , Novozym [®] 435 and Lipozyme [®] IM 6 | Novozym [®] 435 was the most effective lipase for methanolysis. | (Shimada <i>et al.</i> , 1999) |
| Free: <i>R. oryzae</i> , <i>C. rugosa</i> , <i>P. camembertii</i> , <i>P. cepacia</i> and <i>P. fluorescens</i> . Immobilized: Lipozyme [®] RM IM, Lipozyme [®] TL IM, <i>C. antarctica</i> A and B and <i>R. miehei</i> . | The lipase with the highest conversion was <i>P. fluorescens</i> . Lipozyme [®] RM IM also achieved high conversion. | (Soumanou and Bornscheuer, 2003a) |
| Novozym [®] 435, Lipozyme TL-IM, and Lipozyme RM-IM | A mixture of 1/3 Novozym [®] 435 and 2/3 Lipozyme RM-IM (by weight) had the optimal performance. | (Yücel and Demir, 2012) |

2.5.1 Enzyme screening

One of the challenges that has hampered the development of enzymatic biodiesel production at industrial scale is the high cost of lipase (Jaeger and Eggert, 2002). To avoid cost constraints, the activity of the lipase must be both enhanced and prolonged, and the lipase must be tolerant to the desired solvents and substrates (Fukuda *et al.*, 2001). To address these concerns, several studies screen lipases based on their ability to produce biodiesel, and immobilize lipase on support materials so that it can be more easily reused. Table 2.1 presents a summary of various lipase screening studies.

Comparing these studies, the best lipase for biodiesel production is quite specific to the nature of the reaction being performed, for example the alcohol and oil substrates used and the amount of water present in the system. The commercially immobilized lipases considered in these studies typically have high activities in comparison to the free lipases. The demonstrated advantages of immobilized lipase include improved reusability and stability.

Many non-commercial immobilized lipases have also been considered. For example, a porous kaolinite immobilization medium improves lipase activity (Iso *et al.*, 2001), and cotton membranes are good immobilization supports (Nie *et al.*, 2006). Kumari *et al.* compared a variety of free lipases, commercially immobilized lipase on anion exchange resins, lipase immobilized on a microporous resin, cross-linked enzyme aggregates, and protein-coated microcrystals (2007). From that study, the protein-coated microcrystals had the highest percent conversion, but involved a very complicated formation procedure.

Finally, several groups considered sol-gel immobilized lipase. Hsu *et al.* achieved high conversions and considered process optimization with phyllosilicate clay sol-gels from cetyltrimethyl ammonium chloride and tetramethylorthosilicate (Hsu *et al.*, 2001b; Hsu *et al.*, 2003; Hsu *et al.*, 2004). The immobilized lipase reacted more slowly, but it achieved higher conversion, was more reusable, more thermally stable, and not affected by methanol inhibition in comparison to the free lipase (Hsu *et al.*, 2001; Hsu *et al.*, 2003; Hsu *et al.*, 2004). Similarly, lipase immobilized in a TMOS (tetramethylorthosilicate) and iso-BTMS (iso-butyltrimethoxysilane) sol-gel had good methanol resistance, good reusability and more activity than free lipase (Nouredini *et al.*, 2005). Orçaire *et al.* considered silica aerogels reinforced with silica quartz fibre felt and dried with supercritical carbon dioxide (Orçaire *et al.*, 2006). As in the other studies, sol-gel immobilized lipase exhibited improved reusability and higher activity than free lipase, but at high substrate concentrations a severe diffusion limitation was noted due to the plugging of the aerogel pores (Orçaire *et al.*, 2006). Moreira *et al.* (2007) also used sol-gels to immobilize lipase –

tetraethoxysilane (TEOS) and poly(vinyl alcohol) (PVA) sol-gels had high activity at elevated temperatures (50°C) and high ethanol to oil molar ratios (18:1). The sol-gels were much more active than free lipase, and the viscosity of the biodiesel produced was comparable to that of commercial diesel (Moreira *et al.*, 2007).

2.5.2 Optimization

As well as screening for the best source and preparation of lipase for biodiesel production, considerable current research focuses on optimizing the reaction conditions, such as the substrate molar ratio, solvent presence and type, temperature, water content, substrate flow rate, and type of acyl acceptor, to achieve the highest percent conversion and reusability of the enzyme (Akoh *et al.*, 2007). Table 2.2 provides a review of the major results gathered from some current studies on the optimization of reaction parameters for biodiesel production.

Table 2.2: Enzymatic biodiesel production reaction optimization literature results.

| Lipase | Parameters | Results | Reference |
|---|--|--|--|
| Novozym® 435 | Oil; substrate ratio; enzyme amount; temperature | Optimal conditions: methanol:oil = 3.8:1, 100% waste frying oil, 15 wt% enzyme, and 44.5°C. | (Azócar <i>et al.</i> , 2010) |
| Calcium alginate immobilized <i>R. oryzae</i> | Alcohol; enzyme amount; time; temperature; substrate ratio | Optimal conditions: methanol, 30°C, 1:3 (oil:alcohol), 24 h, and 10 wt% enzyme:oil. Pure enzyme had higher conversion than the whole cell immobilized biocatalyst. | (Balasubramaniam <i>et al.</i> , 2012) |
| Lipoprime 50T | Solvent; temperature; substrate ratio; time | Methanolysis in <i>n</i> -hexane was slow while in <i>t</i> -butanol had high reaction rates. Optimal conditions: 40°C, oil:alcohol = 1:6 – 1:8, and 1.5 h. | (Bendikiene <i>et al.</i> , 2011) |
| Immobead 150 immobilized | Solvent | Alkane solvents had high yields and rates. Isooctane and <i>n</i> -hexane were optimal. | (Gagnon and Vasudevan, 2011) |
| Phyllosilicate sol-gel immobilized | Alcohol; enzyme amount | Methanol, ethanol and <i>n</i> -butanol had the highest conversion, and the optimal enzyme amount was 150 mg/mL. | (Hsu <i>et al.</i> , 2001b) |

Continued on next page...

Table 2.2 continued

| Lipase | Parameters | Results | Reference |
|---|---|--|-----------------------------------|
| Phyllosilicate sol-gel immobilized | Temperature; solvent | Optimal reaction temperature: free lipase: 40°C and immobilized: 40°C – 70°C. Hexane had higher yield than solvent-free. | (Hsu <i>et al.</i> , 2003) |
| Phyllosilicate sol-gel immobilized | Temperature; flow rates; time | Optimal conditions using a recirculating packed column reactor were 50°C, 30 mL/min flow rate, and 48 h. | (Hsu <i>et al.</i> , 2004) |
| Novozym® 435 and Lipozym® TM IM mixture | Enzyme amount; enzyme; solvent amount; substrate amount; time | Optimal conditions: 4 wt% enzyme:oil, 49% Novozym® 435 , 55 vol% <i>tert</i> -butanol to oil, 5.12:1 methanol:oil, and 20 h. | (Huang <i>et al.</i> , 2010) |
| Porous kaolinite immobilized | Solvent; temperature; water content | Methanol and ethanol required solvent, but 1-propanol and 1-butanol did not. 1-propanol had the highest solvent-free activity. Optimal conditions: 50°C and 0.3 wt% water. | (Iso <i>et al.</i> , 2001) |
| <i>R. oryzae</i> | Enzyme amount; water content | Reaction rate increased with increasing enzyme amount until 25 IU/mL. Without water, lipase was inactive and insufficient water caused irreversible inactivation. | (Kaieda <i>et al.</i> , 1999) |
| Novozym® 435 | Enzyme amount; substrate ratio; temperature; time | Optimal conditions using refined cotton seed oil and methanol were 30% enzyme, 1:4 oil:alcohol, 30°C, and 7 h. | (Köse <i>et al.</i> , 2002) |
| Sol-gel immobilized | Substrate ratio; temperature | Optimal conditions using palm oil and ethanol were 1:18 oil:alcohol and 58°C. | (Moreira <i>et al.</i> , 2007) |
| Sol-gel immobilized | Temperature; substrate ratio; water content; enzyme amount; alcohol | Optimal conditions: 35°C, 1:15.2 oil:ethanol, 1:7.5 oil:methanol, 0.5 g water (methanol) or 0.3 g water (ethanol), and 475 mg lipase (methanol). Methanol reduced the reusability of the enzyme. | (Noureddini <i>et al.</i> , 2005) |

Continued on next page...

Table 2.2 continued

| Lipase | Parameters | Results | Reference |
|--|--|--|-----------------------------------|
| Novozym® 435 | Temperature; enzyme amount; substrate ratio; water addition; acyl acceptor | Optimal conditions: 45°C, 3 wt% enzyme, 3:1 methanol:oil, and no water. Methyl acetate improved the lipase half-life while maintaining high yield. | (Ognjanovic <i>et al.</i> , 2009) |
| Commercial immobilized | Temperature; water; substrate ratio; alcohol | Optimal conditions: 40°C, 0.4 – 0.6 water activity, 1:3 and 1:6 oil:alcohol. Butanol was the most efficient alcohol. | (Salis <i>et al.</i> , 2005) |
| Commercial free and immobilized | Temperature; solvent | Optimal temperature: 40°C - 50°C, hexane was a good solvent, and solvent-free reactions were successful. | (Soumanou and Bornscheuer, 2003a) |
| Commercial free and immobilized | Oil; alcohol | The highest conversion occurred with palm olein and methanol was the best alcohol. | (Soumanou and Bornscheuer, 2003b) |
| Lipozyme® RM IM | Temperature; enzyme amount; substrate ratio | Optimal conditions in a closed batch reactor: 67°C, 4.5 wt% enzyme, and 1:2 palmitic acid:ethanol. | (Vieira <i>et al.</i> , 2006) |
| Commercial immobilized lipases | Substrate ratio; temperature; time | Optimal conditions: 40°C, 10 h, and 1:12 oil:methyl acetate. | (Xu <i>et al.</i> , 2003) |
| Lipozyme® TL IM | Temperature; enzyme amount ; alcohol | Optimal conditions with three-step alcohol addition of 1 molar each: 40°C, 10 wt% enzyme, and methanol. | (Xu <i>et al.</i> , 2004) |
| Novozym® 435, Lipozyme TL-IM, and Lipozyme RM-IM | Time; temperature; enzyme amount; substrate ratio | Optimal conditions vary depending on lipase used: 3.9-6.2 h; 39.5-55.8°C; 4.4-21.2% enzyme; 1.6:1-4.1:1 oil:alcohol. | (Yücel and Demir, 2012) |

Based on these results, the best operating conditions are dependent on the type of lipase, alcohol, and oil used for the reaction. Immobilized lipase at approximately 40°C with an oil to methanol molar ratio of 1:3 (the stoichiometric ratio) are consistently successful reaction conditions.

Chang *et al.* used a statistical approach to determine the optimal reaction parameters using response surface methodology with a 5-level 5-factor central composite rotatable design (Chang *et al.*, 2005). The optimal reaction parameters for the reaction of canola oil with methanol using Novozym® 435 in a hexane reaction medium were 38°C, 12.4 hour reaction time, 42.3 wt% enzyme, 1:3.5 oil to methanol ratio, and 7.2 wt% water. The predicted conversion was 99.4%, while the actual achieved conversion for this reaction was 97.9%. These results are comparable to those previously reported in the literature.

2.5.3 Glycerol removal

The presence of glycerol in the reaction medium may cause enzyme inhibition (Samukawa *et al.*, 2000; Vasudevan and Briggs, 2008). Removal of glycerol by dialysis using an ultrafiltration flat sheet membrane for continuous methanolysis was very successful, and increasing the removal of glycerol improved the conversion of the reaction significantly – 20% conversion without glycerol compared to 10% conversion with 5.0 g glycerol in the reaction medium (Bélafi-Bakó *et al.*, 2002). Using a membrane separation technique, as opposed to the typical glycerol removal via settling, is much more practical for a continuous biodiesel production process (Bélafi-Bakó *et al.*, 2002).

The presence of silica beds has also been used to adsorb glycerol in biodiesel streams (Mazzieri *et al.*, 2008; Samukawa *et al.*, 2000; Yori *et al.*, 2007). One complication of this process is that one of the reaction substrates, methanol, causes the glycerol saturation capacity of the silica gel to be reduced (Mazzieri *et al.*, 2008) and glycerol to desorb from the silica gel (Yori *et al.*, 2007). Also, silica gel adsorbs methanol which can also lead to a reduced biodiesel yield (Wang *et al.*, 2006).

2.5.4 Alcohol deactivation

To minimize the tendency for lipase to be inhibited by methanol and ethanol substrates, several procedures have been considered including lipase pre-treatment, alternative acyl acceptors to replace methanol, and step-wise addition of methanol (Bélafi-Bakó *et al.*, 2002; Chen and Wu, 2003; Du *et al.*, 2004; Ruzich and Bassi, 2010a; Ruzich and Bassi, 2010b; Ruzich and Bassi, 2011; Samukawa *et al.*, 2000; Shimada *et al.*, 1999; Shimada *et al.*, 2002; Watanabe *et al.*, 2000; Watanabe *et al.*, 2001; Watanabe *et al.*, 2002; Xu *et al.*, 2003; Xu *et al.*, 2004).

Lipase pre-treatment by incubation with methyl oleate and soybean oil for twelve hours helped prevent deactivation of Novozym® 435 by methanol, increased the initial reaction rate, reduced the effect of water on the reaction rate, and helped prevent activity loss even after twenty uses (Samukawa *et al.*, 2000). Another method that helped reduce Novozym® 435 inhibition by methanol and ethanol was a pre-treatment by immersion with *tert*-butanol which increased the fatty acid methyl ester yield from 2.5% to 24.5% (Chen and Wu, 2003). In addition, periodic regeneration of the enzyme with a 2-butanol or *tert*-butanol wash allowed continuous use for seventy days while maintaining the conversion above 70% (Chen and Wu, 2003). The conclusion of this study was that the alcohol is adsorbed onto the immobilized enzyme support thereby blocking the oil substrate from reaching the reaction site and consequently preventing the reaction from progressing (Chen and Wu, 2003).

Another approach to preventing alcohol deactivation of lipase involves using methyl acetate as the acyl acceptor as opposed to methanol or ethanol. Du *et al.* (2004) showed that an oil to methyl acetate molar ratio of 1:12 can be used with Novozym® 435 without deactivating the enzyme for both crude and refined soybean oil, and there is no activity loss in a 0.5 L bioreactor after 100 cycles. In a similar study, methyl acetate as an acyl acceptor gave a higher methyl ester yield and minimal activity loss (Xu *et al.*, 2003).

The most common approach for preventing methanol inactivation of lipase in biodiesel production is three-step methanolysis. In these studies, methanol deactivation is prevented by adding methanol in three steps of one mole of methanol per mole of oil each to achieve the stoichiometric ratio of three moles of methanol per mole of oil. In one study, continuous methanol addition had the best conversion of 97% (Bélafi-Bakó *et al.*, 2002). Several studies have shown that both three-step methanolysis with one mole ratio of methanol in each step (Shimada *et al.*, 1999; Watanabe *et al.*, 2000; Watanabe *et al.*, 2001; Watanabe *et al.*, 2002; Xu *et al.*, 2004) and a two-step process with one mole ratio of methanol in the first step and two mole ratios of methanol in the second step (Shimada *et al.*, 2002) both help to prevent methanol inhibition.

2.5.5 Kinetics and reaction mechanism

The kinetics of enzymatic biodiesel production has not been widely studied. Al-Zuhair (2005) considered the kinetics and developed a mathematical model based on the reaction mechanism with vegetable oil as a substrate. The model was compared to the experimental results from an ion-exchange resin immobilized lipase and silica gel immobilized lipase with reasonable agreement with the initial reaction rate (Al-Zuhair, 2005). A ping-pong mechanism was used with Michaelis Menten kinetics, and, in

contrast to many other studies, both the substrates (oil and alcohol) could be studied independently since an organic solvent was used to keep the bulk volume constant. The inhibition effects of the oil and alcohol were dependent on the immobilization support and as the oil concentration increased, the inhibition effect of the alcohol decreased (Al-Zuhair, 2005). A subsequent study using free lipase rather than immobilized lipase found that the model underestimated the inhibition effects of both substrates, and that the reaction was more inhibited by the alcohol than the oil (Al-Zuhair *et al.*, 2007). Comparing solvent-free and *n*-hexane based reaction media using lipase immobilized on ceramic beads using ping-pong bi-bi kinetics with competitive inhibition by both substrates, a higher yield could be achieved without solvent and that the rate determining step is the surface reaction rather than mass transfer (Al-Zuhair *et al.*, 2009).

Based on a kinetics study on biodiesel production with methyl acetate as the acyl acceptor and the immobilized lipase Novozym® 435, three consecutive second-order reversible reactions were describe for the interesterification of triglycerides and methyl acetate and a kinetic model with a ping-pong bi-bi mechanism with substrate competitive inhibition was developed (Xu *et al.*, 2005). The three reactions are: triglycerides to diglycerides, diglycerides to monoglycerides, and monoglycerides to triacetylglycerol. From the kinetic constants, the first reaction step, triglycerides to diglycerides, was the rate limiting step for the overall interesterification reaction (Xu *et al.*, 2005). Similarly, three reversible reactions can be elucidated for the transesterification of triglycerides to fatty acid alkyl esters and glycerol using an alcohol rather than methyl acetate (Figure 2.4).

In depth studies of the kinetic mechanism of enzyme catalyzed reactions by Cleland are commonly used as starting points for the kinetic studies described in the literature including a series of ping-pong bi-bi mechanisms with substrate and product inhibition (Cleland, 1963a; Cleland, 1963b; Cleland, 1963c). Lipase catalyzed transesterification has been successfully described by a ping-pong bi-bi mechanism (Al-Zuhair 2005; Al-Zuhair *et al.*, 2007; Al-Zuhair *et al.*, 2009; Cheirsilp *et al.*, 2008; Dossat *et al.*, 2002; Xu *et al.*, 2005). In such a kinetic mechanism, the first substrate (ester) binds to the enzyme, forms an enzyme intermediate and the first product (alcohol) is released before the second substrate (alcohol) can bind to the enzyme to form an intermediate and release the second product (ester) (Al-Zuhair *et al.*, 2007; Cheirsilp *et al.*, 2008; Rizzi *et al.*, 1992; Yadav and Devi 2004). Figure 2.5 shows this reaction mechanism when applied to the production of biodiesel via transesterification.

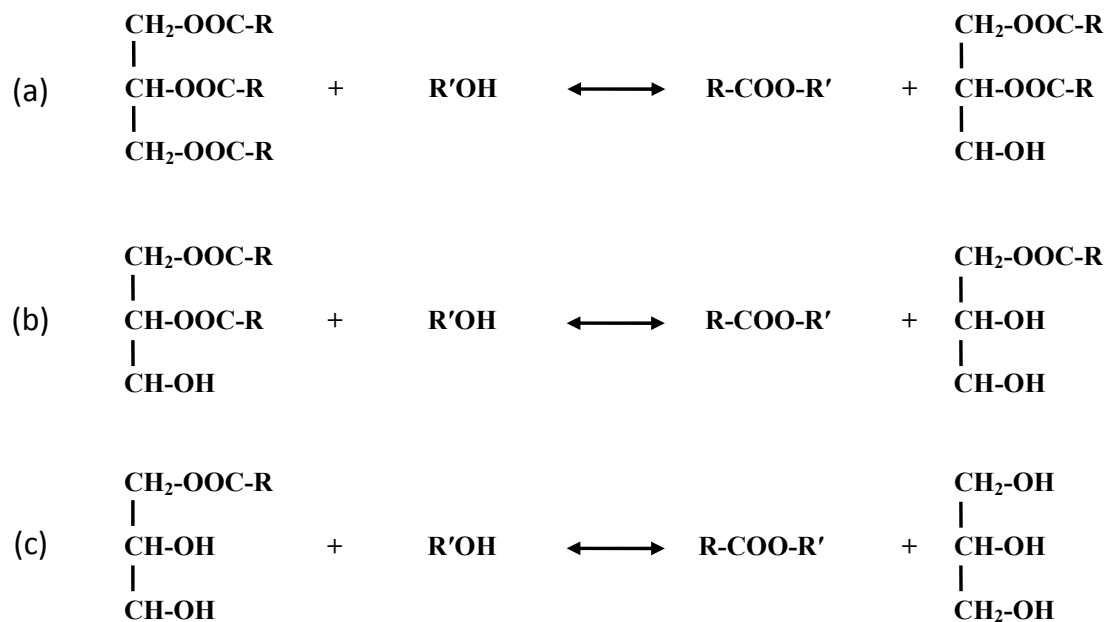


Figure 2.4: Intermediate reactions for the transesterification of triglycerides with alcohol to produce fatty acid alkyl esters and glycerol: (a) triglycerides to diglycerides, (b) diglycerides to monoglycerides, and (c) monoglycerides to glycerol.

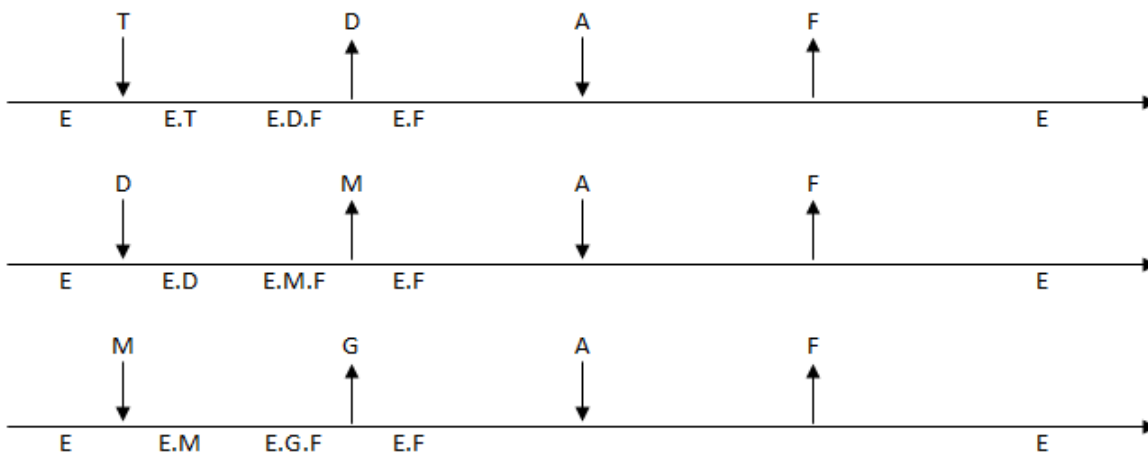


Figure 2.5: Schematic representation of the ping-pong bi-bi kinetic mechanism for the transesterification of triglycerides to produce biodiesel. Adapted from Cheirsilp *et al.* (2008).

The mechanistic steps are as follows: the free enzyme (E) reacts with the triglyceride (T) to produce an enzyme-triglyceride complex (E.T) from which the second complex (E.D.F) releases the diglyceride (D). The third complex (E.F) reacts with the alcohol (A) and releases the fatty acid alkyl ester (F). Similar mechanisms exist for the diglyceride (D) to monoglyceride (M) reaction and the monoglyceride (M) to glycerol (G) reaction as shown in Figure 2.5. This is consistent with the results obtained using TLC analysis of the reaction intermediates by Kaieda *et al.* (1999) supporting the notion that each ester bond of the triglyceride undergoes a two step mechanism: first the ester bond is hydrolyzed to produce partial glycerides and free fatty acids, followed by esterification of the free fatty acids with the alcohol to produce the fatty acid alkyl ester.

The initial rate equation with inhibition of one substrate (Equation 2.1) is often used to model the kinetics of lipase catalyzed transesterification for the production of biodiesel (Al-Zuhair, 2005; Dossat *et al.*, 2002; Xu *et al.*, 2005).

$$v_i = \frac{V_{maxF}[A][T]}{K_{mT}[A](1 + [A]/K_{IA}) + K_{mA}[T] + [A][T]} \quad (2.1)$$

where v_i is the initial reaction velocity, V_{maxF} is the maximum initial reaction velocity, $[A]$ is the alcohol concentration, $[T]$ is the triglyceride concentration, K_{mT} is the apparent Michaelis Menten constant for the triglyceride, K_{IA} is the inhibition constant for the alcohol, K_{mA} is the apparent Michaelis Menten constant for the alcohol.

Al-Zuhair *et al.* considered the initial inhibition effects of both substrates by involving a solvent so that the initial oil and alcohol concentrations could be independently varied and studied (Al-Zuhair *et al.*, 2007; Al-Zuhair *et al.*, 2009). The equation used for the kinetic modeling was similar to Equation 2.1 with the addition of a K_{IT} term to take into account the effect of triglyceride inhibition. These studies show comparable inhibition constants for the triglyceride and alcohol which were quite large (approximately 3000-4500) indicating that the effect of inhibition was low (the inhibition constant represents the dissociation of the inhibitor from the enzyme-inhibitor complex so smaller numbers indicate higher inhibitory effects).

Alternatively, a complete rate equation (Equation 2.2) for a ping-pong bi-bi mechanism with inhibition of both substrates and both products has been developed and can be used as a more sophisticated model for the entire reaction rather than solely the initial conditions (Rizzi *et al.*, 1992; Yadav and Devi, 2004).

$$v = \frac{V_{maxR}V_{maxF} \left([A][B] - \frac{[P][Q]}{K_{eq}} \right)}{V_{maxR}R + V_{maxF}F} \quad (2.2)$$

with:

$$R = [A][B] + K_{mB}[A] \left(1 + \frac{[A]}{K_{IA}} \right) + K_{mA}[B] \left(1 + \frac{[B]}{K_{IB}} \right) + \frac{K_{mA}}{K_{IQ}}[A][Q] + \frac{K_{mA}}{K_{BP}}[P][B] + \frac{K_{mB}}{K_{AQ}}[A][Q]$$

$$F = \frac{K_{mP}}{K_{eq}}[Q] \left(1 + \frac{[Q]}{K_{IQ}} \right) + \frac{K_{mQ}}{K_{eq}}[P] \left(1 + \frac{[P]}{K_{IP}} \right) + \frac{1}{K_{eq}}[P][Q] + \frac{K_{mQ}}{K_{eq}K_{IA}}[A][P]$$

$$\frac{1}{K_{BP}} = \frac{1}{K_{IP}} + \frac{K_B K_{IA}}{K_A K_{IP} K_{IB}}$$

$$\frac{1}{K_{AQ}} = \frac{1}{K_{IQ}} + \frac{K_A K_{IB}}{K_B K_{IQ} K_{IA}}$$

The reaction for this model is: $A+B \leftrightarrow P+Q$; v is the reaction velocity; V_{maxR} and V_{maxF} and the maximum velocities of the reverse and forward reactions; $[A]$, $[B]$, $[P]$, and $[Q]$ represent the concentrations of components A, B, P, and Q; K_{eq} is the equilibrium constant; K_{mA} , K_{mB} , K_{mP} , and K_{mQ} are the Michaelis constants for A, B, P and Q; and K_{IA} , K_{IB} , K_{IP} and K_{IQ} are the inhibition constants for A, B, P and Q.

2.6 Reactor design

Some common immobilized biocatalyst continuous reactors are stirred tank reactors, fluidized bed reactors, and packed bed reactors (Hartmeier, 1988; Messing, 1975). Stirred reactors are simple and inexpensive, but are more common for aerobic fermentations than immobilized biocatalysis because the intensive stirring introduces unnecessary shearing forces on the immobilized biocatalysts (Hartmeier, 1988). Fluidized bed reactors have beds that are loosely filled with catalyst particles and the substrate is forced upwards through the bed. Although fluidized beds are advantageous for immobilized biocatalysts, the retention of biocatalyst particles is challenging if the viscosity of the substrate is high (Hartmeier, 1988).

2.6.1 Packed bed reactors

Packed bed reactors can accommodate the highest density of catalyst particles, and, therefore, the highest possible substrate conversion is attainable (Hartmeier, 1988). In addition, packed bed reactors

help minimize diffusion limitations of immobilized enzymes because the reactor ensures proper mixing between the immobilized catalyst and the reaction medium thereby improving external mass transfer (Messing, 1975). Packed bed reactors have the simplest reactor design to achieve a high degree of contact between the solid catalyst particles and the liquid substrates (Thoenes, 1994).

Using a packed bed reactor, immobilized enzymes can easily be reused and continuous processing is feasible. However, one challenge of a packed bed reactor is based on the lifetime of the biocatalyst – it is impractical to shut down the reactor to change the catalyst particles frequently (Thoenes, 1994). Care must be taken to ensure the catalyst has a long lifetime within the reactor so it can run continuously with little maintenance.

For packed bed reactors, particle diameters are typically between 3 and 10 mm, and the height of the reactor is typically between 10 and a few hundred times the particle diameter (Thoenes, 1994). Continuous enzymatic methanolysis in packed column reactors commonly utilizes columns with a height of approximately 5.5 times the internal diameter (Hsu *et al.*, 2003; Nie *et al.*, 2006; Shimada *et al.*, 1999; Watanabe *et al.*, 2000).

Several packed bed reactor studies have been completed using the commercially immobilized Novozym® 435. Hama *et al.* developed a bench scale solvent-free packed bed reactor with a glycerol separating tank and achieved final fatty acid methyl ester contents above 96% using either 10 passes on a single reactor bed (Hama *et al.*, 2011a) or 550 h continuous production using five reactors in series (Hama *et al.*, 2011b). Similarly, Shimada *et al.* and Watanabe *et al.* developed a continuous, three step, fixed bed reactor with Novozym® 435 that achieved 98% (Shimada *et al.*, 1999) and 96% (Watanabe *et al.*, 2000; Watanabe *et al.*, 2001) conversion with good enzyme reusability and without enzyme deactivation. Other packed bed reactor studies using Novozym® 435 also have promising results: 76% molar conversion with no activity loss after 7 days (Chang *et al.*, 2009), 83% conversion and 30 days continuous production without conversion decrease (Chen *et al.*, 2011), and 75.2% conversion using a *tert*-butanol co-solvent (Shaw *et al.*, 2008).

Considering alternative immobilized lipases, Hsu *et al.* (2004) successfully developed a recirculating packed column reactor with lipase immobilized on ten packages of commercial paper coffee filters. Nie *et al.* (2006) developed a continuous reactor that achieved 92% conversion by immobilizing lipase on a cotton membrane for use in a three-step methanolysis continuous fixed bed reactor with nine columns packed with immobilized lipase. Wang *et al.* (2001) developed a lipase-Fe₃O₄ immobilized on cotton for

use in both a single bed reactor and four packed beds in series. A textile cloth immobilized lipase was used in a three step packed bed reactor with a hexane solvent and gravity driven glycerol separation achieving a 91% fatty acid methyl ester product (Chen *et al.*, 2009). After three hours in a single packed bed reactor using an immobilized lipase of mixed sources and stepwise methanol addition, 98% conversion was achieved dropping to 90% after 108 h due to glycerol accumulation in the reactor (Lee *et al.*, 2010).

A study using Lipozyme® IM-20 compared the performance of batch reactors and tubular reactors for biodiesel production. The tubular reactor required the addition of glass beads to increase the void space in the reactor, and had higher reactor rates, caused less stress on the lipase, and was more flexible in terms of recycle rates (Mukesh *et al.*, 1993).

2.6.2 Modelling

Few studies exist in the literature dealing with modelling enzymatic packed bed reactors for biodiesel production. Most optimization studies are purely empirical using response surface methodology to model and optimize the experimental data (Chen *et al.*, 2011; Ognjanovic *et al.*, 2009; Shaw *et al.*, 2008). Halim *et al.* (2009) used a combination of response surface methodology and mass transfer studies to optimize an immobilized lipase packed bed reactor for biodiesel production. First, the experimental data was modelling using response surface methodology and plots of a reaction controlled model with that of a mass transfer controlled model were subsequently compared to determine which fit the data better. The authors found that the mass transfer controlled model had better fit ($R^2=0.9441$) than the reaction controlled model ($R^2=0.7184$) indicating the importance of considering the mass transfer in addition to the reaction kinetics.

According to Fogler (1999), the reaction and flow in a packed bed can be described by the differential equation shown as Equation 2.3.

$$-U \frac{dC_A}{dz} = k_C S_B (C_A - C_A^S) \quad (2.3)$$

where U is the superficial molar velocity, k_C is the mass transfer coefficient, S_B is the external surface area of the catalyst, C_A is the bulk concentration of substrate A , C_A^S is the concentration of A at the catalytic surface, and z refers position along the length of the reactor. Equations 2.4 and 2.5 can be used to solve Equation 2.3 for a packed bed reactor where Sh is the Sherwood number, D_{AB} is the

diffusion coefficient, d_p is the particle diameter, Q is the volumetric flow rate, A is the reactor cross-sectional area and ε is the reactor void fraction.

$$k_c = \frac{Sh \times D_{AB}}{d_p} \quad (2.4)$$

$$Q = UA\varepsilon \quad (2.5)$$

The Sherwood number is a function of the Reynolds number and the Schmidt number, but the exact relation between the dimensionless numbers is typically determined experimentally. Considering a series of 16 packed and fluidized bed studies, Dwivedi and Upadhyay (1977) developed an equation for the Sherwood number (Sh) to fit a wide range of data as shown in Equation 2.6 for Reynolds numbers less than 10 where the Reynolds number of the particle (Re_p) and the Schmidt number (Sc) are described by Equations 2.7 and 2.8 respectively, μ is the liquid dynamic viscosity, and ρ is the liquid density (Dwivedi and Upadhyay, 1977; Seguin *et al.*, 1996).

$$Sh = \frac{1.1}{\varepsilon} Re_p^{0.28} Sc^{\frac{1}{3}} \quad (2.6)$$

$$Sc = \frac{\mu}{\rho \times D_{AB}} \quad (2.7)$$

$$Re_p = \frac{\rho \times U \times d_p}{\mu} \quad (2.8)$$

The diffusion coefficient (D_{AB}) used in these equations can be estimated by the Wilke and Chang equation as shown in Equation 2.9 where φ is the association factor for the solvent (1.0 for unassociated solvents), v_A is the molal volume for the solute ($v_A = M_A/\rho_A$), and M_X is the molar mass for component X (Treybal, 1980).

$$D_{AB} = \frac{117.3 \times 10^{-18} \times (\varphi \times M_T)^{0.5} \times T}{\mu v_A^{0.6}} \quad (2.9)$$

The void fraction of the packed bed can be estimated for uniformly sized spheres and small reactor diameters by Equation 2.10 where d_R is the reactor diameter (Rase, 1990).

$$\varepsilon = 0.4 \left(1 + 0.42 \frac{d_p}{d_R} \right) \quad (2.10)$$

Finally, the differential term in Equation 2.3 (dC_A/dz) can be determined from the kinetics of the reaction. Combining Equations 2.3 through 2.10 with the reaction kinetics of Equation 2.2 will provide a complete model of both the kinetics and mass transfer in a packed bed reactor for enzymatic biodiesel production.

Santacearia *et al.* (2007) employ a similar set of equations for an immobilized enzyme packed bed reactor for free fatty acid esterification. The reaction kinetics obtained from batch experiments was combined with external mass transfer equations to model the oleic acid conversion in the packed bed reactor (Santacearia *et al.*, 2007; Tesser *et al.*, 2005). In the system described, a unique immobilized catalyst was developed that incorporated springs to help prevent problems arising from catalyst swelling. Since the authors did not have a uniform spherical catalyst, an alternative Sherwood correlation was developed for their catalyst.

Considering an immobilized enzyme packed bed reactor, Rahman *et al.* (2011) used an ordered bi-bi reaction mechanism and external mass transfer equations to describe esterification to produce farnesyl laurate using Lipozyme[®] RM IM. Comparing a reaction limited model to a mass transfer limited model, the reactor was found to be mass transfer limited (Rahman *et al.*, 2011). Halim *et al.* (2009) performed a similar analysis comparing reaction and mass transfer limited models for a Novozym[®] 435 packed bed reactor for biodiesel production and also found that the reaction was mass transfer limited.

Considering solely the external mass transfer in a Lipozyme[®] TL IM packed bed reactor for the hydrolysis of palm olein, Chew *et al.* (2008) used a first order apparent reaction rate along with the external mass transfer correlations. The authors presented only the initial reaction rate data since the apparent reaction rate assumption was only valid for the initial conditions and determined that significant external mass transfer effects existed that could not be neglected especially as the reactor is scaled-up (Chew *et al.*, 2008).

Chapter 3

Experimental Background

The following sections present preliminary results that demonstrate the feasibility of the enzyme immobilization protocol along with the methodology development. Lipase was successfully entrapped in sol-gels with good activity and enhanced thermal stability. A commercially available immobilized lipase, Novozym[®] 435, was used to produce methyl oleate and some of the challenges associated with its application were identified.

3.1 Lipase entrapment in a sol-gel matrix

Lipase was entrapped in an 80% propyltrimethoxysilane (PTMS) and 20% tetramethoxysilane (TMOS) sol-gel following a procedure adapted from that of Clifford and Legge (2005). The precursors (PTMS and TMOS) were sonicated in the presence of water ($\text{H}_2\text{O}:\text{Si} = 12$) and hydrochloric acid ($\text{HCl}:\text{Si} = 0.0002$) for approximately two hours. The hydrolysis of this mixture formed an aqueous sol which was kept on ice to prevent untimely gelation. A solution of lipase (Novozymes[®] N44035) and 50 mM phosphate buffer at pH 7 (enzyme:buffer = 1:2 by volume) was subsequently added to the precursor solution. The enzyme and precursor solution gelled slowly while covered at 4°C for 24 hours. Upon gelation, the sol-gel was allowed to dry further until the drying rate was less than 1 mg/hr. Finally, the gel was crushed into a fine powder and washed twice with 50 mM phosphate buffer at pH 7, then with isopropyl alcohol, and finally with hexane. The sol-gel powder was sized using a micro sieve (number 200 mesh) and only particles less than 80 μm in diameter were used for the analysis. Approximately 12 g of sol-gel were produced using this procedure.

To determine the degree of lipase immobilization in the sol-gel, a sample of the enzyme-buffer solution loaded onto the sol-gel and the first phosphate buffer wash were analyzed for total protein content using a Waters HPLC system with an Agilent Zorbax Bio Series GF-250 column. The HPLC was calibrated using BSA standards as per a BCA protein assay kit from Pierce Biotechnology. The mobile phase was 1 mL/min of 200 mM phosphate buffer with pH 7, the sample injection volume was 20 μL , and the UV detection wavelength was 280 nm. Based on the difference between the amount of protein loaded into

the gels and the amount of protein in the wash, the degree of immobilization was determined. It was determined that 44.3% of the lipase loaded onto the sol-gel was entrapped (1.89 mg-lipase/g-sol-gel).

The sol-gels were analyzed for activity using the hydrolysis of linoleic acid ethyl ester to linoleic acid as the basis for activity determination. In this reaction, 5 mL of 500 mM linoleic acid ethyl ester in diisopropylether was combined with 50 mg of sol-gel and 50 μ L of 50 mM phosphate buffer (pH 7). The reaction was conducted at 30°C with agitation at 500 rpm. Each hour, a 10 μ L sample was removed from the reaction vial and diluted in 990 μ L hexane containing 50 μ L of 5 mM pentadecanoic acid as an internal standard and 5 μ L of the derivitizing agent BSTFA. Prior to analysis of the reaction products, the solution was held at 60°C for one hour to allow the TMS derivitization to occur. The formation of the reaction product, linoleic acid, was analyzed using a Varian CP-3800 gas chromatograph equipped with a Varian FactorFour VF-5ms fused silica capillary column with dimensions 0.25 mm x 0.25 m x 30 m and an oven temperature of 220°C.

The initial activity of the sol-gel is defined as the moles of linoleic acid (LA) produced per unit of time per mass of lipase. The initial activity of the sol-gel was 12.00 μ mol LA/(min mg-lipase) with a relative standard deviation of 3.68%. In addition, the presence of non-enzymatic activity was determined. Two systems were considered: one with blank sol-gel (sol-gel without lipase) and one without sol-gel. In both systems no measurable linoleic acid was produced which confirmed that the reaction observed in the lipase entrapped sol-gel reaction medium was inherently enzymatic.

Finally, the stability of the sol-gel activity was considered with respect to linoleic acid under storage conditions of 4°C. As shown in Figure 3.1, the sol-gel entrapped lipase maintained a stable linoleic acid activity up to 146 days of storage at 4°C. Nouredini *et al.* (2003) studied sol-gel immobilized lipase stability and activity and found that after 120 h of incubation at 40°C sol-gels retained 95% of their activity, but free lipase lost 67% activity after 24 h of incubation at 40°C and had almost no activity after 96 h of incubation.

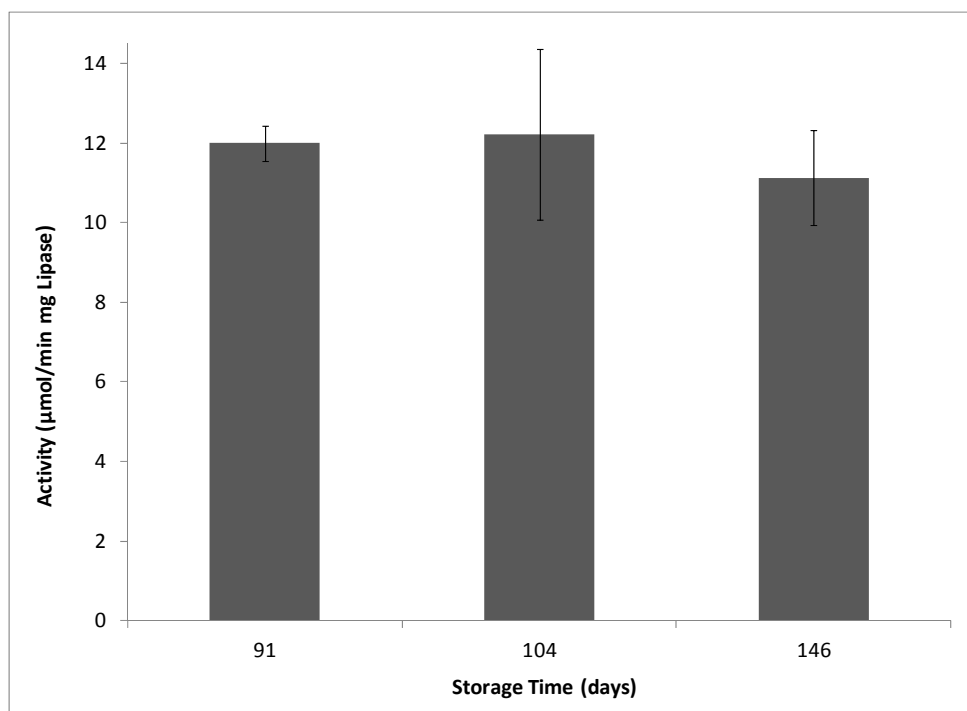


Figure 3.1: Linoleic acid activity of the lipase sol-gel based on 91, 104 and 146 days of storage at 4°C. The error bars represent the standard error with n=2-6.

3.2 Thermal properties of sol-gel entrapped lipase

Immobilization of lipase in sol-gels was shown to improve the thermostability of the enzyme (Noureddini *et al.*, 2002; Noureddini *et al.*, 2003). To analyze the thermostability of the sol-gel entrapped lipase, the sol-gels were incubated in a Pierce Reacti-Therm™ Heating Module at 70°C for the desired period of time. Samples were periodically taken and assayed for activity at 30°C in the presence of linoleic acid ethyl ester and buffer as previously described. A decline in activity was observed with increasing incubation time from 100% at time zero to approximately 50% after three days of incubation at 70°C (Figure 3.2). Noureddini *et al.* (2002) found sol-gel entrapped lipase to be stable up to 70°C, while free lipase had severe activity loss at 40°C.

To investigate the activity of the sol-gel at increased temperatures, the linoleic acid assay was performed at 30°C and at 70°C with neither of the sol-gel samples incubated before the assay. From Figure 3.3, the reaction at 70°C has a higher initial reaction rate than that at 30°C (28.7 mM LA/h vs. 16.0 mM LA/h), but the 12 h linoleic concentration for both temperatures was the same (approximately 100 mM).

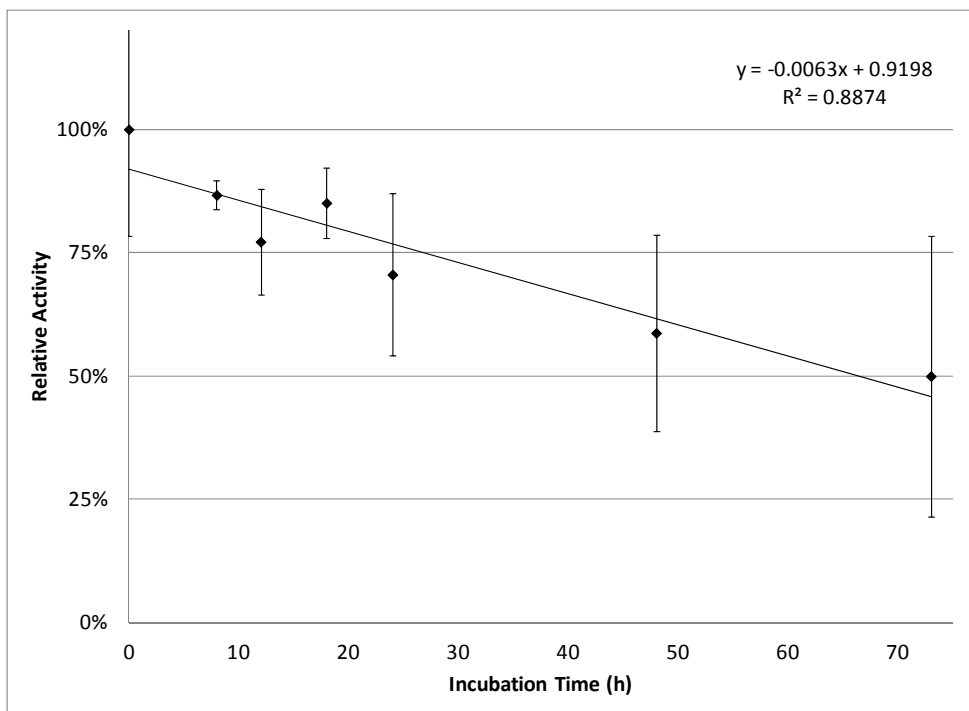


Figure 3.2: Relative activity of the sol-gel entrapped lipase after incubation at 70°C. The error bars represent the standard error with n=2-6.

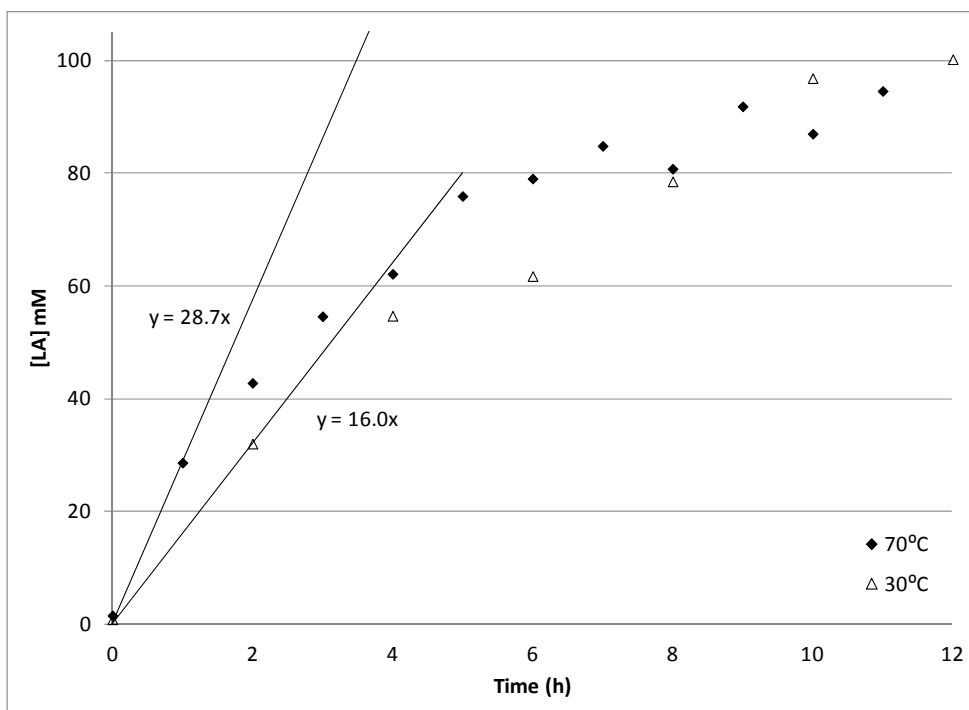


Figure 3.3: Linoleic acid concentration profile as a function of time for sol-gel immobilized lipase at 70°C and 30°C for 12 h. The slopes of the lines represent the initial reaction rates.

3.3 Methyl oleate synthesis with Novozym® 435

To determine the feasibility of producing methyl oleate, a biodiesel component, using sol-gels, a commercially immobilized lipase (Novozym® 435, Novozymes North America Inc., Washington, DC) was investigated. Novozym® 435 is a lipase from *Candida antarctica* immobilized on a macroporous acrylic resin (Sigma-Aldrich Canada Ltd., Oakville, ON). As a case study, this commercially available lipase is useful since there is a broad spectrum of literature available on the use of Novozym® 435 for biodiesel production (Chang *et al.*, 2005; Chen and Wu, 2003; Du *et al.*, 2004; Hernández-Martín and Otero, 2008; Köse *et al.*, 2002; Lai *et al.*, 2005; Orçaire *et al.*, 2006; Salis *et al.* 2005; Samukawa *et al.*, 2000; Shimada *et al.*, 1999; Watanabe *et al.*, 2000; Watanabe *et al.*, 2001; Xu *et al.*, 2003).

An assay for methyl oleate production was employed using 5.94 g of triolein (60% purity), 50 mg of Novozym® 435, and 162 µL of methanol (1:1 methanol:triolein unless noted otherwise). Samples were combined and agitated in a vial maintained at 40°C. The course of the transesterification reaction was followed with time: 10 µL aliquots periodically taken and diluted with 990 µL of hexane. The reactions were followed for 6 h unless otherwise noted.

Since alcohols are known to inhibit enzymes, it is expected that as the concentration of methanol is increased beyond a certain tolerance there will be a negative impact on the observed activity and level of conversion (Kargi and Shuler, 2001). The required stoichiometric ratio of methanol to triolein for this transesterification reaction is 3:1. As shown in Figure 3.4, the optimal methanol molar ratio required to maximize the concentration of methyl oleate produced after 6 h was 0.5 to 1.5. Ratios in this range likely minimize alcohol-mediated inhibition of the enzyme while providing adequate substrate for the reaction. As this is a batch reaction, the amount of methyl oleate produced is limited by the amount of alcohol that can be present in the system without deactivating the enzyme.

Enzymatic reactions are very temperature sensitive where low temperatures limit the kinetic energy of the system and high temperatures cause enzyme denaturation, both of which result in lower rates of reaction (Kargi and Shuler, 2001). Since the reaction medium for the formation of methyl oleate is very viscous, the potential to decrease the viscosity by increasing the temperature or by introducing non-viscous solvents is of great interest. Therefore, the effect of temperature on the conversion of triolein and methanol to methyl oleate was investigated for both solvent-based and solvent-free systems.

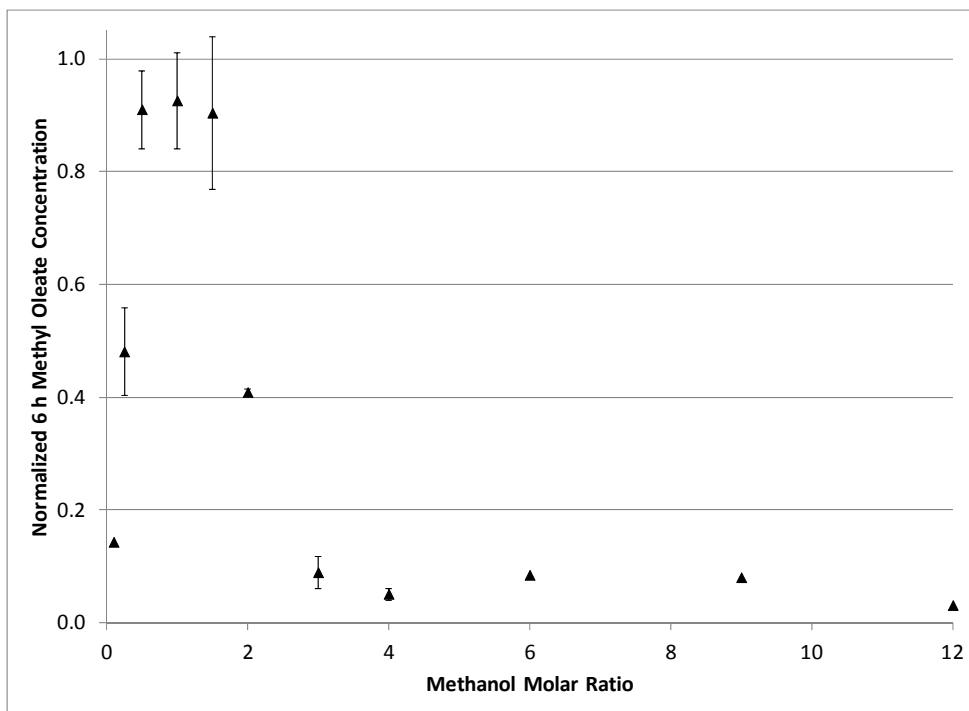


Figure 3.4: Normalized final methyl oleate concentration at various methanol molar ratios for 6 h at 40°C (normalized to the Novozym® 435 batch maximum). The error bars represent the standard deviation with n=2-5.

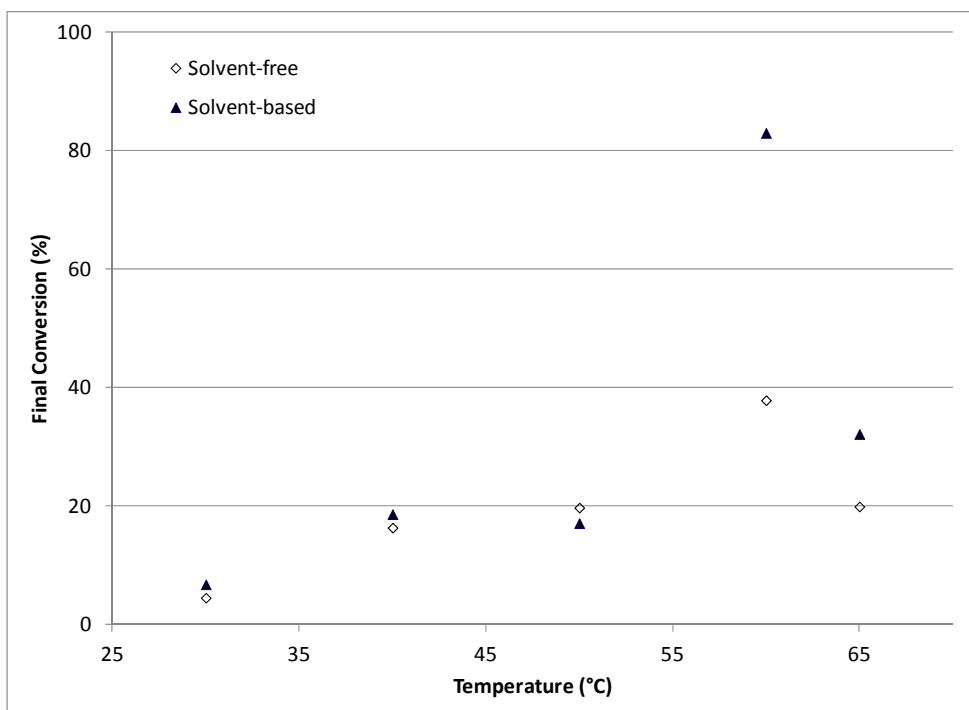


Figure 3.5: Percent conversion of methanol to methyl oleate as a function of reaction temperature after 6 h for both solvent-free and solvent-based (50% hexane) reaction media with a methanol to triolein molar ratio of 1:1.

As seen in Figure 3.5, an optimum temperature for product formation was observed at 60°C, both in the absence and presence of the organic solvent (50% hexane). In the solvent-based system the conversion was more than double that of the solvent-free system. This can likely be attributed to the improved mixing in the solvent-based system as the hexane reduces the viscosity thereby allowing for an improvement in the mixing.

Figure 3.6 compares the methyl oleate formation at 40°C with a 1:1 molar ratio of methanol to triolein with and without solvent. The solvent-free reaction medium consisted of triolein, methanol and immobilized lipase, while the solvent-based medium consisted of triolein, methanol, immobilized lipase, and 50% hexane by volume. The solvent-based medium and the solvent-free medium initially showed the same extent of conversion which increased linearly for the first 12 h. However, as the reaction progressed beyond 12 h, the solvent-based system continued to increase in methyl oleate production whereas the solvent-free system plateaued. As discussed previously, this may be attributed to the mixing limitations in the solvent-free medium. After 24 h, the solvent-based system achieved a percent conversion that was approximately three times that of the solvent-free system (79% conversion for solvent-based and 26% conversion for solvent-free).

In a similar study except that the methanol to triolein molar ratio was increased to 1.5:1 (Figure 3.7), similar observations were made. At the beginning of the reaction period the conversion of methanol to methyl oleate was comparable between the solvent-based and solvent-free systems, but the solvent-free system reached a plateau after about 23 h, while the solvent-based system continued to show an increase in conversion up to 30 h when the conversion leveled off. Unlike at lower methanol to triolein ratios, the initial conversion of the solvent-free system was slightly higher than that of the solvent-based system. Also, the point at which the solvent-free system leveled off was much later (about 23 h as compared to 12 h in the previous study). When the ratio of methanol is increased it can be assumed that more reactant is available to proceed further without deactivating the lipase despite the poor mixing. The reaction in the solvent-free medium was still limited by poor mixing since the solvent-based system surpassed the solvent-free system conversion before leveling off (50% conversion for solvent and 30% conversion for solvent-free).

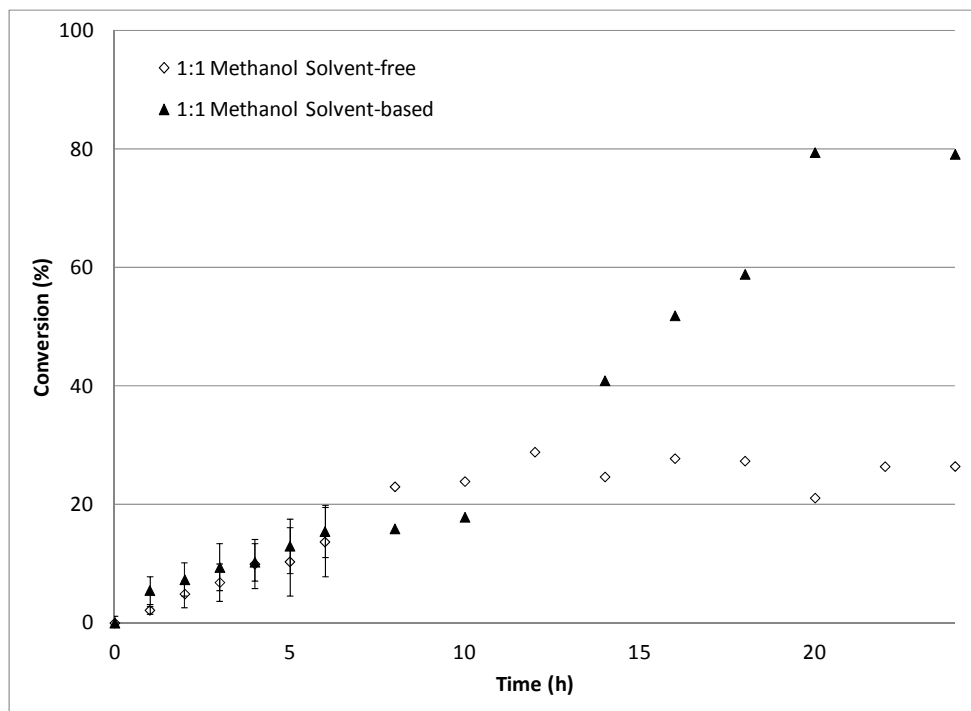


Figure 3.6: Percent conversion of methanol to methyl oleate at a methanol to triolein molar ratio of 1:1 in solvent-free and solvent-based (50% hexane) reaction media at 40°C. Error bars represent the standard error with n=3-4.

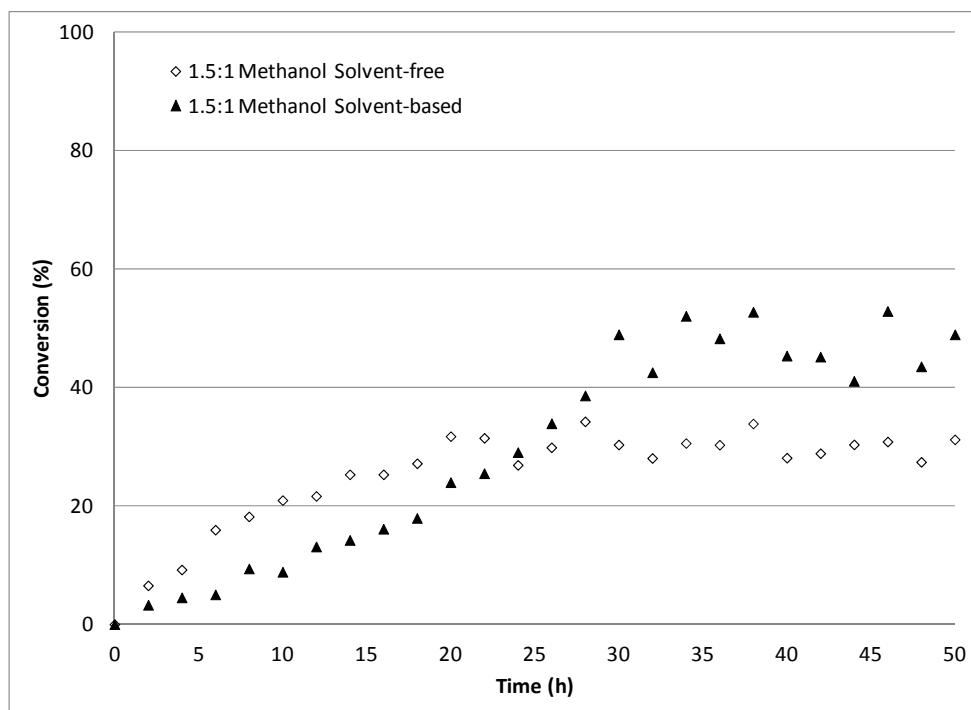


Figure 3.7: Percent conversion of methanol to methyl oleate at a methanol to triolein molar ratio of 1.5:1 in solvent-free and solvent-based (50% hexane) reaction media at 40°C.

Lipase undergoes interfacial activation at oil-water interfaces and the lipase activity is typically proportional to the interfacial area, but excessive water can cause the competing hydrolysis reaction to proceed as opposed to the transesterification reaction (Nouredinni *et al.*, 2005). Therefore, to determine whether a small amount of water would be beneficial for these reaction conditions, a set of experiments was performed with and without 3% water added to the solvent-free and solvent-based (50% hexane) reactions at a methanol to triolein molar ratio of 1:1 at 40°C. For both the solvent-free and solvent-based systems, adding this small amount of water reduced the achievable conversion during the six hour time frame by about 75% (Figure 3.8).

3.4 Sol-gel methyl oleate formation

To demonstrate that the sol-gel immobilized lipase had methyl oleate activity, an experiment was conducted with sol-gels of different compositions (Figure 3.9). The 6 h methanol to methyl oleate conversion observed for the 80% PTMS sol-gel was comparable to that of Novozym[®] 435, but the 20% PTMS sol-gel was considerably lower. Although comparable results are observed between Novozym[®] 435 and the 80% PTMS sol-gel, it will be noted that to achieve this level of conversion 350 mg of sol-gel (approximately 0.66 mg lipase) were used in comparison to 50 mg of Novozym[®] 435.

The supplier's reported activities for each of the enzyme preparations (Table 3.1) show that Novozym[®] 435 has half the activity compared to Novozyme[®] N44035 which is the lipase used in the preparation of the sol-gel. Based on the measured methyl oleate activities, the lipase immobilized in the sol-gel had approximately 6 and 70 times more activity than Novozym[®] 435 for the 20% and 80% PTMS sol-gels, respectively. The results also indicate that the more hydrophobic sol-gel (80% PTMS) was significantly more active in relation to the more hydrophilic preparation. This is expected as the interfacial activation of lipase at hydrophobic interfaces is well documented (Krebs and Gerstein, 2000; Sarda and Desnuelle, 1958). These results indicate that the 80% PTMS sol-gel is a good candidate for the immobilization of sol-gels on silica supports for use in a packed bed enzymatic reactor to produce methyl oleate.

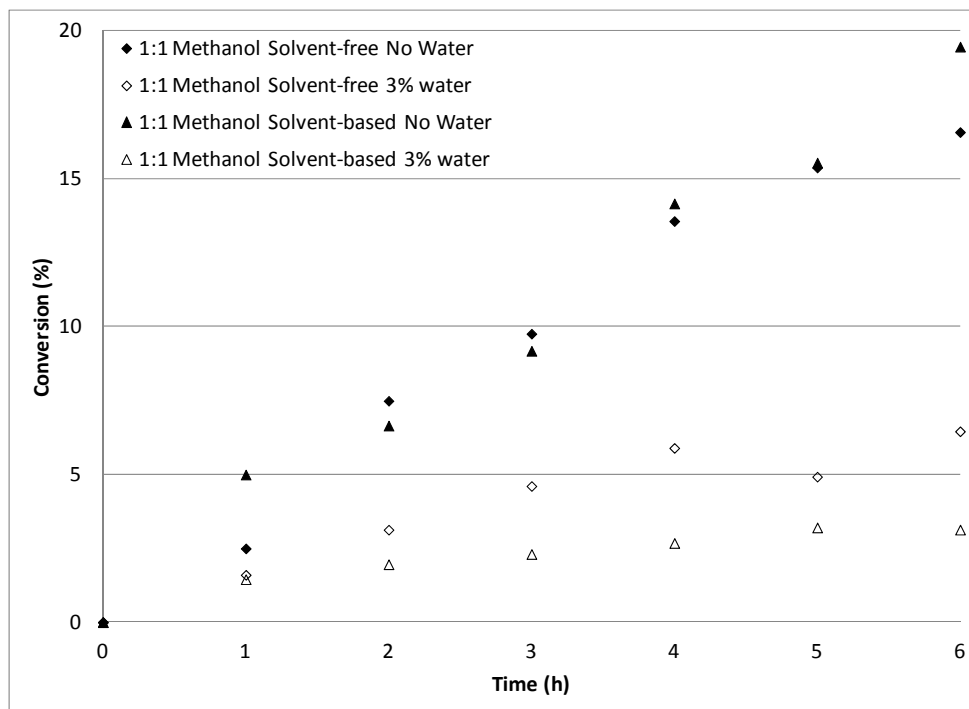


Figure 3.8: Percent conversion of methanol to methanol oleate at a methanol to triolein molar ratio of 1:1 for solvent-free and solvent-based (50% hexane) systems with and without the addition of 3% water.

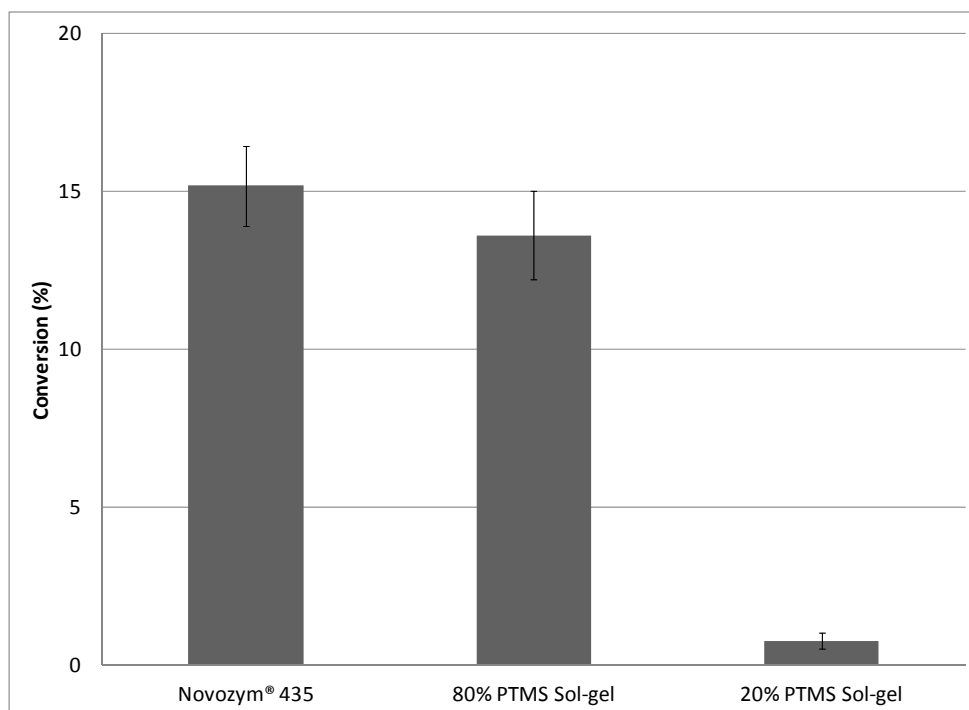


Figure 3.9: Methanol to methyl oleate conversion using immobilized lipase from Novozym® 435, 80% PTMS sol-gel and 20% PTMS sol-gel with a molar ratio of triolein to methanol of 1.5:1 at 40°C. Error bars represent the standard error with n=2.

Table 3.1: Reported and measured activities for Novozym 435®, 80% PTMS sol-gel and 20% PTMS sol-gel.

| Enzyme preparation | Reported activity | Measured activity |
|----------------------------|----------------------|-------------------|
| Novozym® 435 (N435) | 10 000 PLU/g-N435* | 53.46 U/g-N435† |
| 80% PTMS sol-gel | 20 000 PLU/g-lipase* | 3707 U/g-lipase† |
| 20% PTMS sol-gel | 20 000 PLU/g-lipase* | 331 U/g-lipase† |

*PLU = 1 µmol propyllaurate formed per minute

†U = 1 µmol methyl oleate formed per minute

Chapter 4

Study of Support Materials for Sol-gel Immobilized Lipase*

Overview

A variety of support materials for sol-gel immobilized lipase were considered based on their ability to provide superior sol-gel adhesion, load protein, and synthesize methyl oleate. A standard approach was developed to formulate the supported lipase sol-gels and to allow comparison of the resulting hybrid materials. These supported sol-gels are proposed as an alternative immobilization regime to overcome some challenges associated with enzymatic biodiesel production such as enzyme stability and cost. The support materials considered were 6-12 mesh silica gel, Celite® R633, Celite® R632, Celite® R647, anion exchange resin, and Quartzel® felt. Each support material exhibited unique properties that would be beneficial for this application including: Quartzel® felt had the highest initial sol-gel capacity; silica gel had the most uniform coating of deposited sol-gel; the anion exchange resin had the highest protein loading (1060 µg lipase/g) and reaction rate (1.25 mmol/min g); the Celite® support series were the most thermally stable and had the lowest water content; Celite® R632 had the highest sol-gel adhesion (275 mg sol-gel/g material), 6 h biodiesel conversion per gram of supported material (68%), and enzymatic activity (9.4 mmol/min g-lipase). The three supports with the highest enzymatic properties (conversion, activity and reaction rate) were Celite® R632, anion exchange resin, and Quartzel®. These supports had superior performance in comparison to the unsupported lipase sol-gels. Based on this study the lipase sol-gel support material with the most potential for biodiesel production is Celite® R632.

Keywords

Enzyme immobilization; sol-gel entrapment; lipid transesterification; lipase; supported sol-gel; biodiesel

* This chapter was submitted for publication in *Biocatalysis and Biotransformation* and is currently under review
Study of Support Materials for Sol-gel Immobilized Lipase
S.M. Meunier and R.L. Legge, *Biocatal. Biotransform.*, submitted July 2012, Manuscript ID GBAB-12-404.R1.

4.1 Introduction

Growing environmental concerns have resurfaced interest in alternative fuels that are sustainable, renewable and biodegradable. Biodiesel is one such environmentally-friendly fuel that can be produced from natural oils and fats, can be used on its own or blended with petroleum-based diesel fuels, and emits lower exhaust emissions and greenhouse gases (Tan *et al.*, 2010). Biodiesel is a mixture of fatty acid alkyl esters that can be produced via transesterification of triglycerides in the presence of an alcohol with a glycerol by-product.

Industrially, biodiesel is produced using alkaline catalysts which have very high conversions and reaction rates, but are burdened with high energy requirements and extensive downstream recovery and purification steps (Meher *et al.*, 2006). Enzyme-based transesterification can overcome some of the challenges associated with alkaline transesterification requiring milder operating conditions, minimal downstream processing and produce a very high purity product with lower waste production (Fukuda *et al.*, 2001; Akoh *et al.*, 2007; Marchetti *et al.*, 2007; Vasudevan and Briggs, 2008).

There are limitations that accompany enzymatic biodiesel production including the potential for inactivation of the enzyme and the high cost of enzymes (Robles-Medina *et al.*, 2009). Immobilizing enzymes can help overcome these limitations as immobilization renders them more chemically and thermally stable, and they are more easily recovered and reused (Macario *et al.*, 2009; Bajaj *et al.*, 2010). Lipases immobilized in sol-gels also benefit from enhanced lipase activity (Aucoin *et al.*, 2004; Reetz, 1997). In a recent review of biodiesel production via immobilized enzymes, Zhang *et al.* (2012) concluded that immobilized enzymes have the potential in the near future to be competitive with conventional chemical catalysis for the production of biodiesel.

Since enzyme immobilization in sol-gels can cause internal mass transfer limitations (Bajaj *et al.*, 2010), a double immobilization procedure is proposed in which lipase is immobilized in a sol-gel and supported on an inert material. The benefits of this system include both the advantages of sol-gels and enzyme immobilization in addition to improving internal mass transfer and the practicality of supported materials. Researchers have immobilized sol-gels on support materials such as cotton fabric (Li *et al.*, 2007), silica quartz fiber felt (Nassreddine *et al.*, 2008; Orçaire *et al.*, 2006), diatomaceous earth (Furukawa *et al.*, 2002a; Furukawa *et al.*, 2002b; Furukawa and Kawakami, 1998; Kawakami and Yoshida, 1996; Kawakami *et al.*, 2003; Koszelewski *et al.*, 2010; Meunier and Legge, 2010; Meunier and Legge, 2012), and silica gel (Pogorilyi *et al.*, 2007).

In this study, four materials were chosen for development as supports that are analogous in composition to sol-gel. Silica gel has been used successfully for supporting urease sol-gels (Pogorilyi *et al.*, 2007). Diatomaceous earth is a common enzyme immobilization material; Celite® 545 has been used successfully for ω -transaminase, protease and lipase sol-gels (Furukawa *et al.*, 2002a; Furukawa *et al.*, 2002b; Furukawa and Kawakami, 1998; Kawakami and Yoshida, 1996; Kawakami *et al.*, 2003; Koszelewski *et al.*, 2010), and Celite® R632, R633, and R647 supported lipase sol-gels have been used for methyl oleate production (Meunier and Legge, 2010; Meunier and Legge, 2012). Quartz fiber felt is a useful support material for lipase sol-gels (Nassreddine *et al.*, 2008; Orçaire *et al.*, 2006). Finally, an ion exchange resin was chosen for its valuable separation and immobilization properties (Wang *et al.*, 2010).

This study encompasses a variety of support materials, applies a consistent sol-gel immobilization technique and compares each of the materials formed on the basis of their surface, coating, and enzymatic characteristics. The surface characteristics of the materials are compared via SEM imaging to determine the presence of a visible sol-gel coating. The coating properties considered are the adhesion of sol-gel to the support surface, the protein loading of the supported sol-gel, and the water capacity and thermal stability of the coated and uncoated support materials. The enzymatic properties considered are methyl oleate production capacity, enzymatic activity, and reaction rate. Based on these results, the support materials with the greatest potential are identified for further study.

4.2 Experimental

4.2.1 Materials

Novozym® 435 was a gift from Novozymes North America Inc. (Franklinton, NC) – its reported activity is 10 000 PLU/g. Lipase (NS44035, Novozymes North America Inc., Franklinton, NC) with a reported activity of 20 000 PLU/g was immobilized in 80% PTMS – trimethoxypropylsilane and 20% TMOS – tetramethyl orthosilicate (Sigma-Aldrich Canada Ltd, Oakville, ON) sol-gels. The lipase sol-gels were supported on desiccant activated silica gel 6-12 mesh (Eagle Chemical Co., Mobile, AL), Celite® (World Minerals, Santa Barbara, CA), analytical grade anion exchange resin AG3-X4 (BioRad Laboratories, Richmond, CA), and Quartzel® felt (Saint-Gobain Quartz USA, Louisville, KY). Ultrapure water was from a Milli-Q water purification system (Millipore, Billerica, MA). All other chemicals used were reagent grade from local suppliers.

4.2.2 Methods

4.2.2.1 Support lipase sol-gel immobilization

The support materials chosen for consideration and their known properties are provided in Table 4.1.

The lipase was immobilized using a method adapted from previous work (Meunier and Legge, 2010) using 80% PTMS and 20% TMOS which resulted in a sol-gel with high hydrophobicity for enhanced lipase activity (Clifford and Legge, 2005) and superior gelation properties. A precursor mixture containing 0.08 mol PTMS, 0.02 mol TMOS, 1 mol ultrapure water and 20 μ L HCl (0.1 M) was hydrolyzed for 1 h in a sonicating water bath at room temperature. The hydrolyzed precursor mixture was then evaporated under vacuum for 30 min at 40°C. Subsequently, 14 mL of lipase and phosphate buffer (50 mM, pH 7.0) was added to the precursor mixture. This mixture was then added to the desired support material based on a predetermined sol-gel capacity to maximize the amount of sol-gel on the support without allowing excess sol-gel to gel separately from the supported material (Table 4.1). After thorough mixing, the support and sol-gel was deposited in a Petri dish, sealed and aged for 24 h at 4°C, then dried unsealed at 4°C until the drying rate slowed to less than 1 mg/h. Once dry, the gels were washed with phosphate buffer (5 mL/g sol-gel) twice, isopropyl alcohol (3 mL/g sol-gel), and hexane (5 mL/g sol-gel). After washing, the excess solvent was evaporated from the gels overnight and the gels were then stored in a sealed container at 4°C until use.

Unsupported lipase sol-gels were prepared in a similar manner omitting the mixing step with the support. Since the unsupported sol-gels adhere to the Petri dish upon gelation, they were crushed into a powder upon removal and the washing solutions removed via centrifugation at approximately 1250 xg for 10 min.

Table 4.1 Properties of the lipase sol-gel support materials. Pore diameter and particle size are as provided by the suppliers. Initial sol-gel capacity is defined as the amount of liquid sol-gel required to fully wet the support without excess material.

| Support | Pore diameter (μm) | Particle size (μm) | Initial sol-gel capacity (mL/g) |
|-----------------------------|--|--|--|
| Silica Gel | 0.005 | 1680 – 3360 | 0.3 |
| Celite® R633 | 6.5 | 297 – 595 | 1 |
| Celite® R632 | 7.0 | 595 – 1410 | 1 |
| Celite® R647 | 0.007 | 595 – 1410 | 1 |
| Anion Exchange Resin | large | 74 – 149 | 1.5 |
| Quartzel® Felt | - | - | 62.5 |

4.2.2.2 Scanning electron microscopy

The surface coating of the supported lipase sol-gels was studied qualitatively using a Hitachi S570 SEM (Hitachi High Technologies, Berkshire, England). The samples were coated with gold in preparation for microscopy and an electron beam energy of 15 kV was used. Images were taken at a variety of magnifications for comparison, but only those taken at 3000x are presented.

4.2.2.3 Protein measurement

The methodology for protein determination of the supported sol-gels has been previously described (Meunier and Legge, 2010). Samples from the original enzyme solution and the two phosphate buffer washes were analyzed for protein content using a Varian HPLC (Agilent Technologies, Mississauga, ON) equipped with an Agilent Zorbax Bio Series GF-250 column calibrated using a BSA protein standard (Pierce Biotechnology Inc., Rockford, IL). The HPLC mobile phase was 200 mM phosphate buffer (pH 7.0) and the absorbance wavelength was 280 nm. Based on a protein mass balance, the amount of protein remaining in the supported sol-gels was determined.

4.2.2.4 Adhesion of sol-gel

The adhesion of sol-gel to the support (mg sol-gel per g support material) was determined based on the change in mass of the support before and after the sol-gel immobilization and washing procedures. The ratio of lipase to sol-gel (mg lipase per g sol-gel) was also measured and calculated from the ratio of protein loading to sol-gel adhesion.

4.2.2.5 Thermogravimetric analysis

The water retention and thermal stability of the supported sol-gels and the neat supports was determined based on thermogravimetric analysis using a Q500 TGA (TA Instruments, New Castle, DE). The TGA analysis method used a temperature ramp from 30°C to 400°C at 10°C/min under N₂ at 50 mL/min and air cooling for 10 min.

4.2.2.6 Enzymatic transesterification of lipids

GC-MS analysis was used to determine the enzymatic activity of the supported lipase sol-gels as previously published (Meunier and Legge, 2010). A reaction vial containing 1 g of supported lipase sol-gel, 4 mmol triolein, and 4 mmol methanol was heated to 40°C and agitated for 6 h. Hourly, 10 µL aliquots were sampled from the reaction vial and diluted with 990 µL hexane and 100 µL of heptadecanoic acid methyl ester (internal standard) and subsequently analyzed for methyl oleate content using a Varian GC-MS (CP-3800 gas chromatograph, Saturn 2000 mass spectrometer/mass

spectrometer) equipped with a CP-Wax 52 CB fused silica column (CP8513, Varian Inc., Mississauga, ON). The GC injector temperature was 250°C with a split ratio of 50 and a helium gas flow of 1 mL/min. The column oven temperature was held at 170°C for 10 min, ramped at 10°C/min to 250°C, and held at 250°C for 2 min. The methyl oleate detection limit was approximately 0.7 mM.

4.3 Results and discussion

4.3.1 Surface coating

In most cases, the SEM images collected confirm a visible presence of sol-gel on the surface of the support material that is consistent with the nature of the unsupported sol-gel (Figure 4.1a). However, it is evident that each of the support materials is coated with sol-gel in a different manner. The silica gel exhibits an ideal sol-gel surface coverage – without sol-gel the silica gel has a rough surface (Figure 4.1b), but when coated with sol-gel the surface is smooth and appears uniform (Figure 4.1c). In contrast with the silica gel surface coverage, all three diatomaceous earth supports exhibit coating that is non-uniform (Figure 4.1d and e for Celite® R633) – there are visible sections of sol-gel coating on the diatomaceous earth. The sol-gel tends to form preferentially on itself rather than on the diatomaceous earth indicating stronger cohesive forces than adhesive forces. This is consistent with observations of Celite® sol-gel coatings previously reported (Meunier and Legge, 2010). The anion exchange resin does not show any evidence of sol-gel coating on the surface at 3000x magnification (Figure 4.1f and g). Since the coating and enzymatic properties considered show evidence that sol-gel is indeed immobilized on the anion exchange resin, the lack of visible sol-gel in the SEM images is likely due to the similarities between the surface properties of the anion exchange resin and the sol-gel. The SEM images of the Quartzel® felt show sol-gel immobilized on the individual fibers (Figure 4.1h and i) and also bonding individual fibers to each other (not shown). Unlike the sol-gel formed on the other surfaces, the sol-gel formed on the Quartzel® fibers is rougher than the uncoated fibers. This could be due to mechanical issues hindering the sol-gel formation on the cylindrical surface.

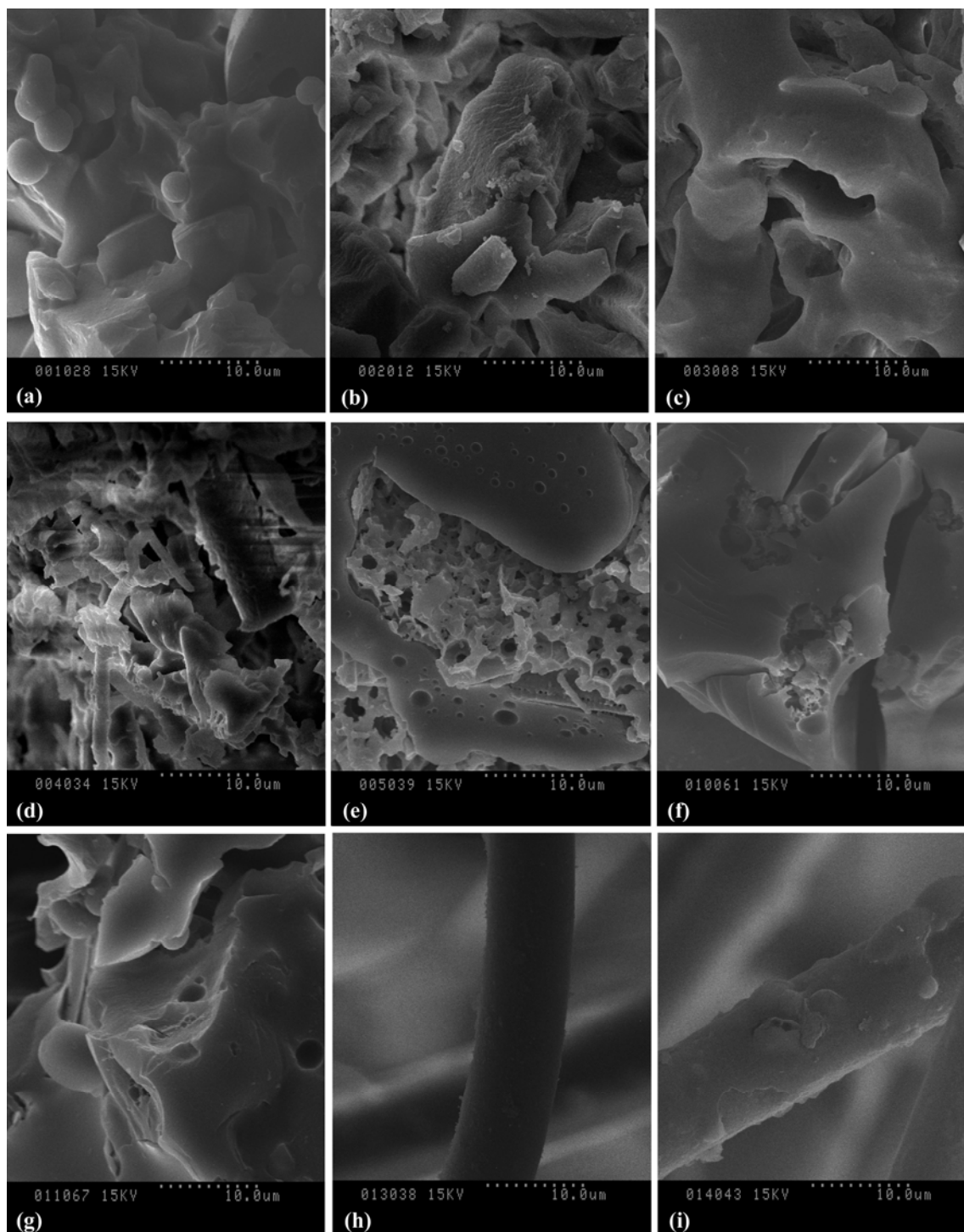


Figure 4.1: SEM images at 3000x (a) unsupported lipase sol-gel; silica gel (b) without and (c) with sol-gel immobilized on the surface; Celite® R633 (d) without and (e) with sol-gel immobilized on the surface; anion exchange resin (f) without and (g) with sol-gel immobilized on the surface; and Quartzel® felt (h) without and (i) with sol-gel immobilized on the surface.

4.3.2 Coating properties

The adhesion of sol-gel on the support material and the loading of protein in the supported sol-gel were compared to determine the presence of preferential sol-gel or lipase loading for each of the support materials tested (Figure 4.2). Silica gel (SG), Celite® R632 (R632), and anion exchange resin (AE) all have similar ratios of lipase to sol-gel (3.7, 3.1, and 4.3 µg lipase/mg sol-gel respectively). Celite® R633 (R633) and Celite® R647 (R647) both have an affinity to load lipase over sol-gel (9.1 and 14.6 µg lipase/mg sol-gel respectively). A possible explanation for the difference between the different Celite® supports is that the R632 has a much lower water adsorption capacity than the other two supports which could cause R632 to preferentially load sol-gel without entrapping the lipase in its pores. Quartzel® felt (QF) has a strong affinity for sol-gel over the lipase (0.86 µg lipase/mg sol-gel) possibly due to the cylindrical nature of the sol-gel formation which does not provide a well-defined pore structure to effectively entrap the protein. Based on these results, the highest protein loadings and adhesion levels are attained by AE and R632 (protein loadings above 800 µg lipase/g material and adhesion levels above 200 mg sol-gel/g material). Coating on glass beads was also explored, but the sol-gel did not adhere to the surface of the beads without surface modification.

TGA was conducted to ascertain the water capacity and thermal stability of the materials studied. The weight loss of the neat supports and the supported sol-gels (Figure 4.3) show that adding sol-gel to the support material causes no change or an increase in the water content of the materials given that the weight change is primarily due to the presence of water. One notable exception to this is AE, which exhibits less of a weight loss with sol-gel, but a substantially larger weight loss than any of the other support materials. Based on the thermograms (not shown), it is evident that AE is not thermally stable at temperatures above approximately 250°C, thus at high temperatures, the weight change is attributed to degradation of the anion exchange resin. Therefore, the addition of the sol-gel increases the overall stability of the material likely due to the presence of the highly stable silicon. Neat QF has a very low density and the sample weight is very close to the detection limits of the TGA so the thermograms for the neat QF are highly variable. Overall, the Celite® series of support materials displays the highest thermal stability and lowest water content.

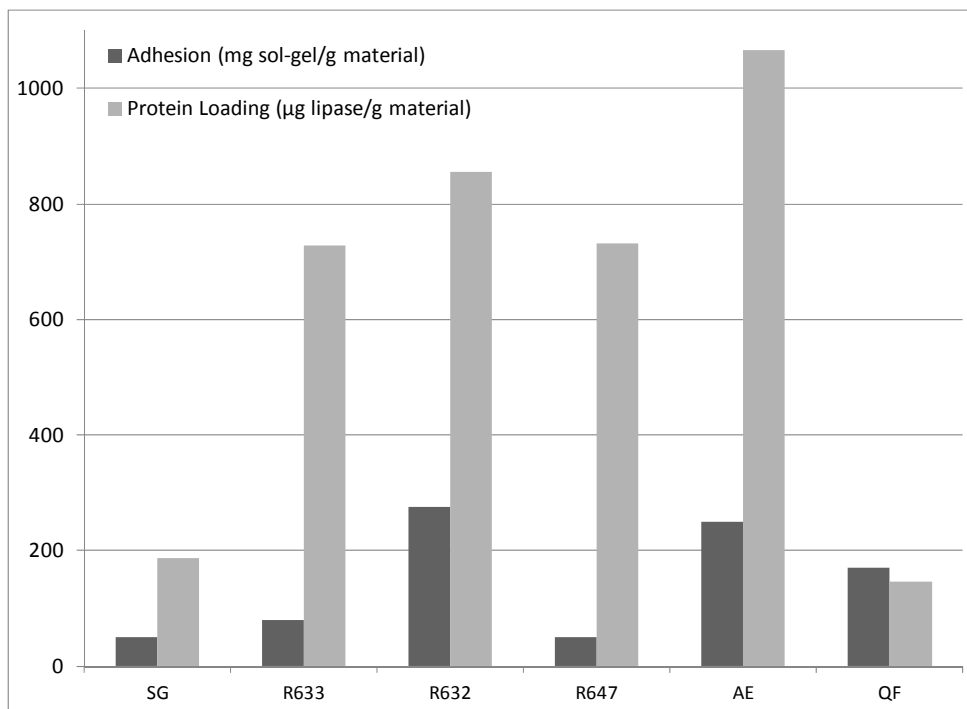


Figure 4.2: Adhesion of sol-gel (mg sol-gel/g material) and protein loading (µg lipase/g material) for each support material. Supports: SG (silica gel), R633 (Celite® R633), R632 (Celite® R632), R647 (Celite® R647), AE (anion exchange resin), and QF (Quartzel® felt). Due to the low density of QF, data are presented on a per cm² basis rather than a per gram basis.

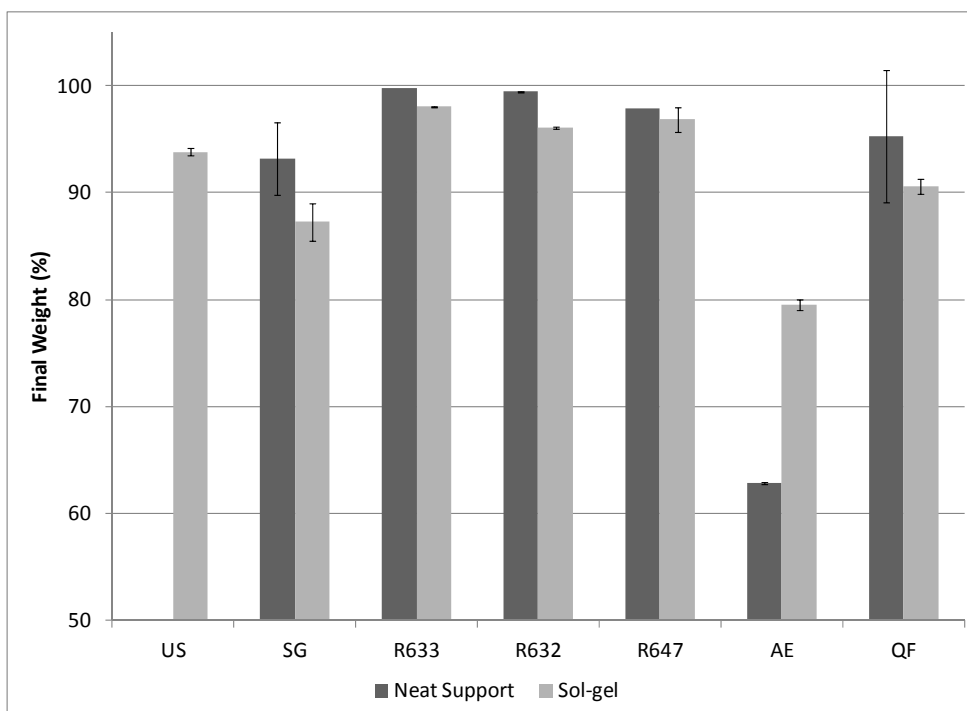


Figure 4.3: Final weight percent of the supports with and without sol-gel based on TGA. Supports: SG (silica gel), R633 (Celite® R633), R632 (Celite® R632), R647 (Celite® R647), AE (anion exchange resin), and QF (Quartzel® felt). Error bars represent a 90% confidence interval.

4.3.3 Enzymatic properties

Based on the methyl oleate concentration profiles for the batch reactions as a function of time (Figure 4.4), the conversion of methanol to methyl oleate (%) after 6 hr, the initial reaction rate (mM/min g), and the initial enzymatic activity (mmol/min g-lipase) were calculated (Table 4.2). The 6 h conversion is calculated based on the final methyl oleate concentration with respect to the starting concentration of methanol for the reaction; the initial reaction rate is based on initial slope for the concentration profile; and the initial enzymatic activity is calculated from the initial reaction rate based on the amount of lipase present in the reaction (Figure 4.4).

For each of the supported lipase sol-gels, with the exception of SG and QF, the percent conversion of methanol to methyl oleate was comparable to or beyond that of the unsupported sol-gel (Table 4.2). Although the silica gel appeared to be a promising support material based on the coating properties, it did not produce any detectable methyl oleate. This is likely due to protein inactivation caused by an interaction between the silica gel and the lipase during the immobilization process. Although the series of Celite® supports all have similar sol-gel coatings (Figure 4.1), Celite® R632 exhibits a substantially higher percent conversion than Celite® R633 and Celite® R647, indicating that the enzymatic properties of the sol-gel coating were more dependent on the ability of the support material to achieve good sol-gel and protein loadings than consistent support coverage. Although the anion exchange resin did not have a sol-gel coating that was visible by SEM, its high percent conversion confirms the presence of very active lipase. QF exhibited a very small percent conversion, but due to its low density it is reported on a per cm² basis rather than a per g basis like the other support materials, so the values are not directly comparable. R632 and AE achieved enhanced percent conversion in comparison to that of US, with R632 having the highest conversion of 68%. Therefore, the Celite® R632 is considered the most promising support to reduce mass transfer limitations that inhibit reactants and products from diffusing to and from the entrapped lipase.

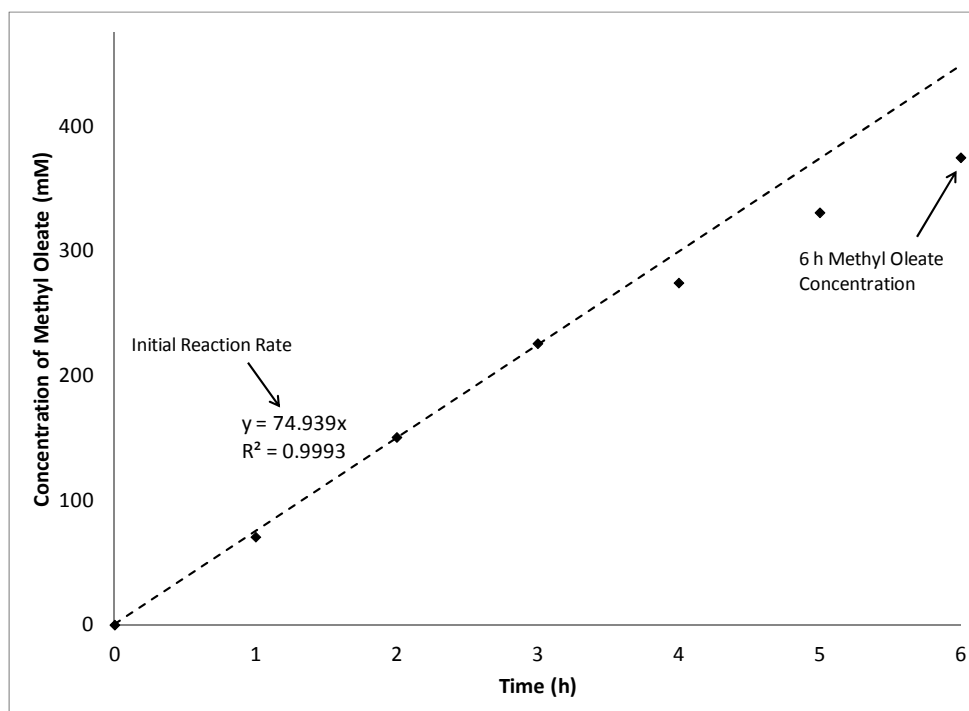


Figure 4.4: Kinetic profile for a typical lipid transesterification reaction with Celite® R632 as the support.

Table 4.2: Enzymatic properties of the supported lipase sol-gels: percent conversion of methanol to methyl oleate (MO) after 6 h of reaction, initial reaction rate, and enzymatic activity. For Quartzel® felt, the conversion and reaction rate are presented in terms of cm^2 rather than g due to the low density of the felt material. All error ranges are based on the 90% confidence interval of replicated experiments.

| Support | 6 h MO conversion (%/g-material) | Reaction rate (mM/min g-material) | Enzymatic activity (mmol/min g-lipase) |
|----------------------|----------------------------------|-----------------------------------|--|
| Unsupported | 36.0 ± 12.1 | 0.617 ± 0.239 | 1.01 ± 0.39 |
| Silica gel | 0 | 0 | 0 |
| Celite® R633 | 31.9 ± 5.3 | 0.529 ± 0.253 | 4.82 ± 2.31 |
| Celite® R632 | 68.1 ± 3.4 | 1.202 ± 0.212 | 9.36 ± 1.64 |
| Celite® R647 | 38.1 ± 2.6 | 0.616 ± 0.142 | 5.61 ± 1.29 |
| Anion exchange resin | 50.8 ± 1.6 | 1.249 ± 0.011 | 7.80 ± 0.69 |
| Quartzel® felt | 8.84 (per cm^2) | 0.181 (per cm^2) | 8.29 |

Similar conclusions can be drawn from the initial reaction rate and enzymatic activity (Table 4.2). Although there is much more variability in the R632 data for these parameters making the reaction rate of R632 not significantly higher than of AE, and the activity not significantly higher than that of AE and QF. In terms of reaction rate, two distinct groups were observed: a high reaction rate group of R632 and AE (approximately 1.2 mmol/min g) and a low reaction rate group of US, R633, and R647 (approximately

0.6 mmol/min g). QF does not follow this trend as it is presented on a per cm² basis rather than per g due to its low density in comparison to the other supports. With the exception of SG, all the supports demonstrated enhanced lipase activity in comparison to the unsupported sol-gel formulation due to the improved mass transfer expected for the supported sol-gel system. However, QF does have a high enzymatic activity since activity is calculated on the basis of the amount of lipase in the reaction media and QF has a very low lipase loading in comparison to the other support materials (Figure 4.2). Based on the enzymatic properties presented (conversion, reaction rate, and activity) R632, AE and QF are the most promising support materials.

For comparison, the activity of the commercially immobilized lipase (Novozym[®] 435) and the free lipase (NS44035) were also assayed under the same reaction conditions. The enzymatic activity of Novozym[®] 435 (8.8 ± 1.1 mmol/min-g) was not significantly different than that of R632, AE, and QF, and NS44035 did not produce methyl oleate at detectable levels.

4.4 Conclusions

A study of potential lipase sol-gel support materials (silica gel, Celite[®] R633, Celite[®] R632, Celite[®] R647, anion exchange resin, and Quartzel[®] felt) was conducted with a comparison of their sol-gel coating and enzymatic capacities to that of unsupported lipase sol-gels demonstrating their potential for biodiesel production. Based on SEM imaging, the silica gel possessed a smooth and uniform coating on the surface; however, it did not exhibit any enzymatic activity. Thermal analysis demonstrated that the anion exchange resin was not stable at high temperatures like the other support materials, and that the Celite[®] series of supports exhibited the highest stability and lowest water content. Based on sol-gel adhesion, protein loading and enzymatic properties, the superior support materials were Celite[®] R632, anion exchange, and Quartzel[®] felt. These supports showed improved enzymatic abilities in comparison to the unsupported sol-gels likely due to the decrease in mass transfer resistance. Based on this analysis, Celite[®] R632 is the most promising support material, and supported lipase sol-gels warrant further study for enzymatic biodiesel production.

4.5 Acknowledgements

This work was supported by the Natural Sciences and Engineering Research Council (NSERC) in the form of a Discovery grant to RLL and an NSERC Postgraduate Scholarship to SMM. We thank Novozymes North America for samples of the lipase formulation, World Minerals for samples of the Celite® support materials, and Saint Gobain Quartz for the Quartzel® samples.

Chapter 5

Evaluation of Diatomaceous Earth as a Support for Sol-gel Immobilized Lipase for Transesterification[†]

Overview

Enzymatic production of biodiesel by triglyceride transesterification is a promising alternative to chemically catalyzed biodiesel production despite the challenges involved with using enzymes. Celite[®] supported lipase sol-gels were investigated as an option for solving some of the challenges associated with the use of enzymes for biodiesel production addressing such problems as activity, stability and reusability of the enzyme. Three types of Celite[®] were considered (R633, R632, and R647) and compared to unsupported lipase sol-gels. Various factors were considered with regards to comparing the support materials. They included surface morphology characterized using surface area analysis and scanning electron microscopy, physical properties including adhesion of the sol-gel to the Celite[®] and the protein loading on the Celite[®], and finally enzymatic properties based on the conversion of methanol to methyl oleate and the enzymatic activity of lipase. All the sol-gels showed good conversion and initial lipase activity, and all the Celite[®] supports had similar sol-gel adhesion and protein loading. Sol-gel immobilized lipase supported on Celite[®] R632 had an average 6 h percent conversion of approximately 60%, and an average initial lipase activity comparable to that of the unsupported sol-gel formulation.

Keywords

Enzyme immobilization, sol-gel entrapment, Celite[®], transesterification, lipase

[†] This chapter is published in the Journal of Molecular Catalysis B: Enzymatic **Evaluation of Diatomaceous Earth as a Support for Sol-gel Immobilized Lipase for Transesterification** S.M. Meunier and R.L. Legge, J. Mol. Catal. B: Enzym., vol. 62, no. 1, pp. 53-57, 2010.

5.1 Introduction

Biodiesel is an alternative to fossil fuels that is becoming increasingly important due to environmental concerns, rising fossil fuel prices, demands for renewable fuel sources, and market requirements for agricultural surpluses (Robles-Medina *et al.*, 2009). Industrially, most biodiesel is produced using alkaline catalysts because this process is cost effective and efficient; however, it is energy intensive and requires significant downstream processing steps such as washing, separation and purification (Ranganathan *et al.*, 2008). Alternatively, transesterification of triglycerides to produce biodiesel can be accomplished enzymatically using lipase. The enzymatic process consumes less energy, produces less waste and by-products, and involves milder operating conditions (Akoh *et al.*, 2008; Fukuda *et al.*, 2001; Marchetti *et al.*, 2007; Vasudevan and Briggs, 2008).

Industrially, enzymatic biodiesel production possesses several challenges including a slow reaction rate, the risk of enzyme inactivation by the alcohol substrate and glycerol by-product, and the high cost of enzymes (Robles-Medina *et al.*, 2009). By immobilizing enzymes, their reusability can be improved thereby reducing their associated costs, and simplifying downstream processing (Akoh *et al.*, 2008). Further, lipase immobilized in sol-gel matrices has improved chemical and thermal stability and has higher activity compared to other immobilization procedures (Reetz, 1997; Reetz *et al.*, 1996).

Sol-gel immobilized lipase can be supported on inert materials to improve the diffusion of substrates and products to and from the enzyme and thus improve the reaction rate (Brányik *et al.*, 2000; Orçaire *et al.*, 2006; Pogorilyi *et al.*, 2007). Studies have shown that lipase supported on Celite® 545 had greater activity, higher thermal stability, and improved reusability in comparison to lipase supported on Amberlite IRA-938® and free lipase (Sağiroğlu 2008; Sağiroğlu *et al.*, 2004; Sağiroğlu and Telefoncu, 2004). Studies have also shown that sol-gel entrapped lipase immobilized on Celite® 545 has improved activity and thermostability compared to lipase deposited directly on Celite® 545 without using the sol-gel method (Kawakami, 1996; Kawakami and Yoshida, 1996).

Deactivation of lipase by methanol is a common challenge for the production of biodiesel via methanolysis. Although the stoichiometric ratio of oil to methanol is 1:3, studies have shown that enzyme deactivation can be significantly reduced by adding methanol in 3 steps of 1 mole ratio each (Shimada *et al.*, 1999; Watanabe *et al.*, 2000; Watanabe *et al.*, 2001; Watanabe *et al.*, 2002; Xu *et al.*, 2004). Our own laboratory work using Novozym® 435 supports this finding with an optimal methanol to triolein mole ratio of 0.5 – 1.5. As an alternative to step-wise methanolysis, one study shows that

continuous addition of methanol was found to achieve the highest biodiesel conversion of 97% (Bélafi-Bakó *et al.*, 2002).

The presence of glycerol is also inhibitory to the enzymatic production of biodiesel (Samukawa *et al.*, 2000). Studies have shown that silica beds are successful for the adsorption of glycerol in biodiesel streams, but methanol is detrimental to this process (Yori *et al.*, 2007; Mazzieri *et al.*, 2008). Methanol desorbs glycerol from the silica (Yori *et al.*, 2007), and adding methanol reduces the saturation capacity of the silica gel by half (Mazzieri *et al.*, 2008). In addition, when silica gel was used to control the amount of water in the biodiesel system, excess silica reduced the biodiesel yield due to methanol adsorption (Wang *et al.*, 2006).

The objective of this study was to better characterize lipase sol-gels supported on diatomaceous earth-based supports and to evaluate their efficacy in terms of the production of biodiesel via enzymatic transesterification. The surface morphology of the Celite® supported lipase sol-gels was characterized using surface area analysis and scanning electron microscopy. The physical properties investigated included the adhesion of sol-gel to the Celite® and the loading of protein on the Celite® sol-gel. Finally, the conversion and enzymatic activity of the hybrid materials were considered. For each property studied, three different types of Celite® were compared and, where applicable, the Celite® supported sol-gel was compared to unsupported sol-gel material. This information is valuable in evaluating an optimal support system for sol-gel immobilized lipase and for understanding the interaction between the support, sol-gel, and lipase.

5.2 Experimental

5.2.1 Materials

Celite® samples were a gift from World Minerals (Santa Barbara, CA). Lipase (NS44035) and Novozym® 435 were gifts from Novozymes North America Inc. (Franklinton, NC). The biological source of NS44035 was not provided by the supplier; the commercial activity of NS44035 is 20 000 PLU/g. The biological source of Novozym® 435 is *C. antarctica* and its commercial activity is 10 000 PLU/g. Tetramethyl orthosilicate (TMOS), trimethoxypropylsilane (PTMS), triolein, and methyl heptadecanoate (HDA-ME) were obtained from Sigma-Aldrich Canada Ltd. (Oakville, ON). Sodium phosphate was obtained from Mallinckrodt Baker (Phillipsburg, NJ). Isopropyl alcohol was obtained from EMD Chemicals (Gibbstown, NJ). Hexane was obtained from Fisher Scientific Company (Ottawa, ON). The silica gel (6–12 mesh) was

obtained from Eagle Chemical Co., Mobile, AL. Ultrapure water was produced using a Milli-Q water purification system from Millipore (Billerica, MA). All other chemicals were obtained from local suppliers and were of reagent grade.

5.2.2 Methods

5.2.2.1 Immobilization of lipase

To immobilize lipase on Celite[®], 0.08 mol PTMS and 0.02 mol TMOS were hydrolyzed in the presence of 1 mol ultrapure water and 200 μ L HCl (0.1 M). The mixture was sonicated in a water bath sonicator for 1 h. The precursor solution was then rotary evaporated in a heated water bath at 40°C for 30 min to remove water and alcohol. A solution of lipase and phosphate buffer (50 mM, pH 7.0) with an approximate protein concentration of 4000 μ g/mL was prepared, and 14 mL was added to the hydrolyzed precursor solution. Nine mL of the resultant mixture was combined with 6 g of the desired Celite[®] support, thoroughly mixed, and deposited in a Petri dish. The Petri dish was sealed and aged at 4°C for 24 h. The gel was then dried unsealed at 4°C until the drying rate was less than 1 mg/h. Once dry, the gel was removed from the Petri dish and washed to remove any protein not entrapped with the following wash sequence: twice with phosphate buffer (50 mM, pH 7.0, 5 mL per 3 mL sol-gel mixture), isopropyl alcohol (2.5 mL per 3 mL sol-gel mixture), and hexane (5 mL per 3 mL sol-gel mixture). Excess solvent was evaporated from the gel at room temperature overnight before the gels were stored in a sealed container at 4°C.

Unsupported gels were prepared in a similar manner except that the evaporated precursor and enzyme mixture was deposited directly into a Petri dish for aging and drying, the dried sol-gel was crushed in a mortar following removal from the Petri dish, and the washing solutions were separated from the sol-gel by centrifugation at 4000 rpm for 10 min.

5.2.2.2 Surface area analysis

The nitrogen physisorption experiments were carried out in a Micrometrics Gemini 2375 surface area analyzer (Micrometrics Instrument Corporation, Norcross, GA). The samples were degassed at 120°C for 15 h under nitrogen flow prior to each measurement. The Celite[®] R647 samples were degassed for an additional 3 h at 300°C. StarDriver software was used to fit the adsorption curve and evaluate the BET surface area.

5.2.2.3 Scanning electron microscopy

The surface morphology of the gels was evaluated using a Hitachi S570 scanning electron microscope (Hitachi High-Technologies, Berkshire, England). The samples were coated with gold prior to analysis. An electron beam energy of 15 kV was used for analysis. Sol-gel clusters were identified visually from the SEM images, and the SEM images were used to determine the percent coverage of sol-gel on the surface of the Celite® particles. For this analysis, 45 random images of each type of Celite® were collected and the percent coverage was determined for each image.

5.2.2.4 Protein determination

The total protein content of the gels was determined from the protein content of the enzyme solution loaded into the sol-gels and the protein content in the two buffer washes. The amount of protein was quantified using a Varian HPLC system (Varian Inc., Mississauga, ON) equipped with an Agilent Zorbax Bio Series GF-250 column (Agilent Technologies, Mississauga, ON) and calibrated using a BCA protein assay kit (Pierce Biotechnology Inc., Rockford, IL). The mobile phase for the HPLC analysis was 200 mM phosphate buffer (pH 7.0), and detection was at an absorbance wavelength of 280 nm.

5.2.2.5 Enzymatic lipid transesterification

The enzymatic activity of the Celite® supported lipase sol-gels was determined by GC-MS analysis. The reactions were carried out at 40°C with agitation for 6 h. The reaction vial consisted initially of approximately 1 g of the supported lipase sol-gel, 4 mmol of triolein, and 4 mmol of methanol. At 1 h intervals a 10 µL sample was removed from the reaction vial and diluted in 990 µL hexane and 100 µL of the internal standard, HDA-ME. The formation of methyl oleate, the reaction product, was followed using a Varian GC-MS system (CP-3800 gas chromatograph, Saturn 2000 mass spectrometer/mass spectrometer) equipped with a CP-Wax 52 CB fused silica column (CP8513, Varian Inc., Mississauga, ON). One µL samples of the diluted reaction mixture were injected into the GC at an injector temperature of 250°C and a split ratio of 50. Helium was used as the carrier gas with a column flow of 1 mL/min. The GC oven temperature was initially set to 170°C for 10 min, ramped at 10°C/min to 250°C, and held at 250°C for 2 min.

5.3 Results and discussion

5.3.1 Surface morphology

Comparison of the textural characteristics of the three types of Celite® considered for this study, R633, R632, and R647 will be found in Table 5.1. The three types of Celite® were chosen based on their particle sizes and pore diameters. Surface area analysis was completed for each of the supports with and without a lipase sol-gel coating. The coated R633 had a significant increase in surface area over the uncoated R633, but the other two supports, R632 and R647, had no significant change in surface area upon coating (Table 5.1). With R633, some sol-gel formation occurred between particles promoting particle agglomeration which could increase the surface area. In addition, the presence of sol-gel clusters on the Celite® confirmed that cohesive forces were perhaps stronger than the adhesive forces during sol-gel formation (Figure 5.1). Sol-gel clusters were visible for all three types of Celite® (Figure 5.1).

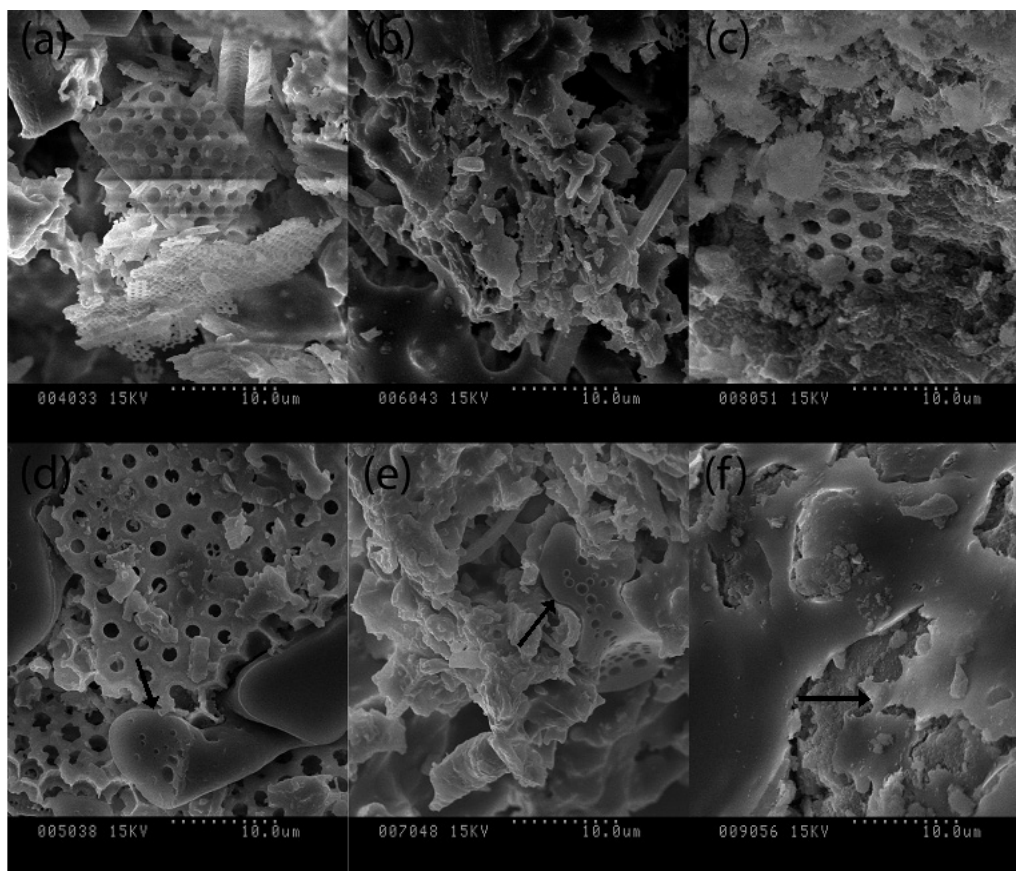


Figure 5.1: SEM images at 3000x magnification of (a) uncoated Celite R633®, (b) uncoated Celite R632®, (c) uncoated Celite R647®, (d) Celite R633® coated with lipase sol-gel, (e) Celite R632® coated with lipase sol-gel, and (f) Celite R647® coated with lipase sol-gel. Arrows identify some clusters of sol-gel on the surfaces of the Celite®.

Table 5.1: Particle size and pore diameter for each type of Celite® based on the manufacturer’s specifications, and surface areas of Celite® without lipase sol-gel (support) and with lipase sol-gel (coated). The confidence limits indicated represent the 95% confidence interval of the mean based on $n \geq 6$.

| Celite® | Particle size (um) | Pore diameter (um) | Support surface area (m ² /g) | Coated surface area (m ² /g) |
|---------|--------------------|--------------------|--|---|
| R633 | 300-600 | 6.5 | 0.90 ± 0.12 | 1.37 ± 0.33 |
| R632 | 600-1400 | 7 | 1.52 ± 0.17 | 1.49 ± 0.23 |
| R647 | 600-1400 | 0.07 | 58.92 ± 0.77 | 64.39 ± 4.50 |

Table 5.2: Quantification of the sol-gel clusters found on each of the Celite® samples. 45 images for each type of Celite® were used for this determination.

| | R633 | R632 | R647 |
|--|--------|--------|--------|
| Surface area imaged (µm ²) | 477000 | 477000 | 477000 |
| Number of sol-gel clusters | 38 | 48 | 2 |
| Average cluster size (µm ²) | 1270 | 1230 | 3670 |
| 95% confidence interval for cluster size | 540 | 480 | 6130 |

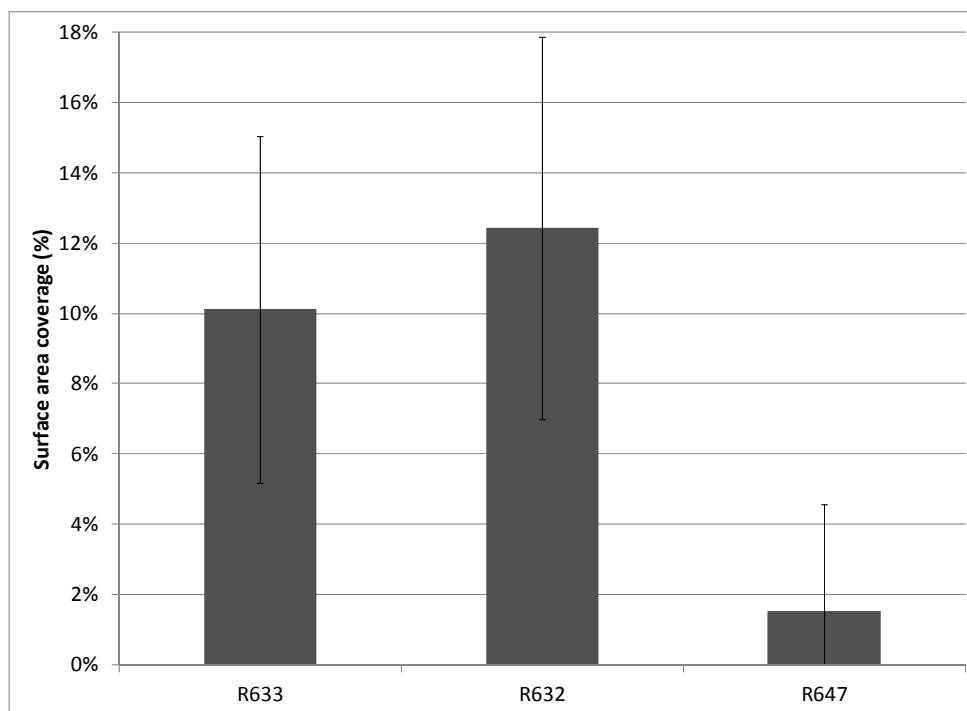


Figure 5.2: Percent sol-gel coverage on the surface of Celite® as determined by SEM image analysis. The error bars represent the 95% confidence intervals of the sample mean based on $n = 45$.

As seen in Figure 5.2, R647 has significantly less percent sol-gel on the surface of the Celite® in comparison with R633 and R632. This indicates that the lipase sol-gel did not adhere as well to the Celite® R647 support. Celite® R647 has a much larger surface area (Table 5.1) than R633 and R632 which may favour sol-gel cohesion over adhesion to the Celite® surface.

5.3.2 Physical properties

Both the Celite® R633 and R632 have a comparable number of sol-gel clusters and average cluster size based on the 45 images recorded for each sample; however, Celite® R647 had very few clusters (Table 5.2). There is no significant difference between the levels of sol-gel adhesion on any of the support materials (Figure 5.3). For R647, although the same mass of sol-gel is immobilized on the support (Figure 5.3), the surface coverage is significantly lower (Figure 5.2). This would suggest that the R633 and R632 favour adhesion of sol-gel as a thinner layer on the surface rather than cohesion of thicker sol-gel clusters as with R647.

Figure 5.4 shows the loading of protein as calculated based on HPLC analysis. The unsupported sol-gel has a high protein loading per gram of material (Figure 5.4 A) because there is no additional mass contributed by the Celite® which is the case for supported sol-gels. When the loading is considered on the basis of sol-gel only (Figure 5.4 B), the unsupported formulation is significantly lower than the Celite® R632 and R647 formulations. For both the material basis and sol-gel basis (Figure 5.4 A and B), R633 has significantly lower protein loading than R632 and R647. Based on the manufacturer's specifications for the Celite®, R633 has a much higher water adsorption capacity than R632 and R647 (R633 240%, R632 84%, and R647 163%). R633 may preferentially absorb the lipase-buffer solution from the sol-gel mixture, whereas the other types of Celite® absorb less water which may promote gelation of the lipase in the sol-gel polymer matrix. In the latter case the lipase would not be washed off the support as in the former case resulting in more protein immobilized on the R632 and R647 supports.

5.3.3 Enzymatic properties

Initial studies were performed to determine the effect of silica and Celite® on the enzymatic activity of the sol-gel. Adding 1 g of silica gel to either the 50 mg Novozym® 435 or 200 mg sol-gel reaction systems reduced the amount of methyl oleate produced after 6 h (Table 5.3). Further, adding 1 g of Celite® R632 to the 200 mg sol-gel system caused no methyl oleate to be produced in 6 h. Therefore, any improved activity in the supported sol-gel appears to be due to the Celite® sol-gel complex rather than the adsorption of glycerol or water in the presence of silica.

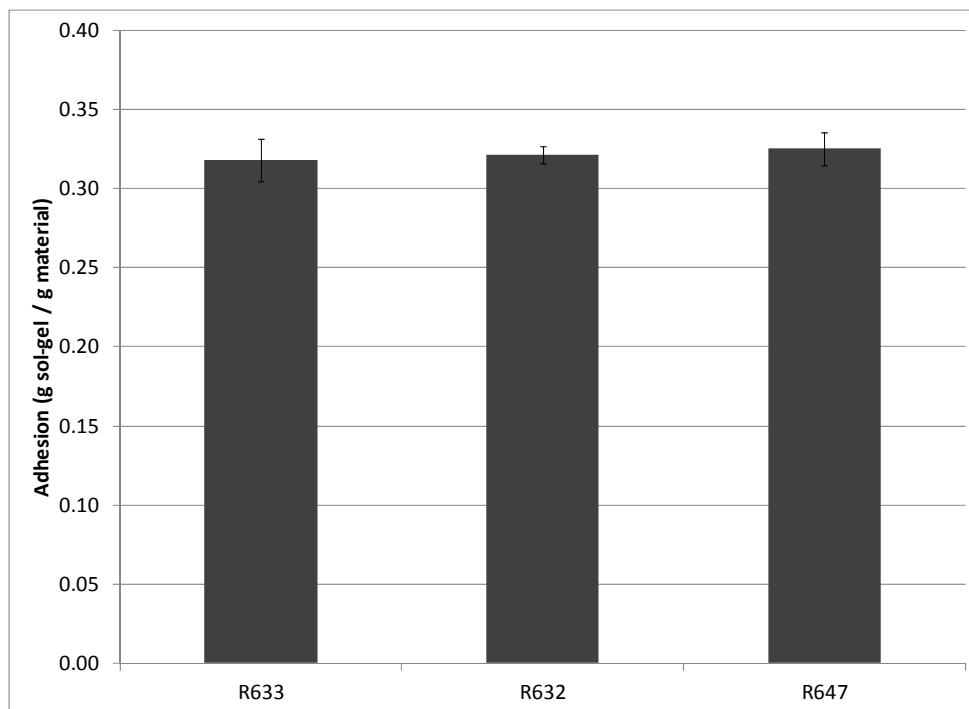


Figure 5.3: Adhesion of sol-gel on the support for each type of Celite® considered. The error bars represent the 95% confidence intervals of the sample mean based on n = 3.

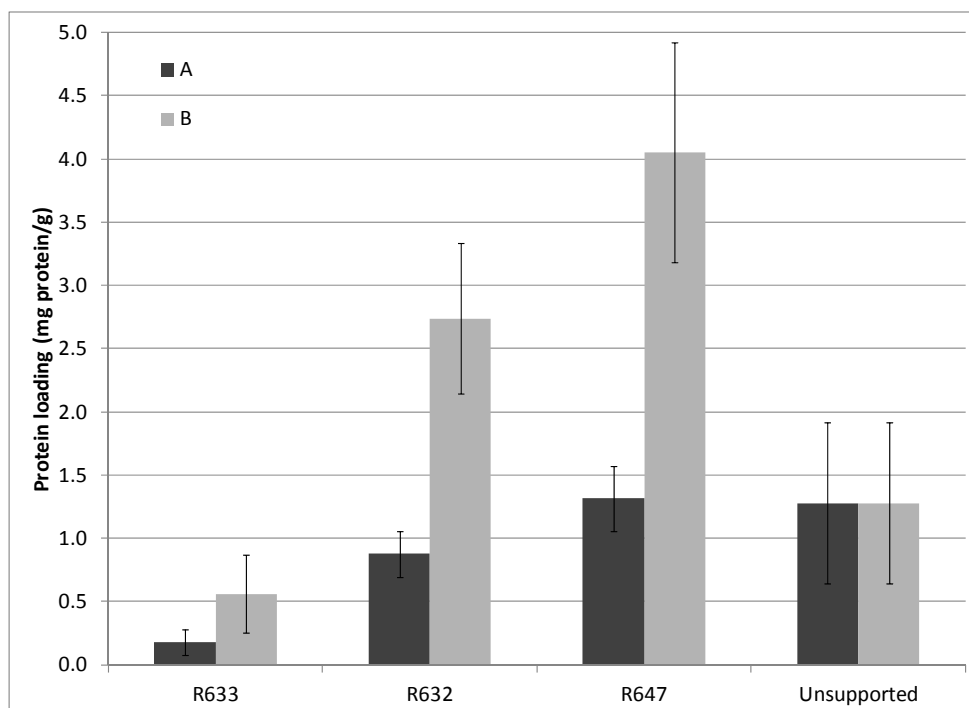


Figure 5.4: Loading of protein per gram for each support: A) the amount of protein per gram of material, and B) the amount of protein per gram of sol-gel. The error bars represent the 95% confidence interval of the sample mean based on n = 3.

Table 5.3: Effect of the presence of silica and Celite® on methyl oleate production with Novozym® 435 and unsupported sol-gel containing lipase.

| Enzyme | Silica | Effect on methyl oleate production |
|-----------------------------------|------------------|---|
| 50 mg Novozym 435 | 1 g silica gel | Reduction |
| 200 mg unsupported sol-gel | 1 g silica gel | Reduction |
| 200 mg unsupported sol-gel | 1 g Celite® R632 | Elimination |

Figure 5.5 shows the percent conversion of methanol to methyl oleate per gram of material based on a 6 h reaction period. R632, R647, and the unsupported sol-gels all show a higher conversion than R633. Since R633 has a lower protein loading than the other gels, a lower conversion per mass is expected. Figure 5.6 shows that Celite® R633 exhibits a high initial lipase activity; however, its low protein loading and low conversion make it a poor support material for transesterification.

Figure 5.6 shows that the initial lipase activity of the Celite® R647 is significantly lower than that of both R633 and R632. This would indicate that the R633 and R632 supports provide a favourable environment for the immobilization of active lipase in comparison to R647. The high percent surface coverage (Figure 5.2) on R632 while maintaining comparable sol-gel adhesion (Figure 5.3) indicates that thinner layers of sol-gel are formed on the surface of this support, therefore the high lipase activity for the R632 lipase sol-gel may be due to improved internal mass transfer.

5.4 Conclusions

Lipase immobilized sol-gels supported on diatomaceous earth are promising for biodiesel production. All three Celite® supports considered (R633, R632, and R647) as well as the unsupported sol-gel exhibited lipase activity and showed conversion ranges from approximately 25% to 65% in 6 h. Similar sol-gel adhesion levels were measured for each of the support materials. Based on the three support materials considered, Celite® R632 exhibited good initial activity and achieved an average conversion of approximately 60% per gram of material after 6 h of reaction. The high surface area coverage of the sol-gel on R632 indicates a thinner coating that would lead to improved internal mass transfer. Thus, comparing the three supports, Celite® R633, R632, and R647, and unsupported lipase sol-gel, Celite® R632 could be considered a promising support for lipase immobilized sol-gels to produce biodiesel via enzymatic transesterification.

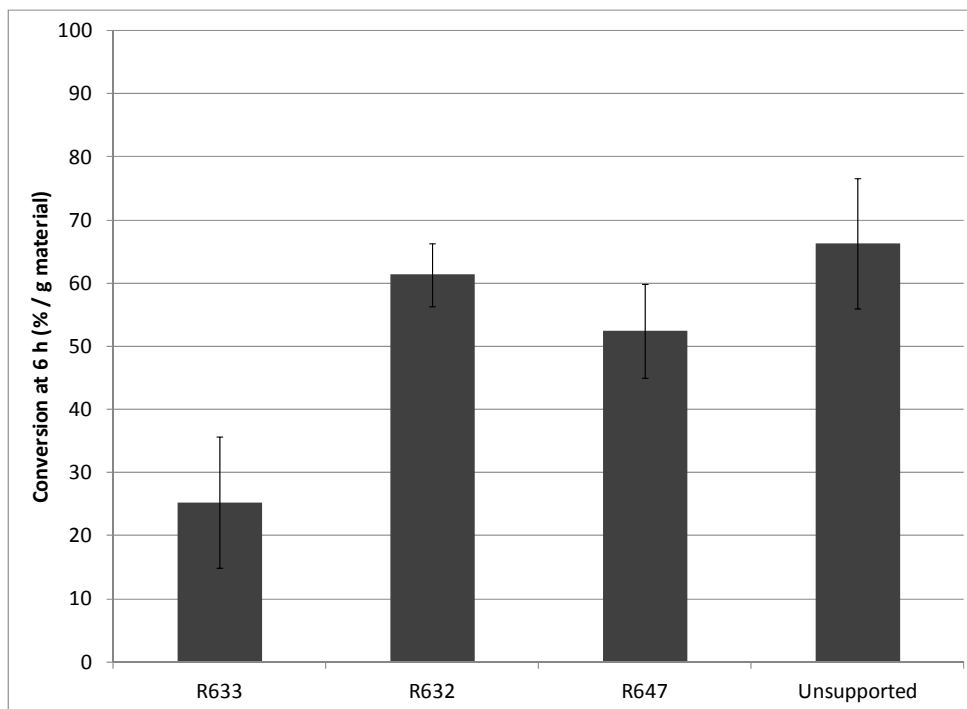


Figure 5.5: Percent methanol conversion per gram of material after 6 h for each sol-gel formulation. The error bars represent the 95% confidence interval of the sample mean based on n = 9.

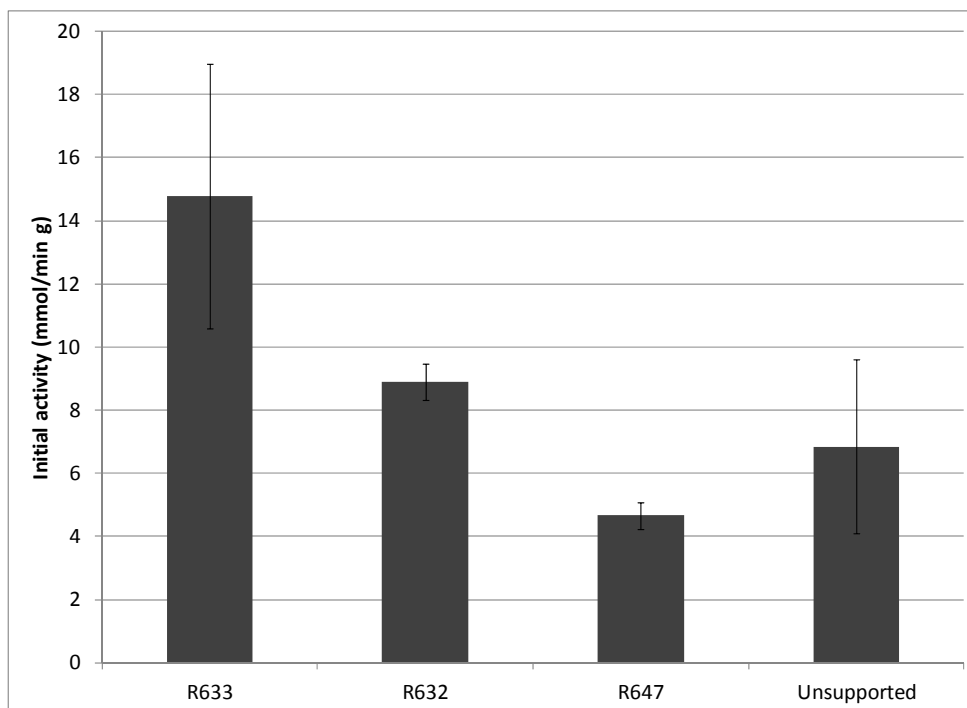


Figure 5.6: Initial lipase activity for each sol-gel formulation measured by the initial amount of methyl oleate produced per minute per gram of protein. The error bars represent the 95% confidence interval of the sample mean based on n = 9.

5.5 Acknowledgements

This work was supported by the Natural Sciences and Engineering Research Council (NSERC) in the form of a Discovery grant to RLL and an NSERC Postgraduate Scholarship to SMM. We thank Novozymes North America for supplying samples of the lipase formulation and World Minerals for supplying samples of the Celite® support materials.

Chapter 6

Evaluation of Diatomaceous Earth Supported Lipase Sol-gels as a Medium for Enzymatic Transesterification to Produce Biodiesel[‡]

Overview

Immobilized lipase has the potential to be the catalyst of choice for biodiesel production since it is efficient, effective, and environmentally friendly; however, the stability and activity of lipase must be addressed before enzymatic biodiesel production processes can be industrially accepted. This study investigates an enzyme immobilization procedure that immobilizes lipase in a sol-gel supported on diatomaceous earth (Celite[®] R632), and determines its potential for biodiesel production in terms of achievable conversion and apparent stability. Four immobilized materials (lipase sol-gels with and without Celite[®] at two protein loading levels) were compared in terms of their immobilized protein content, conversion of methanol to methyl oleate, lipase activity, long term stability, and glycerol-water adsorption. The Celite[®] R632 sol-gel with high protein loading achieved the maximum conversion in the 6 h reaction period (80%). A drying step was found to be advantageous prior to the reaction, and the absorption of glycerol-water on the Celite[®] was only found to be significant at high levels of glycerol. The material was found to be very stable upon storage at 4°C for up to 1.5 years, losing only about 15% of its percent conversion capacity per year. Based on this study, the supported immobilization technique shows significant potential as a novel catalyst for biodiesel production.

Keywords

enzyme immobilization, biodiesel, sol-gel, transesterification

[‡] This chapter is published in the Journal of Molecular Catalysis B: Enzymatic **Evaluation of Diatomaceous Earth Supported Lipase Sol-gels as a Medium for Enzymatic Transesterification of Biodiesel** S.M. Meunier and R.L. Legge, J. Mol. Catal. B: Enzym., vol. 77, pp. 92-97, 2012.

6.1 Introduction

Lipase is a triacylglycerol hydrolase and is responsible for the hydrolysis of ester bonds in triglycerides. At hydrophobic interfaces, lipases are known to undergo interfacial activation which causes a surge in enzymatic activity (Sarda and Desnuelle, 1958). Enzymatic reactions typically have many advantages such as enhanced specificity and efficiency; however, decreased activity and stability are common elements of concern when working with enzymes.

One way to extend the operational stability, and thus decrease the effective cost of the enzyme, is by immobilization. Although biodiesel production with alkali catalysts is known to be the least costly option, processes using immobilized lipase are significantly less costly than those using free lipase (Jegannathan *et al.*, 2011). Jegannathan *et al.* (2011) also show that if immobilized lipase is reused more than five times or the production cost of the lipase is reduced significantly, enzymatic biodiesel production could be competitive with the alkali biodiesel process.

Enzyme entrapment in polymers such as sol-gels provides a stable enzyme support with very strong bonds while not requiring complex chemical preparation (Reetz *et al.*, 1996). Both the thermal and chemical stability and activity of enzymes can be improved via sol-gel immobilization (Pirozzi *et al.*, 2009; Reetz, 1997; Reetz *et al.*, 1996). Further, ω -transaminases encapsulated via a supported immobilization procedure with Celite[®] sol-gels exhibit enhanced activity even at extreme conditions such as high pH and temperature, and can be recycled up to eight times without dramatically reducing the achievable conversion (Koszelewski *et al.*, 2010). Other studies comparing Celite[®] sol-gels show similar results using lipase as the enzyme of interest (Kawakami, 1996; Kawakami and Yoshida, 1996).

Due to environmental and economical concerns, biodiesel has become an invaluable alternative to standard diesel fuels (Robles-Medina *et al.*, 2009). Biodiesel is comprised of fatty acid alkyl esters and is produced via the transesterification of oils. Conventionally, biodiesel is produced using either an alkali or acid catalyst, but using lipase as the catalyst for transesterification could provide significant advantages over these traditional processes. Enzymatic processes self-adapt to changes in raw material quality, produce biodiesel in few processing steps, use little energy, produce little wastewater, and yield high quality by-products (Fjerbaek *et al.*, 2009). The challenges associated with enzymatic transesterification include low reaction rates, high enzyme cost, and the potential for enzyme deactivation (Ganesan *et al.*, 2009).

Since methanol, glycerol and water are all known to have inhibitive effects on lipase each of these components must be closely monitored in the biodiesel production process. Methanol is a substrate as well as a lipase inhibitor in the biodiesel production process; therefore, lower than stoichiometric ratios of methanol are commonly used for biodiesel production to avoid enzyme deactivation (Shimada *et al.*, 1999; Watanabe *et al.*, 2000; Watanabe *et al.*, 2001; Watanabe *et al.*, 2002; Xu *et al.*, 2004). Glycerol is a by-product of enzymatic biodiesel production that is inhibitory to the lipase, but glycerol produced during transesterification can be absorbed by silica beds (Samukawa *et al.*, 2000; Yori *et al.*, 2007; Mazzieri *et al.*, 2008). In terms of water absorption, according to the Celite® supplier, World Minerals, the water absorption capacity of Celite® is up to 500% by weight, depending on the type of Celite® considered. This is a crucial parameter since, although water is necessary for lipase activation in biodiesel production, excess water levels will inhibit the lipase by occupying the enzyme support pore space and limiting contact between the enzyme and substrates (Robles-Medina *et al.*, 2009).

This study considers the enzymatic activity of lipase immobilized in Celite® R632 sol-gels based on a supported immobilization scheme. A comparison is made between the achievable enzymatic conversion of methanol to methyl oleate for unsupported sol-gels and sol-gels supported on Celite® R632 at both high and low protein content levels. Further, the glycerol-water absorption is considered for both Celite® R632 and sol-gel Celite® R632 using thermogravimetric analysis in an attempt to elucidate the possible effects of glycerol and water in a biodiesel process for lipase immobilized in Celite® R632 sol-gels. This information is valuable in evaluating the potential of Celite® R632 sol-gels as a supported immobilization medium for enzymatic biodiesel production.

6.2 Experimental

6.2.1 Materials

Celite® samples were a gift from World Minerals (Santa Barbara, CA). Lipase (NS44035) was a gift from Novozymes North America Inc. (Franklinton, NC). The biological source of NS44035 cannot be disclosed by the supplier; the activity of NS44035 is 20 000 PLU/g. Tetramethyl orthosilicate (TMOS), trimethoxypropylsilane (PTMS), triolein, glycerol, methyl oleate and methyl heptadecanoate (HDA-ME) were obtained from Sigma-Aldrich Canada Ltd. (Oakville, ON). Acetonitrile was obtained from EMD Chemicals (Gibbstown, NJ). Sodium phosphate was obtained from Mallinckrodt Baker (Phillipsburg, NJ). Hexane and hydrochloric acid were obtained from Fisher Scientific Company (Ottawa, ON). Ultrapure

water was produced using a Milli-Q water purification system from Millipore (Billerica, MA). All other chemicals were obtained from local suppliers.

6.2.2 Methods

6.2.2.1 Immobilization of lipase

Four different lipase sol-gels were produced for analysis – with and without Celite® R632 as a support material and with high and low concentrations of lipase (Table 6.1).

To immobilize lipase in diatomaceous earth sol-gels, 0.08 mol PTMS and 0.02 mol TMOS were hydrolyzed in the presence of 1 mol ultrapure water and 200 μ L HCl (0.1 M). The mixture was sonicated for one hour to allow for complete hydrolyzation of the precursors. The precursor solution was then rotary evaporated in a heated water bath at 40°C for 30 min to remove excess water and alcohol. A solution of lipase and phosphate buffer (50 mM, pH 7.0) with an approximate protein concentration of 4 mg/mL was prepared, and 14 mL was added to the hydrolyzed precursor solution. For the high lipase concentration Celite® sol-gels, the lipase solution was used undiluted at a concentration of approximately 12 mg/mL. The resultant mixture was added to the support material with approximately 3 mL sol-gel mixture for every 2 g of Celite® R632. After thorough mixing, the sol-gel Celite was deposited in a Petri dish, sealed and aged at 4°C for 24 hours. The Celite® sol-gel was then dried uncovered at 4°C until the drying rate was less than 1 mg/h. Finally, the supported gel was removed from the Petri dish and washed twice with phosphate buffer (50 mM, pH 7.0, 5 mL buffer per gram of sol-gel for each wash) to remove any protein that was not completely immobilized within the gel. Excess solvent was evaporated from the gel at room temperature overnight prior to storing the gels in a sealed container at 4°C.

Unsupported gels were prepared in a similar manner except that the evaporated precursor and enzyme mixture was deposited directly into the Petri dish for aging and drying, the dried sol-gel was crushed in a mortar upon removal from the Petri dish, and the washing solutions were separated from the sol-gel by centrifugation.

Table 6.1: Description of the lipase preparations used for analysis in terms of the support material, sol-gel formulation, and lipase solution concentration.

| Lipase preparation | Support material | Sol-gel | Lipase solution |
|---------------------------|-------------------------|-------------------|------------------------|
| C-SG-4 | Celite® R632 | 80% PTMS/20% TMOS | 4 mg/mL |
| C-SG-12 | Celite® R632 | 80% PTMS/20% TMOS | 12 mg/mL |
| U-SG-4 | Unsupported | 80% PTMS/20% TMOS | 4 mg/mL |
| U-SG-12 | Unsupported | 80% PTMS/20% TMOS | 12 mg/mL |
| Free | Unsupported | No Sol-gel | 4 mg/mL |

6.2.2.2 Protein measurement

The total protein content of the gels was calculated using a mass balance of the protein content of the enzyme solution loaded to the sol-gels and content in the two buffer wash solutions. The degree of immobilization was calculated as the percentage of protein in the sol-gel compared to the amount of protein desired in the supported sol-gel. The amount of protein was quantified using a Varian HPLC system (Varian Inc., Mississauga, ON) equipped with an Agilent Zorbax Bio Series GF-250 column (Agilent Technologies, Mississauga, ON) and calibrated using a BCA protein assay kit (Pierce Biotechnology Inc., Rockford, IL). The mobile phase for the HPLC analysis was 200 mM phosphate buffer (pH 7.0) and detection was at a wavelength of 280 nm.

6.2.2.3 Enzymatic lipid transesterification

The enzymatic activity of the supported lipase sol-gels was determined by GC-MS analysis. The reactions were carried out at 40°C with agitation for 6 h. The reaction mixture consisted initially of approximately 1 g of the supported lipase sol-gel, 4 mmol of triolein and 4 mmol of methanol (total reaction volume 3.89 mL). Each hour, a 10 µL sample was removed from the reaction vial and diluted in 990 µL hexane with 100 µL of the internal standard, HDA-ME. The formation of methyl oleate, the reaction product, was followed using a Varian GC-MS system (CP-3800 gas chromatograph, Saturn 2000 mass spectrometer/mass spectrometer) equipped with a CP-Wax 52 CB fused silica column (CP8513, Varian Inc., Mississauga, ON). 1 µL samples of the diluted reaction mixture were injected into the GC at an injector temperature of 250°C and a split ratio of 50. Helium was used as the carrier gas with a column flow of 1 mL/min. The GC oven temperature was initially set to 170°C for 10 min, ramped at 10°C/min to 250°C, and held at 250°C for 2 min.

The enzymatic activity of the dried sol-gel formulations was carried out in the same manner as the original gels with the exception that prior to the enzymatic assay the gels were dried overnight in a 60°C oven. At this point, no further change in mass was observed from the drying process and thus any remaining water was assumed to be completely removed from the sol-gel formulation.

Using the GC-MS method described, a calibration was completed based on a methyl oleate standard (40 mM – 800 mM) and used as the basis for all methyl oleate concentrations provided. From the GC-MS chromatograms, methyl oleate was the only visible peak indicating that no side reactions occurred. The enzymatic activity of the lipase was determined from the slope of the methyl oleate concentration-time profile over the weight of immobilized enzyme material used.

6.2.2.4 Desorption of glycerol and water

The desorption of glycerol and water from Celite® R632 upon equilibration was measured using a thermogravimetric analyzer (Q500 TGA, TA Instruments, New Castle, DE). Prior to analysis, each sample was immersed in the desired solution containing glycerol and water at various concentrations (0%, 10%, 25%, 50%, 75% and 100% by volume glycerol) and equilibrated for 24 hours. The sample was then washed with water to remove excess glycerol and air dried overnight. The TGA analysis method ramped the temperature from 30°C to 400°C at 10°C/min followed by air cooling for 10 min under 50 mL/min N₂ gas. The onset of desorption (temperature at which 0.025% mass loss is achieved), the peak desorption rate (maximum mass loss rate achieved), the peak temperature (temperature at the peak desorption rate), and the total mass loss (percent mass lost at the end of the analysis) were determined from the weight loss curve and the derivative weight loss curve.

6.3 Results and discussion

6.3.1 Physical properties

Comparing the protein content and the degree of immobilization of the four different lipase sol-gels formed, several phenomena were observed (Figure 6.1). First, for both the low and high protein level sol-gels, the unsupported sol-gels have higher protein contents in comparison to the Celite® supported sol-gels. Since there is additional material added to the Celite® sol-gels, lower protein content per gram is expected for these gels.

The protein level immobilized in the sol-gel was not proportional to target load for the sol-gel during the formation procedure (Figure 6.1). For the Celite® sol-gels the protein content was approximately double when triple the lipase was loaded, but for the unsupported sol-gels the protein content was approximately triple as expected. One possible explanation for the lack of proportionality for the Celite® sol-gels is that the excess of lipase in the triple unsupported formulation caused protein aggregation and subsequent immobilization. This effect might not be as pronounced for the lower levels of lipase

because there is not enough lipase in the formulation and for the triple lipase Celite® system because the presence of Celite® reduces the apparent protein concentration.

The observed degree of protein immobilization for the Celite® sol-gels is comparable to that for the unsupported sol-gels (Figure 6.1). When the amount of lipase is tripled, the degree of immobilization decreases slightly for both the Celite® and unsupported sol-gels. Since there is excess lipase in the triple lipase sol-gels, there is more opportunity for lipase that is incompletely entrapped to be easily removed during the washing steps.

The high protein content unsupported sol-gel (U-SG-12) did exhibit much more variability than the other immobilization regimes (Figure 6.1). This is likely caused by the potential for aggregation, incomplete immobilization and lipase deactivation during the sol-gel formation procedure. With such high levels of protein and without the Celite® support material, the lipase is much more exposed and thus more sensitive to environmental changes. This enhanced potential for enzyme deactivation and poor immobilization can conceivably greatly reduce the reproducibility of the lipase sol-gel immobilization procedure.

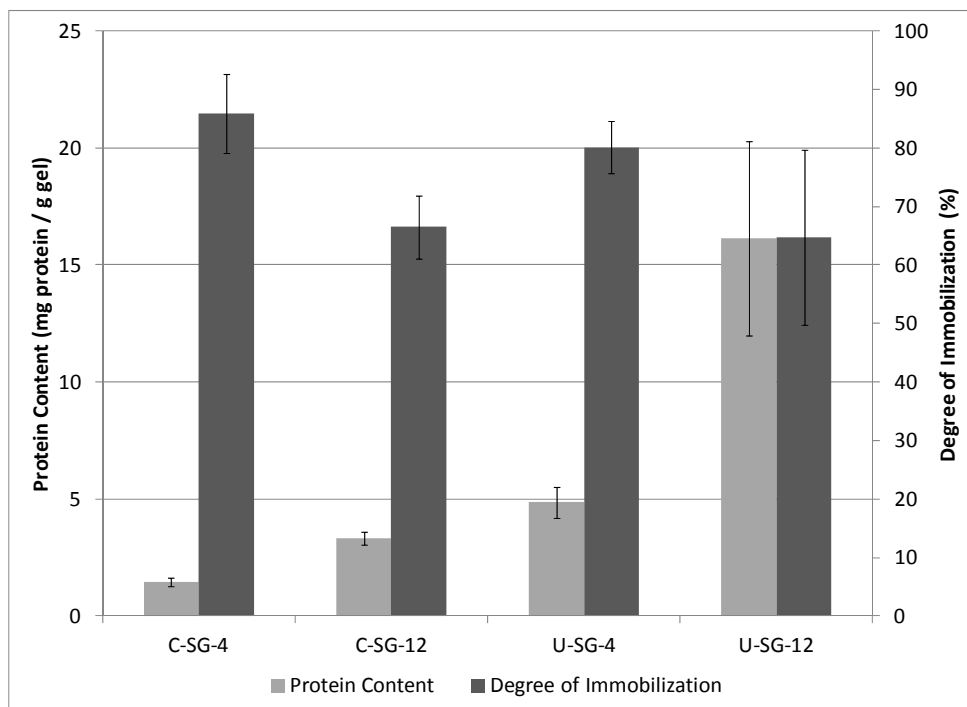


Figure 6.1: Protein content and degree of protein immobilization for four sol-gel formulations. Error bars represent a 95% confidence interval.

6.3.2 Enzymatic properties

Free lipase at a comparable level to that found in the immobilized lipase preparation C-SG-4 was assayed to determine a base methyl oleate conversion level for comparison to the immobilized preparations. Based on GC-MS analysis, no measurable methyl oleate was detected during the 6 h reaction.

Based on the percent conversion after 6 h for methyl oleate production (Figure 6.2), the Celite® R632 sol-gels exhibited an increased conversion when the amount of lipase loaded onto the gels was tripled. In addition, the Celite® supported sol-gels achieved slightly more conversion when dried due to an excess of water absorbed on the support material since Celite® is absorbent and lipase is inhibited by excess water content.

The unsupported sol-gels demonstrate the opposite trend – the sol-gel preparation with triple lipase achieved a lower percent conversion than the regular lipase loading and the dried gel preparations have lower conversion than those that are not dried. As discussed with regards to the protein content of the gels, this formulation does have much more variability than the other formulations which could be caused by aggregation, incomplete immobilization, and deactivation of the protein due to the excess quantities of protein. Since there is no Celite® present in the unsupported sol-gels to remove the water, drying the enzyme preparation may result in inactivation of the lipase rather than removing the excess water and thereby causing the reduction in product concentration.

In comparison to the Celite® supported sol-gel, adding neat Celite® to the unsupported sol-gel (SG + Celite®) greatly reduces the percent conversion likely due to reactant, product and water absorption by the Celite® thereby preventing the reaction from progressing. Comparing the supported and unsupported sol-gel formulations, the addition of the Celite® as a support material for the sol-gel increases the percent conversion to methyl oleate for both sol-gel formulations.

Comparing the activity of the different sol-gel preparations on a mass basis (Figure 6.3) reveals that the dried unsupported and supported sol-gels all have comparable activities. This demonstrates the beneficial effects of using Celite® and providing a support since the Celite® sol-gels contain much less enzyme per gram of material in comparison to the unsupported sol-gels (Figure 6.1). The unsupported sol-gel preparation with the higher level of lipase (U-SG-12) does have a slightly lower activity in comparison with the other materials when dried which is likely due to the excess lipase in the preparation which is either inactive and/or inaccessible to the substrates.

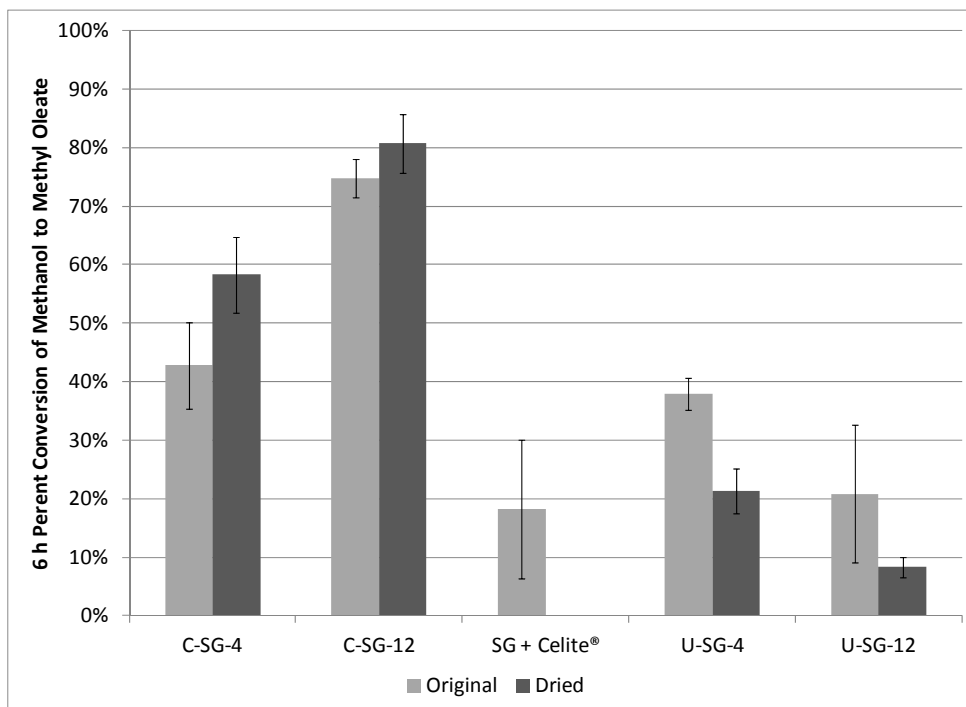


Figure 6.2: Percent conversion of methanol to methyl oleate based on a 6 h batch reaction for each sol-gel formulation without and with a drying step prior to the enzymatic assay. Error bars represent a 95% confidence interval.

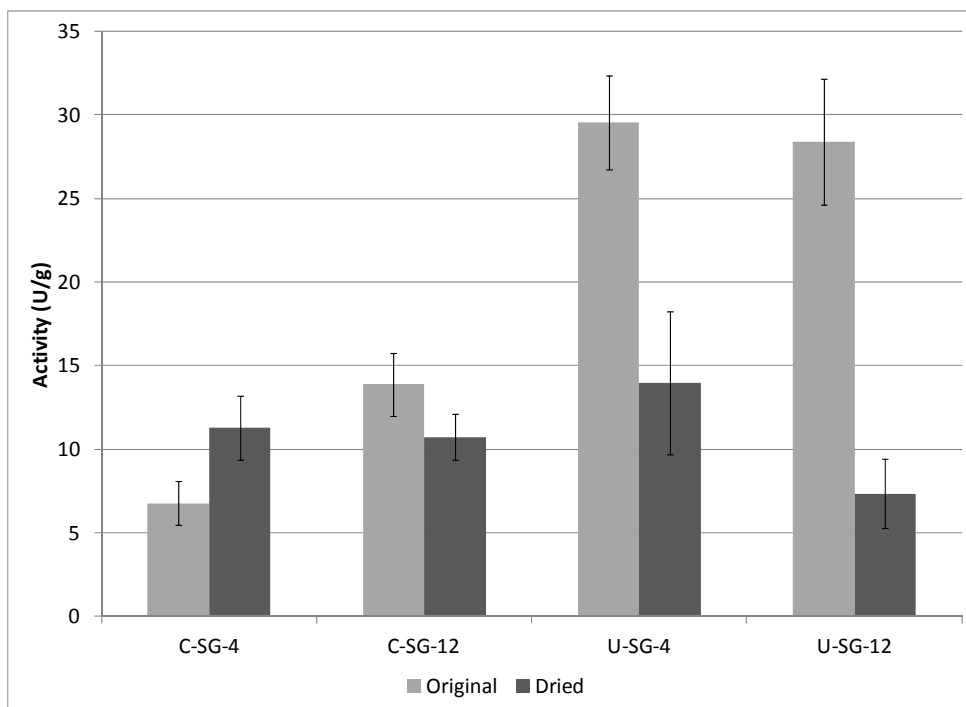


Figure 6.3: The enzymatic activity on a per gram of material basis for each sol-gel formulation as determined from the conversion of methyl oleate and the protein content of the gels. Both the sol-gel formations without and with a drying step prior to the reaction were considered. Errors bars represent a 95% confidence interval.

The unsupported sol-gels have a much higher activity than the Celite® sol-gels when assayed without a drying step. The adsorptive properties of the Celite® and the inhibition of lipase caused by excess water are the expected causes of this phenomenon. Despite the increased lipase content (Figure 6.1) in the high concentration lipase unsupported sol-gel (U-SG-12), the activity is comparable to the regular lipase level unsupported sol-gel (U-SG-4). Therefore, the excess lipase in this system may not be accessible to the substrates or has been rendered inactive.

The Celite® supported sol-gels and the unsupported sol-gels were also compared based on their stability over a period of approximately 1.5 years (Figure 6.4). The unsupported and Celite® supported sol-gel formulations show almost identical trends with a very gradual decrease in product output over time. The unsupported sol-gel (U-SG-4) has a 0.05% decrease in product concentration per day while the Celite® supported sol-gel (C-SG-4) has a 0.04% decrease per day. This is about an 18% (U-SG-4) and 15% (C-SG-4) decrease in product concentration per year. This indicates that a very stable enzyme formulation has been developed with a long shelf life when stored at 4°C.

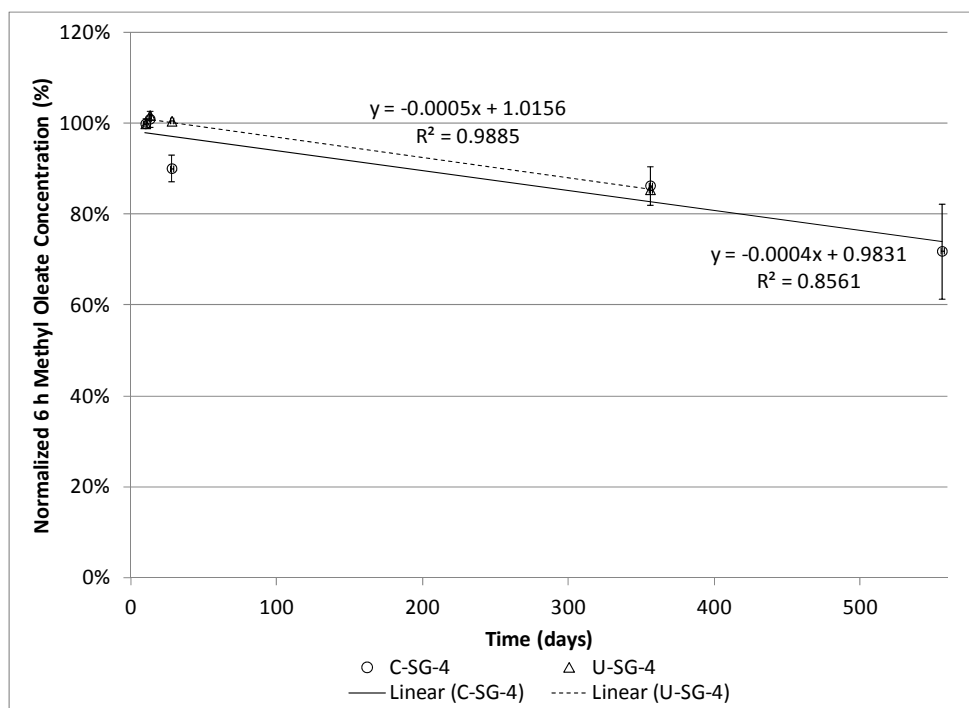


Figure 6.4: Average percent conversion of methanol to methyl oleate for sol-gels after storage at 4°C for unsupported (Δ) and Celite® R632 supported sol-gels (o). The lines represent the lines of best fit for the unsupported sol-gel (broken) and the Celite® R632 supported sol-gel (solid). Error bars represent a 95% confidence interval.

6.3.3 Adsorptive properties

A TGA spectrum (Figure 6.5) shows typical weight-time and derivative weight-time profiles for a sample of Celite® R632 sol-gel (C-SG-4). The peak desorption and total mass loss parameters are indicated on the graph. These profiles are used to determine the onset of desorption, peak desorption rate, peak temperature, and total mass loss.

Based on the weight change with respect to temperature data obtained from the TGA analysis, the temperature at which desorption was established for each case (10%, 25%, 50%, 75%, and 100% glycerol for both neat Celite® and the Celite® sol-gel C-SG-4, data not shown) was compared. The average onset of desorption for all cases was $113.3 \pm 1.2^\circ\text{C}$. This indicates that the observed desorption is caused by a combination of the water and the glycerol rather than the components separately.

The peak desorption rate obtained from the TGA analysis is a measure of the level of adhesion of solvent to the Celite® or Celite® sol-gel with respect to the cohesion of solvent molecules to each other. High peak desorption rates indicate that the solvent coheres more strongly to itself and low peak desorption rates signify that the solvent molecules adhere very well to the support material. The total mass loss indicates the absorptive capacity of the Celite® or Celite® sol-gel with respect to the applicable glycerol-water solution. At the end of the TGA analysis, any glycerol-water absorbed and retained by the material is desorbed and thus quantified by the total mass loss.

Considering both the peak desorption rate (Figure 6.6) and the total mass loss (Figure 6.7) when neat Celite® and Celite® sol-gels are incubated in glycerol-water solutions similar trends are evident. Both the peak desorption rates and the total mass loss are higher in each case for the neat Celite® than for the Celite® sol-gel. It is likely that the sol-gel provides a protective barrier that reduces absorption of the glycerol-water solution.

Additionally, the amount of solution absorbed does generally increase with increasing percentage of glycerol in the equilibrating solution. One notable exception is the decrease for the neat Celite® from 75% glycerol to 100% glycerol. This shows that the water is necessary for absorption of glycerol onto the Celite®. However, this is not the case for the Celite® sol-gel. The increasing adsorption trend of the supported sol-gel material is not affected by eliminating the water from the equilibrating solution.

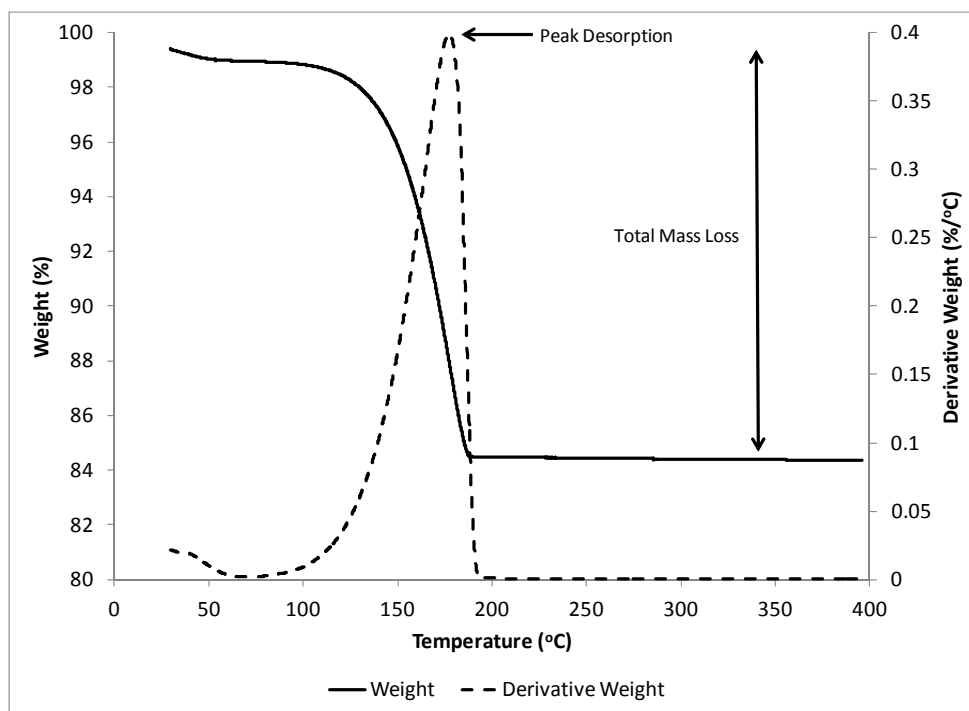


Figure 6.5: Typical TGA profile including the sample weight (solid) and the derivative weight (broken). The peak desorption point and the total mass loss are indicated on the graph. The sample shown is Celite® R632 sol-gel (C-SG-4) at 50% glycerol equilibrating solution.

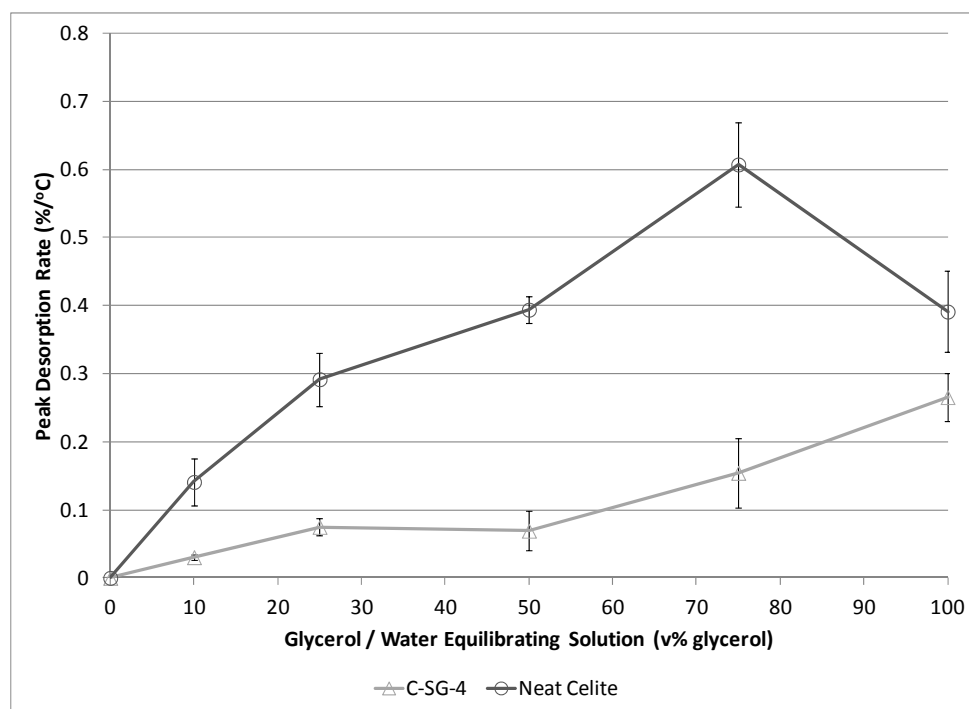


Figure 6.6: Peak desorption rates for Celite® R632 sol-gels (Δ) and plain Celite® R632 (o) based on different levels of glycerol in the equilibrating solution. Error bars represent a 95% confidence interval.

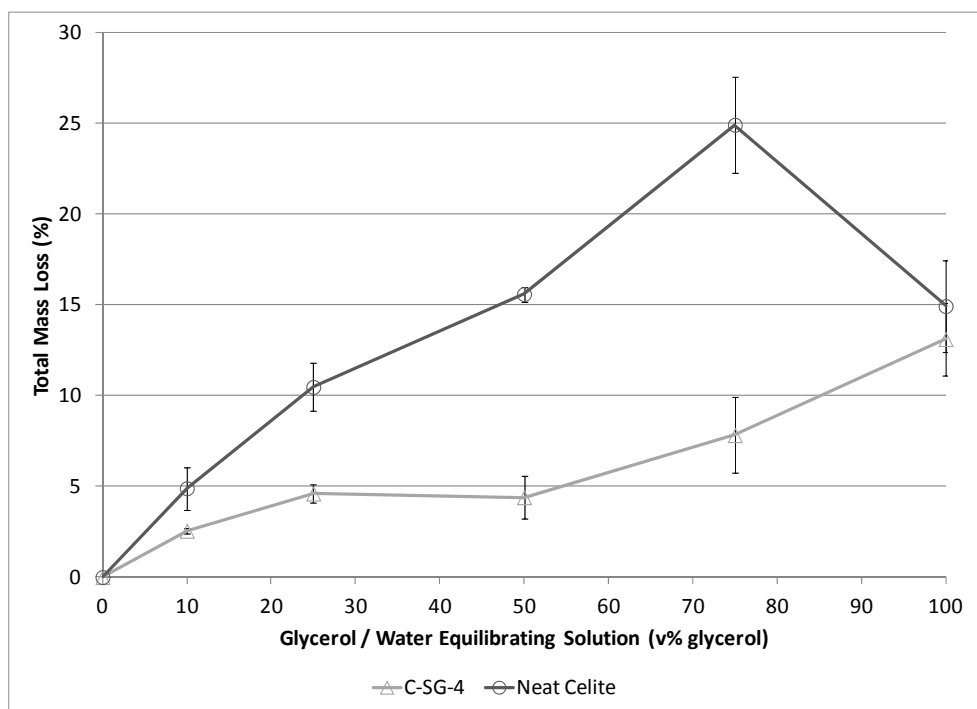


Figure 6.7: Total percentage mass loss for Celite® R632 sol-gels (Δ) and plain Celite® R632 (o) based on different levels of glycerol in the equilibrating solution. Error bars represent a 95% confidence interval.

When the equilibrating solution consisted solely of water, there was no evidence of desorption from the neat Celite® or sol-gel Celite® (Figures 6.6 and 6.7). This is evidence that the water is not readily retained by the Celite® material despite its absorptive properties.

The peak desorption temperature as determined by the TGA is a measure of the strength of cohesion of the glycerol-water solution to the Celite® or Celite® sol-gel material. The peak desorption temperatures for each solution were different (Figure 6.8), ranging from 132°C to 187°C, and showed similar trends to those observed for the peak desorption rate (Figure 6.6) and the total mass loss (Figure 6.7). One phenomena observed is the similarity between the values for the 100% glycerol solution absorption when comparing the regular Celite® and the sol-gel supported Celite® (Figure 6.8), indicating that the difference caused by the sol-gel is most prominent when water is present in the equilibrating solution. According to Clifford and Legge (2005), both contact angle measurements and TGA indicate that PTMS-TMOS sol-gels are hydrophobic and that increasing the proportion of PTMS increases the hydrophobicity of the sol-gels. Therefore, the hydrophobicity of the sol-gel appears to have a stronger effect when pure water is used as the equilibrating solution rather than when glycerol-water solutions are used.

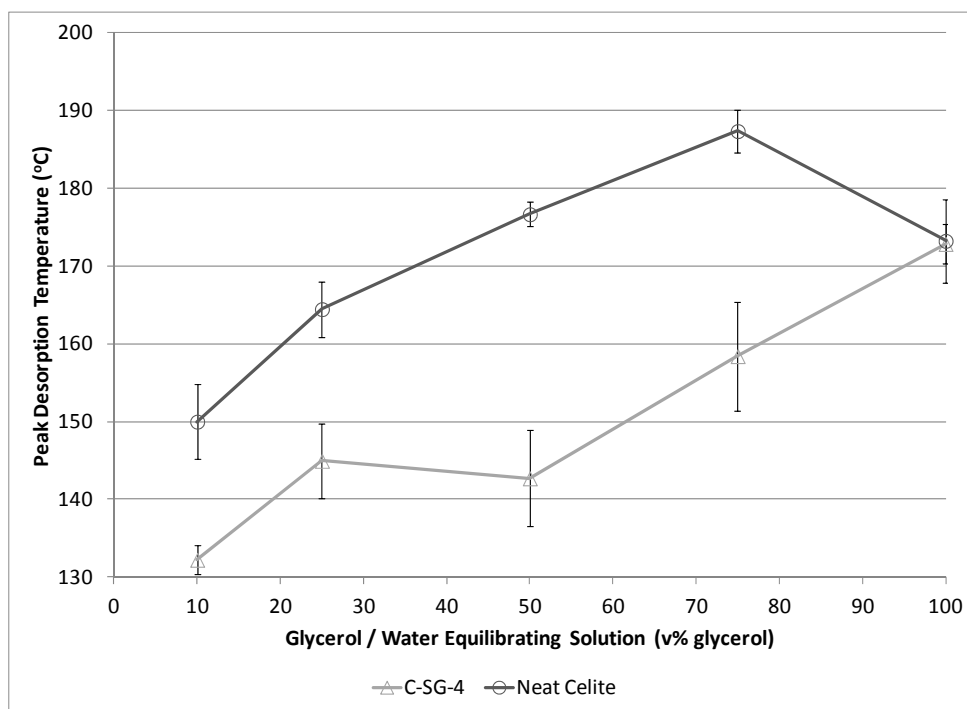


Figure 6.8: Peak desorption temperatures for Celite® R632 (Δ) sol-gels and plain Celite® R632 (o) based on different levels of glycerol in the equilibrating solution. Error bars represent a 95% confidence interval.

These phenomena are important in a biodiesel production processes since glycerol is a by-product of the reaction. The highly absorptive properties of the Celite® sol-gel will inhibit the lipase and prevent the reaction from proceeding. Care must be taken to ensure that glycerol is removed when the reaction is run on a continuous basis. However, at low levels of glycerol (i.e. 10% by volume), very little glycerol is absorbed in the Celite® sol-gel material (approximately 2.5% by mass), so this phenomena becomes more of a concern as the concentration of glycerol increases.

6.4 Conclusions

A procedure to immobilize lipase in sol-gels supported on Celite® R632 was developed and shown to be valuable for the transesterification of triolein to produce methyl oleate. Three main properties were considered for comparison: protein loading, enzymatic activity, and glycerol-water adsorption, for four different sol-gel preparations: unsupported sol-gel low protein level (U-SG-4), Celite® sol-gel low protein level (C-SG-4), unsupported sol-gel high protein level (U-SG-12), and Celite® sol-gel high protein level (C-SG-12).

Based on the amount of protein retained with respect to that loaded onto the sol-gel, the immobilization procedure is more effective (i.e. incomplete protein immobilization is minimized) at the low protein levels. The water absorbed by the Celite® during sol-gel preparation must be removed as it inhibits the lipase – the maximum production of methyl oleate (80% in 6 h) was achieved with the high protein content Celite® sol-gel (C-SG-12) after a pre-drying step. Over a 1.5 yr time frame, both the unsupported and Celite® supported sol-gels exhibited high stability when stored at 4°C. The sol-gel was found to provide a protective barrier that inhibits the absorption of the glycerol-water solution. Therefore, the removal of glycerol is key in preventing the inhibition of the lipase, but is only a concern at very high levels of glycerol (approximately 75% glycerol by volume).

Based on this study, a Celite® supported sol-gel immobilized lipase was developed that achieves high production of methyl oleate in a short reaction time. Although the immobilization procedure is straightforward, some subtleties of the new material exist including a desirable pre-drying step to remove water absorbed during immobilization, and the potential for glycerol-water absorption when high quantities of glycerol are present. In addition to the high conversion, the immobilization regime is highly stable over 1.5 years without sophisticated storage requirements.

6.5 Acknowledgements

This work was supported by the Natural Sciences and Engineering Research Council (NSERC) in the form of a Postgraduate Scholarship to SMM and a Discovery Grant to RLL. We thank Novozymes North America for supplying samples of the lipase formulation and World Minerals for supplying samples of the Celite® support materials.

Chapter 7

Kinetic Modelling of the Production of Methyl Oleate by Celite® Supported Lipase Sol-gels

Overview

This study illustrates the benefits of Celite® supported lipase sol-gels for the transesterification of triolein to produce methyl oleate. Different methanol concentrations and temperatures were tested to identify any effects due to methanol or temperature. A ping-pong bi-bi kinetic model was developed and validated taking into account the inhibition effects of methanol and glycerol as well as the temperature effect on the enzyme. Although initial reaction rate kinetic models are useful for predicting the kinetics when no products are present in the reaction medium, a complete kinetic model beyond the initial conditions that considers glycerol inhibition is important. The model developed was consistent with the experimental data ($R^2=0.95$) showing an increase in methyl oleate production capacity with increasing methanol concentration up to an optimal range of 1.3 M to 2.0 M depending on the temperature. Increasing the temperature increased the initial reaction rate, but no thermal inactivation of the enzyme was observed over the temperature range examined. Based on the kinetic constants obtained, the maximum velocity of the reverse reaction is about 25% slower than that of the forward reaction and glycerol inhibition has a more significant effect on the reaction kinetics than methanol inhibition. The model that was developed is of fundamental importance for understanding the effects of methanol and glycerol inhibition as well as the effect of temperature on the production of methyl oleate using lipase-mediated enzymatic transesterification.

Keywords

enzyme immobilization, biodiesel, sol-gel, transesterification, kinetic modelling, Celite®

7.1 Introduction

Biodiesel is a clean burning fuel that consists of a mixture of fatty acid alkyl esters and can be produced via the transesterification of triglycerides. Biodiesel is typically produced using an alkaline or acid catalyst – chemical catalysts produce very high yields, but there are issues with high energy consumption, significant downstream processing, the necessity for wastewater treatment, and low selectivity leading to undesirable side reactions (Al-Zuhair, 2005; Bajaj *et al.*, 2010; Fukuda *et al.*, 2001; Shah *et al.*, 2004; Soumanou and Bornscheuer, 2003). Alternatively, lipase can be used to catalyze transesterification reactions without the associated drawbacks of chemical catalysts. Enzymes do, however, have their own shortcomings – high cost, potential for deactivation, and low reaction rates (Akoh *et al.*, 2007; Fukuda *et al.*, 2001; Ganesan *et al.*, 2009; Marchetti *et al.*, 2007; Robles-Medina *et al.*, 2009; Vasudevan and Briggs, 2008).

Economically, it is essential to immobilize lipase for reuse if an enzymatic transesterification process is to be competitive with the alkaline process (Al-Zuhair, 2007; Jegannathan *et al.*, 2011). Immobilized enzymes, specifically those immobilized in sol-gels, are known to have increased activity, selectivity, and stability as well as being more easily separated and reused (Aucoin *et al.*, 2004; Pirozzi *et al.*, 2009; Reetz *et al.*, 1996; Reetz, 1997). Combined with the challenges of chemical catalysis, these benefits make immobilized enzymes especially appealing for fatty acid alkyl ester production.

In an attempt to further improve enzymatic activity and stability, reduce any complications caused by mass transfer limitations, and facilitate separation of the enzyme from the reaction media for reuse, there has been a significant amount of research on immobilizing sol-gels on a variety of inorganic support materials. Immobilizing lipase sol-gels on diatomaceous earth supports has proven to produce a very stable and active biocatalyst for the enzymatic production of fatty acid methyl esters (Meunier and Legge, 2010; Meunier and Legge, 2012).

Enzymatic transesterification is complicated by the potential for lipase inactivation by the alcohol substrate, glycerol product, and temperature. The required stoichiometric ratio of triglyceride to alcohol is 1:3; however, the alcohol concentration is typically limited by lipase inhibition. In several studies, a methanol concentration less than the stoichiometric amount was necessary to prevent adverse effects of alcohol inhibition during transesterification (Shimada *et al.*, 1999; Watanabe *et al.*, 2000; Watanabe *et al.*, 2001; Watanabe *et al.*, 2002; Xu *et al.*, 2004).

When glycerol inhibition affects the enzymatic production of fatty acid methyl esters, the removal of glycerol from the reaction media via dialysis (Bélafi-Bakó *et al.*, 2002), silica bed adsorption (Mazzieri *et al.*, 2008; Samukawa *et al.*, 2000; Yori *et al.*, 2007), or gravitational settling (Chen *et al.*, 2009; Hama *et al.*, 2011a; Hama *et al.*, 2011b) has been explored.

Enzymatic transesterification is advantageous due to low temperature requirements and lower operating costs associated with the decreased energy requirements. However, working with enzymes that are very sensitive to temperature can add undesirable constraints to the operating conditions. Immobilization of lipase in sol-gels has been shown to reduce the temperature and alcohol sensitivity of the enzyme (Hsu *et al.*, 2001a; Hsu *et al.*, 2001b; Reetz *et al.*, 1996; Reetz, 1997). Immobilized enzymes show improved thermal stability in comparison to free enzymes, but there is still the limitation that although higher temperatures increase the enzymatic activity they also cause thermal deactivation of the enzyme (Balcão *et al.*, 1996).

Ping-pong bi-bi mechanisms have been widely used for the kinetic modelling of biodiesel production via enzymatic transesterification (Al-Zuhair, 2005; Al-Zuhair *et al.*, 2007; Al-Zuhair *et al.*, 2009; Cheirsilp *et al.*, 2008; Dossat *et al.*, 2002; Xu *et al.*, 2005). Comprehensive kinetic equations for enzyme-catalyzed reactions, including ping-pong bi-bi mechanisms with competitive inhibition by both substrates and products, have been developed and are widely used as a starting point for enzymatic kinetic studies (Cleland, 1963a; Cleland, 1963b; Cleland, 1963c). Kinetic studies of enzymatic biodiesel production are often based on the initial rate version of the ping-pong bi-bi kinetic equation, and, therefore, only account for substrate inhibition since glycerol is not present in the system initially (Al-Zuhair, 2005; Al-Zuhair *et al.*, 2007; Al-Zuhair *et al.*, 2009; Dossat *et al.*, 2002; Xu *et al.*, 2005). Equation 7.1 is often used for initial reaction rate studies based on the reaction $T + A \leftrightarrow G + M$ where T is the triglyceride, A is the alcohol, G is the glycerol, and M is the methyl oleate:

$$v_i = \frac{V_{maxF}[T][A]}{[T][A] + K_{mA}[T] + K_{mT}[A](1 + [A]/K_{IA})} \quad (7.1)$$

where: v_i is the initial reaction rate, V_{maxF} is the maximum initial reaction velocity, $[A]$ and $[T]$ are the alcohol and triglyceride concentrations respectively, K_{mA} and K_{mT} are the apparent Michaelis constants for the alcohol and triglyceride respectively, and K_{IA} is the alcohol inhibition constant.

The objective of this study was to model the kinetics of the transesterification of triolein and methanol for the production of methyl oleate and glycerol using Celite® supported lipase sol-gels. A series of

experiments were completed with various temperatures and methanol concentrations to determine the effect of these parameters. The initial rate kinetic equation was originally considered, but a more comprehensive model was subsequently developed and validated which includes the effect of glycerol inhibition. The kinetic study presented provides a fundamental understanding the effects of glycerol and methanol inhibition on the enzyme as well as the benefits of Celite® supported sol-gels containing immobilized lipase.

7.2 Experimental

7.2.1 Materials

Novozym® 435 was a gift from Novozymes North America Inc. (Franklinton, NC) containing lipase from *Candida antarctica* with a reported activity of 10 000 PLU/g. Lipase PS “Amano” SD (Amano Enzyme USA Co., Elgin, IL) with a activity of 25 800 U/g from *Burkholderia cepacia* was immobilized in sol-gels composed of 80% trimethoxypropylsilane and 20% tetramethyl orthosilicate (Sigma-Aldrich Canada Ltd, Oakville, ON). The lipase sol-gel was supported on Celite® R632 from World Minerals (Santa Barbara, CA). Ultrapure water was from a Milli-Q water purification system from Millipore (Billerica, MA). All other chemicals used were reagent grade.

7.2.2 Methods

7.2.2.1 Immobilization of lipase

Celite® R632 supported lipase sol-gels were produced as previously reported (Meunier and Legge, 2010). Trimethoxypropylsilane (14 mL) and tetramethyl orthosilicate (2.95 mL) were combined with ultrapure water (17.4 mL) and 0.1 M HCl (200 µL) and sonicated for 1 h to allow hydrolysis of the precursors. The solution was rotary evaporated at 40°C for 30 min to remove any water or alcohol. 6.5 g of Lipase PS “Amano” SD was dissolved in 18 mL of 50 mM phosphate buffer at pH = 7.0, and 14 mL was added to the rotary evaporated precursor solution. The lipase sol-gel solution was added to the support material in a ratio of 1.5 g mixture/g Celite® R632 and mixed thoroughly. The mixture was then deposited into a Petri dish and sealed for 24 h at 4°C. Finally, the Celite® sol-gel was dried uncovered at 4°C until the drying rate slowed to less than 1 mg/hr. After the Celite® sol-gels were dried, the supported sol-gel was washed with 50 mM pH=7.0 phosphate buffer twice (5 mL buffer/g sol-gel per wash) to remove any free protein. The resulting gels were dried overnight at room temperature and then stored in a sealed container at 4°C until use.

Unsupported lipase sol-gels were prepared in a similar fashion but without the support and sol-gel mixing step. The resulting sol-gel was crushed with a mortar and pestle and the wash solutions separated from the sol-gel by centrifugation at 1250 xg for 10 min.

7.2.2.2 Total protein quantification

The total protein content of the supported sol-gels was determined using a BCA protein assay kit (Pierce Biotechnology Inc., Rockford, IL) using a microplate method with a bovine serum albumin (BSA) standard from 25-2000 µg/mL. The absorbance was measured at 562 nm using a BioTek Synergy 4 Microplate Reader (BioTek US, Winooski, VT). Samples of the stock enzyme solution were compared with samples from the wash solutions and a mass balance performed to determine the amount of protein remaining in the sol-gel.

7.2.2.3 Enzymatic transesterification

To determine the enzymatic transesterification capacities of the supported sol-gels, Celite® sol-gel (1 g), triolein (6.5 mmol), and methanol (4 mmol unless otherwise stated) were combined in a reaction vial and agitated at a controlled temperature for 6 h as previously described (Meunier and Legge, 2010). Ten µL samples were taken every hour from the reaction vial and diluted with 990 µL hexane and 100 µL internal standard (heptadecanoic acid methyl ester). The diluted samples were analyzed for methyl oleate content using a GC-MS (CP-3800 gas chromatograph, Saturn 2000 mass spectrometer/mass spectrometer, Varian Inc., Mississauga, ON) equipped with a CP-Wax 52 CB fused silica column (CP8513, Varian Inc., Mississauga, ON). The injector was set at 250°C with a split ratio of 50; the oven was held at 170°C for 10 min, ramped from 170°C to 250°C at 10°C/min and held at 250°C for 2 min; helium was the carrier gas at a flow rate of 1 mL/min; and the injection volume was 1 µL.

Only the methyl oleate concentration could be measured directly using this GC-MS method, so the concentrations of the other components (alcohol, triolein, and glycerol) were determined using a mass balance based on the reaction stoichiometry. No other components were observed in the GC-MS chromatograms.

7.2.2.4 Kinetic modelling

MATLAB® software (Version 7) from Mathworks, Natick, Massachusetts was employed for parameter estimation. The fitting coefficients were taken as positive values and optimized using built-in Matlab functions for non-linear least squares fitting with the Trust-region algorithm. The ordinary differential equation (ODE) of methyl oleate concentration was solved using a built-in Matlab function, ode45,

which is based on an explicit fourth order Runge-Kutta formula. The relative error tolerance and absolute error tolerance were set at 10^{-4} and 10^{-6} , respectively.

The 5 kinetic constants for the initial rate equation (section 7.3.2) were obtained using the initial reaction rate data from all 13 reaction conditions to ensure a good model fit. To consider the entire 6 h reaction (section 7.3.3), 5 additional kinetic constants were necessary to be used in combination with the 5 constants from the initial rate equation (total of 10 kinetic constants). To obtain the 5 additional kinetic constants, one experimental condition was used ($T = 40^{\circ}\text{C}$ and $[A]^{\circ} = 0.6 \text{ M}$). The remaining 12 reaction conditions ($T = 40, 50, \text{ and } 60^{\circ}\text{C}$ and $[A]^{\circ} = 0.3, 0.6, 0.9 \text{ and } 1.8 \text{ M}$) were used to verify the fit of the kinetic model and to test the model flexibility beyond the primary reaction conditions. The model developed was validated using 83 data points at different temperatures, alcohol concentrations, and times.

7.3 Results and discussion

7.3.1 Comparison of lipase immobilization schemes

Comparing the performance of Novozym[®] 435 (N435), free lipase (Free), unsupported lipase sol-gels (US), and Celite[®] supported lipase sol-gels (CSG) at 40°C and a molar ratio of methanol to triolein of 1.5:1, CSG had the highest conversion after 6 h, initial reaction rate and initial activity compared to N435, US and Free (Table 7.1). Celite[®] supported lipase sol-gels have enhanced transesterification abilities giving them a unique advantage over both unsupported lipase sol-gels, free lipase, and the commercially immobilized Novozym[®] 435.

Table 7.1: Comparison of Novozym[®] 435 (N435), free lipase (Free), unsupported sol-gel (US), and Celite[®] supported sol-gel (CSG) in terms of their final percent conversion, initial reaction rate, and initial activity at 40°C and methanol to triolein molar ratio of 1.5:1. *For N435, the initial activity is based on the weight of N435 rather than the weight of lipase since the amount of lipase in the enzyme preparation is unknown.

| Sample | Final conversion (%) | Initial reaction rate ($\mu\text{M}/\text{min}$) | Initial activity ($\mu\text{mol}/\text{min g-lipase}$) |
|--------|----------------------|--|--|
| N435 | 8.2 | 333 | 43* |
| Free | 3.5 | 257 | 398 |
| US | 38.2 | 1105 | 5712 |
| CSG | 62.2 | 3740 | 9750 |

7.3.2 Kinetic model – initial reaction rate

To evaluate the validity of the initial reaction rate model at different temperatures and methanol ratios, Equation 7.1 was adapted to include a temperature dependent exponential term (T in degrees K) as shown in Equation 7.2 where K_a is the temperature constant.

$$v_i = \frac{V_{maxF}[T][A]}{[T][A] + K_{mA}[T] + K_{mT}[A](1 + [A]/K_{IA})} e^{K_a T} \quad (7.2)$$

This kinetic model demonstrates good agreement between the initial experimental data collected and the model predictions using the kinetic constants in Table 7.2 (Figure 7.1). Both the model and experimental data show an increase in the initial rate with increasing temperature and methanol concentration up to approximately 1 M at which point the alcohol inhibition resulted in a decrease in the initial reaction rate.

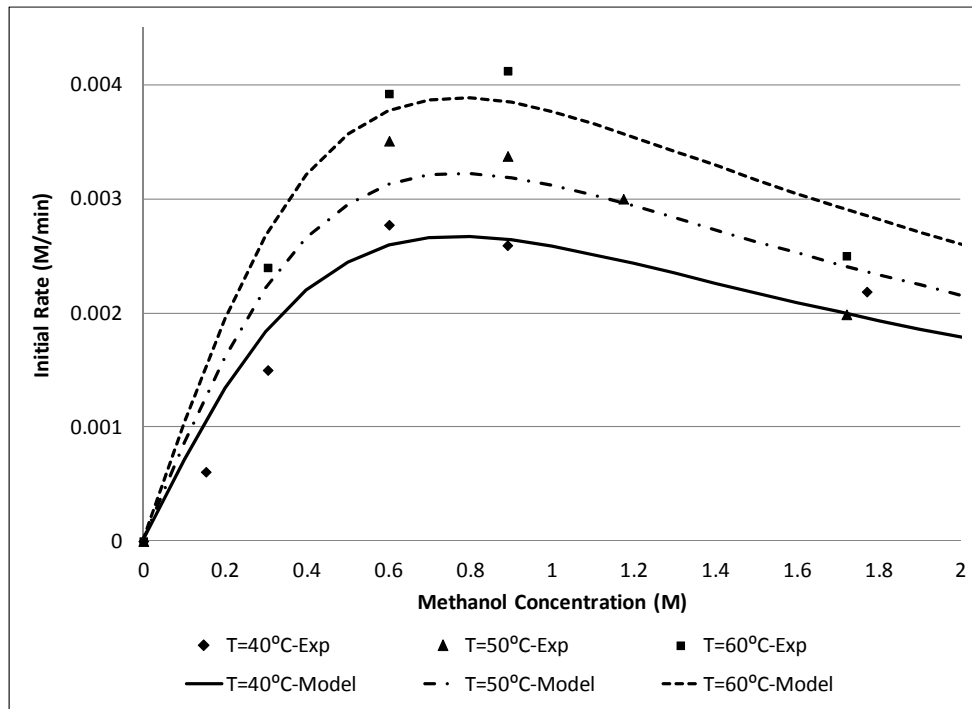


Figure 7.1: Initial reaction rate as a function of methanol concentration at three temperatures (40°C, 50°C, and 60°C). The lines represent the predictions from the model provided by Equation 7.2 and the symbols represent the experimental data.

Table 7.2: Kinetic parameter estimation for the models presented in Equations 7.2 and 7.3.

| Coefficient | Equation 7.2 | Equation 7.3 |
|------------------------|-------------------|-------------------|
| V_{maxR} (mol/L min) | - | 0.8236 |
| V_{maxF} (mol/L min) | 1.136 | 1.136 |
| K_{eq} | - | 0.3709 |
| K_{mA} (mol/L) | 5.5×10^4 | 5.5×10^4 |
| K_{mT} (mol/L) | 1.2×10^4 | 1.2×10^4 |
| K_{mG} (mol/L) | - | 0.7362 |
| K_{mM} (mol/L) | - | 0.6133 |
| K_{IA} (mol/L) | 0.137 | 0.137 |
| K_{IG} (mol/L) | - | 0.0394 |
| K_a | 0.0188 | 0.0188 |

Although Equation 7.2 agrees with the experimental data for the initial reaction rate, significant over-prediction for every data point at the 6 h methyl oleate concentration was found (Figure 7.2 inset). This indicates that the glycerol inhibition is an important consideration for kinetic modelling of the entire concentration profile (Bélafi-Bakó *et al.*, 2002; Dossat *et al.*, 1999; Hong *et al.*, 2011; Watanabe *et al.*, 2000).

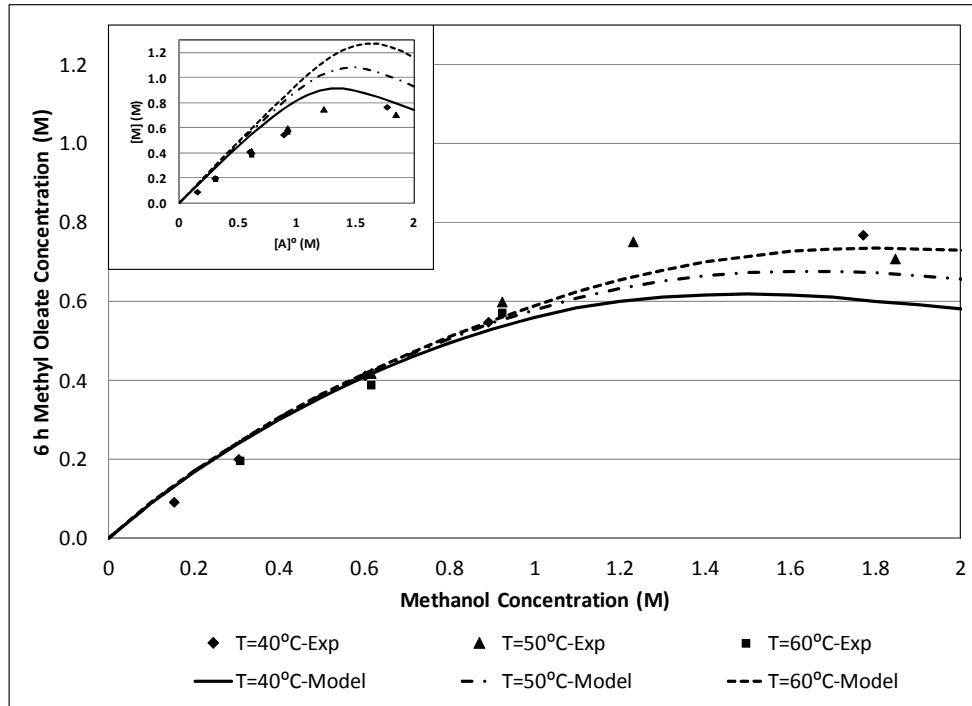


Figure 7.2: Methyl oleate concentration at 6 h with respect to the initial methanol concentration at three temperatures (40°C, 50°C, and 60°C). The lines represent the model predictions and the symbols represent the experimental data. The main plot represents the results from Equation 7.3 while the inset plot (upper left) represents the results from Equation 7.2.

7.3.3 Kinetic model – time-dependent reaction rate

A more comprehensive model (Equation 7.3) was developed by modifying the classic ping-pong bi-bi kinetic model to include only the competitive inhibition terms for the alcohol substrate and the glycerol product (Rizzi *et al.*, 1992).

$$v = \frac{V_{maxR}V_{maxF} \left([T][A] - \frac{[G][M]}{K_{eq}} \right)}{V_{maxR}R + V_{maxF}F} e^{K_a T} \quad (7.3)$$

with:

$$R = [T][A] + K_{mA}[T] + K_{mT}[A] \left(1 + \frac{[A]}{K_{IA}} \right) + \frac{K_{mT}}{K_{IG}} [G][A]$$

$$F = \frac{K_{mG}}{K_{eq}} [M] + \frac{K_{mM}}{K_{eq}} [G] \left(1 + \frac{[G]}{K_{IG}} \right) + \frac{1}{K_{eq}} [G][M]$$

where: v is the reaction rate; V_{maxR} and V_{maxF} and the maximum velocities of the reverse and forward reactions, respectively; $[A]$, $[T]$, $[M]$, and $[G]$ are the concentrations of alcohol, triolein, methyl oleate and glycerol, respectively; K_{eq} is the equilibrium constant; K_{mA} , K_{mT} , K_{mM} , and K_{mG} are the Michaelis constants for alcohol, triolein, methyl oleate and glycerol, respectively; K_{IA} and K_{IG} are the constants for dissociation of the inhibitor from the enzyme-inhibitor complex for alcohol and glycerol, respectively; and K_a is the temperature constant.

The performance of each model was validated based on the final methyl oleate concentration demonstrating the improvement in prediction when glycerol inhibition is considered (Table 7.3 and Figure 7.2). Considering only the final observed methyl oleate concentration, Equation 7.2 provides a very poor fit with a $R^2=0.201$ while Equation 7.3 provides a good fit with a $R^2=0.910$.

7.3.4 Methyl oleate concentration profile

Using only one data set for model fitting ($T = 40^\circ\text{C}$ and $[A]^\circ = 0.6 \text{ M}$) and the remaining data to validate the model, the prediction of the entire methyl oleate concentration profile based on methanol and glycerol inhibition kinetics (Equation 7.3) demonstrates good agreement with the experimental values (Figure 7.3). This model provides an excellent fit for the entire set of experimental results (the fitting parameters presented in Table 7.3 consider only the final concentration), with the accuracy of the model determined as follows: $\text{SSE} = 0.20$, $R^2=0.95$, and $\text{RMSE}=0.049$.

Table 7.3: Comparison of the performance of the two proposed models (Equations 7.2 and 7.3) in terms of their SSE, R^2 , and RMSE for the 6 h methyl oleate concentration.

| Model (Equation) | Sum of squared errors (SSE) | Coefficient of determination (R^2) | Root mean squared error (RMSE) |
|--------------------------------|-----------------------------|--|--------------------------------|
| Initial Rate (7.2) | 0.447 | 0.201 | 0.193 |
| With Glycerol Inhibition (7.3) | 0.050 | 0.910 | 0.064 |

The kinetic parameters used to fit the model (Table 7.2, Equation 7.3) indicate that the maximum velocity of the reverse reaction is approximately 25% slower than that of the forward reaction and glycerol inhibition has a much stronger effect on the reaction rate than methanol inhibition since higher inhibition constants correspond to less of an inhibition effect as they are present in the denominator of the kinetic model. These kinetic constants demonstrate the importance of glycerol inhibition and the reverse reaction when considering the kinetics of enzymatic transesterification. In immobilized enzyme reactors, glycerol is known to adsorb onto the enzymatic support and cause an activity decrease by creating a hydrophilic layer around the enzyme that prevents the hydrophobic substrate (triolein) from accessing the enzyme (Bélafi-Bakó *et al.*, 2002; Dossat *et al.*, 1999; Hong *et al.*, 2011; Watanabe *et al.*, 2000).

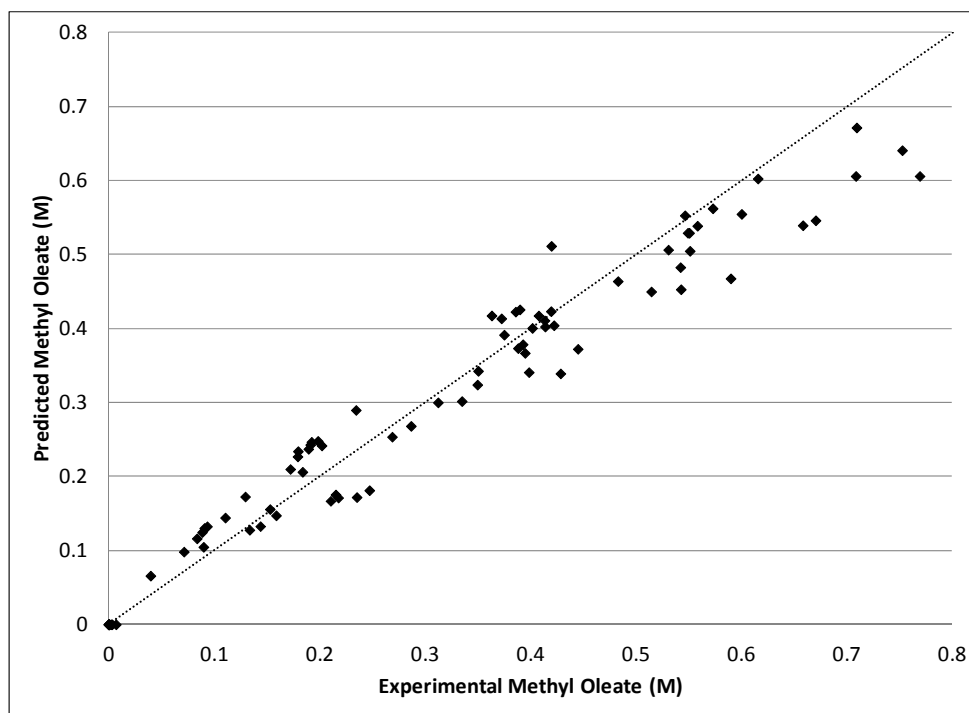


Figure 7.3: Correlation between the predicted and experimental methyl oleate concentration values using the kinetic model described by Equation 7.3.

Comparing the concentration profiles at 3 temperatures (40°C, 50°C, and 60°C) and 4 methanol concentrations (0.3 M, 0.6 M, 0.9 M, and 1.8 M), very good agreement between the model predictions and the experimental data are observed (Figure 7.4). The model does over-predict the methyl oleate concentrations at the low methanol concentration (0.3 M), which is likely due to a mass transfer inhibition caused by the relatively small amount of methanol present in the reaction medium and the insolubility of methanol in triolein since this is a solvent-free system (Ognjanovic *et al.*, 2009). At every temperature considered, the concentration of methyl oleate produced during the reaction increased with increasing initial methanol concentration indicating that at these levels methanol inhibition does not have a detrimental effect on the performance of the enzyme at concentrations up to 1 M (approximately 1:1 molar ratio of methanol:triolein). When the methanol concentration is increased beyond 1 M no further increase in methyl oleate concentration was observed, demonstrating the commencement of methanol inhibition. This is in agreement with the literature where methanol inhibition is documented indicating that less than stoichiometric amounts of methanol are necessary to prevent inhibition and that a 1:1 molar ratio of triolein:methanol is optimal (Lee *et al.*, 2011; Shimada *et al.*, 2002; Xu *et al.*, 2004).

At a high methanol concentration (1.8 M, Figure 7.4d), there is a minimal effect of temperature between 40°C and 50°C which is expected since the optimal temperature for lipase is within this temperature range. These results indicate that the Celite® supported lipase sol-gels are quite temperature and methanol resistant over the range of temperatures and concentrations considered (Figure 7.4). Other studies examining the optimal temperature range of immobilized lipase for the production of biodiesel indicate a lower temperature optimum of 30-40°C with commercially immobilized enzymes (Köse *et al.*, 2002; Salis *et al.*, 2005) compared to sol-gel immobilized lipases which have reported optima between 40 and 70°C (Hsu *et al.*, 2003; Hsu *et al.*, 2004; Moreira *et al.*, 2007). In a recent study, Chesterfield *et al.* (2012) found that thermal denaturation of Novozym® 435 began at 47°C.

Considering the initial reaction rate data (Figure 7.1) and the final methyl oleate concentration (Figure 7.2), it is evident that increasing the temperature increases the initial reaction rate, but has a minimal effect on the final methyl oleate concentration. This indicates that the increased performance from the temperature effect causes the final product concentration to be attained more quickly, but does not cause the final product concentration to increase. It is argued that the inhibitory effect of glycerol supersedes the temperature effect seen initially.

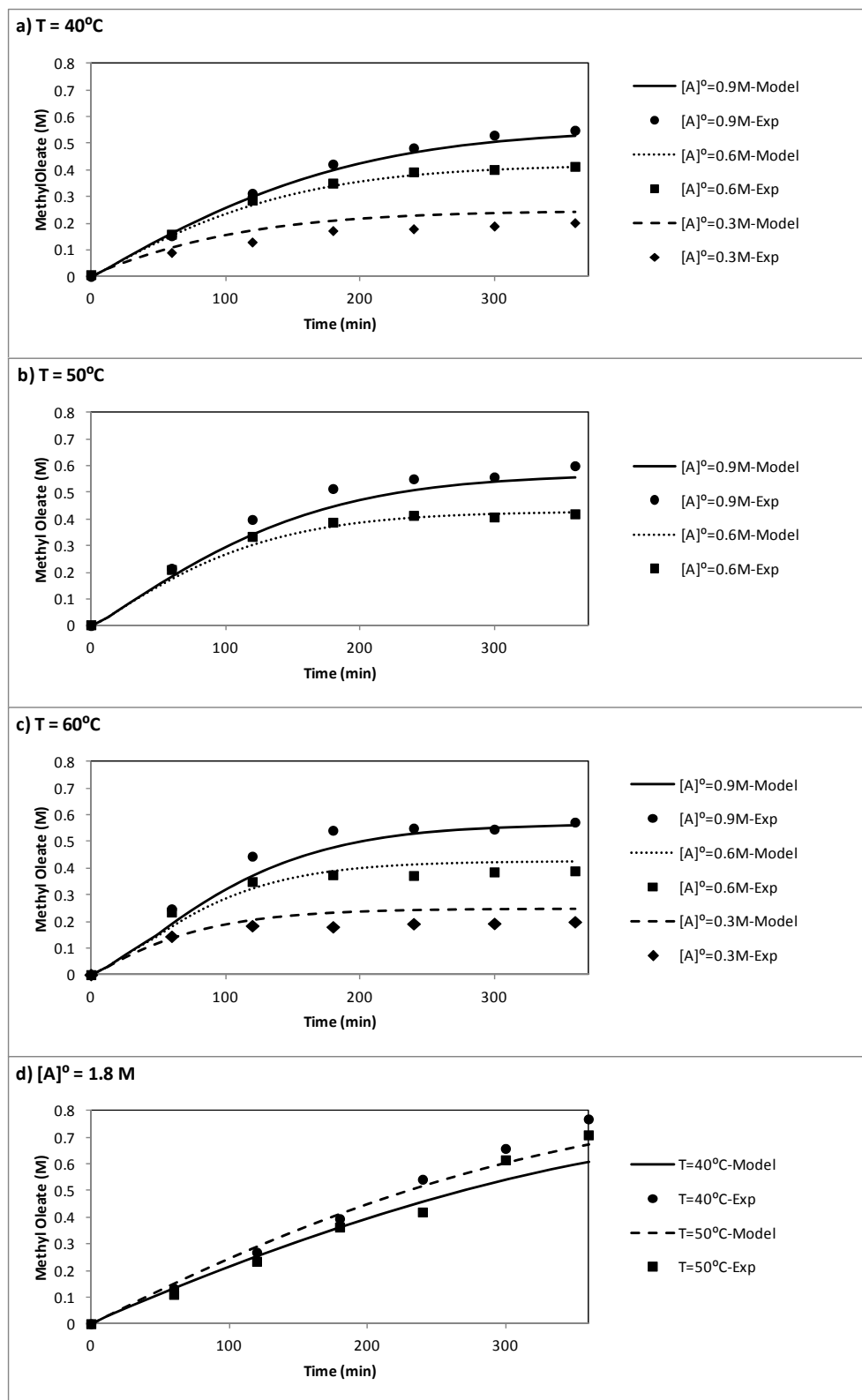


Figure 7.4: Comparison of model predictions (lines) and experimental data (symbols) for four methanol concentrations (0.3 M, 0.6 M, 0.9 M, and 1.8 M) and three temperatures (40°C, 50°C, and 60°C). Plot a) T = 40°C, b) T = 50°C, c) T = 60°C, d) [A]⁰=1.8 M.

7.3.5 Kinetic model predictions for transesterification

Based on the kinetic model, the conditions were extended beyond those tested experimentally to assess the potential of the model developed (Figure 7.5). This model predicts an optimal methanol concentration range of approximately 1.3 M to 2.0 M which is in agreement with experiments that show that increasing the methanol to triolein molar ratio from 1.8 to 3 decreases the 6 h methyl oleate concentration by about 60% (data not presented). From the model predictions, increasing the temperature from 30°C from 70°C shifted the optimal methanol concentration from 1.3 M to 2.0 M indicating that there is a positive interaction between temperature and methanol (Figure 7.5). The optimal alcohol concentration increased linearly with temperature at a rate of 0.017 M/K. Additionally, at higher temperatures the impact of increasing the methyl oleate concentration was more profound than at lower temperatures demonstrating that at higher temperatures higher methyl oleate concentrations can be achieved, but small changes in the initial methanol concentration have a more intense effect on the final product concentration. Since diffusivity in liquids is known to increase with increasing temperature, the mass transfer of glycerol away from the enzyme will improve at higher temperatures resulting in an increase in the reaction rate (Treybal, 1980).

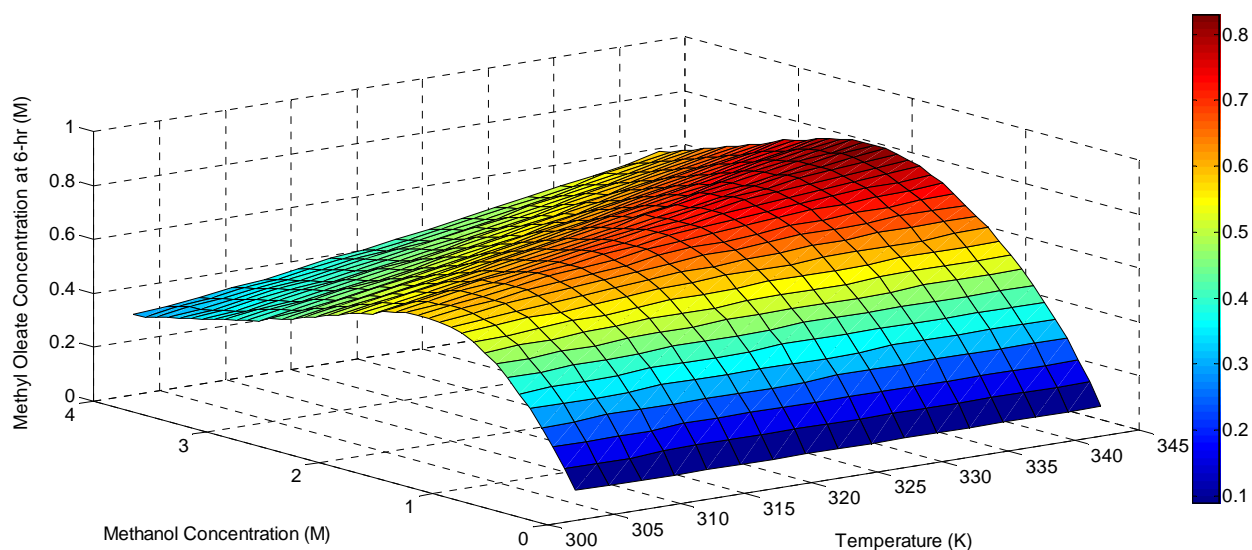


Figure 7.5: Surface plot of the kinetic model (Equation 7.3) predictions for the methyl oleate concentration after 6 h at different initial methanol concentrations (0-4 M) and temperatures (30-70°C).

7.4 Conclusions

Celite® supported lipase sol-gels have superior enzymatic performance over unsupported lipase sol-gels, free lipase, and Novozym® 435. The typical kinetic model for predicting enzymatic transesterification performance was shown to be useful only when considering the initial conditions of the reaction. However, as the reaction progresses, the presence of glycerol in the reaction medium becomes more important and it is essential for a kinetic model to take into account the enzymatic inhibition caused by this product. A kinetic model based on a ping-pong bi-bi mechanism was developed that takes into account both methanol and glycerol inhibition effects on the production of methyl oleate via enzymatic transesterification using Celite® supported lipase sol-gels. The model developed shows excellent agreement with the experimental data at varying temperatures and initial methanol concentrations ($R^2=0.95$). Based on the kinetic parameters, glycerol has a stronger inhibition effect than methanol and the maximum velocity of the reverse reaction is approximately 25% slower than that of the forward reaction. The experimental data show that increasing the concentration of methanol in the reaction medium increases the production of methyl oleate indicating that although methanol is inhibitory, it is not enough to decrease the achievable product concentration within the range of concentrations studied. There is also a positive temperature effect on the enzyme that increases the initial reaction rate, but not the final methyl oleate concentration achieved. The results from the model indicate that there is an optimal methanol concentration range of 1.3 M to 2.0 M that increases with increasing temperature, but no temperature deactivation of the enzyme was observed.

7.5 Acknowledgements

This work was supported by the Natural Sciences and Engineering Research Council (NSERC) in the form of a Postgraduate Scholarship to SMM and a Discovery Grant to RLL. We thank Amano Enzyme USA for supplying samples of the lipase formulation and World Minerals for supplying samples of the Celite® support materials.

7.6 Nomenclature

Acronyms

CSG Celite® supported lipase sol-gel

| | |
|-------|------------------------------|
| Free | Free lipase |
| N435 | Novozym® 435 |
| R^2 | Coefficient of determination |
| RMSE | Root mean squared error |
| SSE | Sum of squared errors |
| US | Unsupported lipase sol-gel |

Parameters

| | |
|----------|---|
| $[A]$ | Alcohol concentration (M) |
| $[G]$ | Glycerol concentration (M) |
| $[M]$ | Methyl oleate concentration (M) |
| $[T]$ | Triglyceride concentration (M) |
| K_a | Temperature constant (dimensionless) |
| K_{eq} | Equilibrium constant (dimensionless) |
| K_{IA} | Alcohol inhibition constant (M) |
| K_{IG} | Glycerol inhibition constant (M) |
| K_{mA} | Apparent Michaelis constant for alcohol (M) |
| K_{mG} | Apparent Michaelis constant for glycerol (M) |
| K_{mM} | Apparent Michaelis constant for methyl oleate (M) |
| K_{mT} | Apparent Michaelis constant for triglyceride (M) |
| T | Temperature (K) |
| v | Reaction velocity (M/min) |
| v_i | Initial reaction velocity (M/min) |

V_{maxF} Maximum velocity of the forward reaction (M/min)

V_{maxR} Maximum velocity of the reverse reaction (M/min)

Chapter 8

Kinetic and Mass Transfer Modelling of Methyl Oleate Production in an Immobilized Lipase Packed Bed Reactor

Overview

This study investigates a Celite® supported sol-gel immobilized lipase packed bed reactor along with the development of a kinetics and mass transfer model for the production of methyl oleate. To determine the reaction kinetics, an initial rate equation accounting for alcohol inhibition was used for both the Celite® supported lipase sol-gel and Novozym® 435. It was found that the Celite® supported sol-gel had a high maximum reaction velocity and was less inhibited by methanol in comparison to Novozym® 435, supporting the practical potential of Celite® supported sol-gels for use in enzyme-based reactors for the production of biodiesel. To describe the continuous packed bed reactor performance, an efficiency correlation was developed to account for the effect of the flow rate and glycerol concentration on the enzymatic activity. These reaction kinetics, mass transfer, and efficiency equations were used to describe the effect of flow rate in the packed bed reactor; the model developed was in good agreement with the experimental data. Increasing the flow rate was found to increase the reactor performance presumably by aiding in the removal of a glycerol layer around the biocatalyst. Additionally, a maximum achievable methyl oleate concentration was observed due to presence of glycerol. Comparing the Celite® sol-gel packed bed reactor performance to that of the Novozym® 435, a higher product conversion was achievable using the Celite® sol-gel in a shorter period of time indicating the superior performance of the supported sol-gel for enzymatic transesterification. The Celite® sol-gel did not exhibit any activity loss over a five day time span supporting the potential for this catalyst in a packed bed reactor for transesterification.

Keywords

Packed bed reactor, lipase immobilization, transesterification, sol-gel, biodiesel, Celite®

8.1 Introduction

The industrial production of biodiesel (fatty acid alkyl esters) from triglycerides is catalyzed chemically by an acidic or alkaline process. The use of these chemical catalysts is complicated by the requirement of higher than ambient operating temperatures (55-80°C), undesirable side-reactions caused by raw material impurities (such as free fatty acids and water), difficult recovery and purification of the products as well as the catalyst, and the need for substantial wastewater treatment (Ganesan *et al.*, 2009). Alternatively, enzymatic transesterification of triglycerides using lipase can overcome these challenges by lowering the operating temperature and providing a more selective reaction with less processing steps and without the need for extensive wastewater treatment (Fjerbaek *et al.*, 2009). The major drawbacks of enzymatically catalyzed biodiesel production are the high cost of the enzyme, low reaction rate, and the potential for enzyme inhibition and deactivation over time (Robles-Medina *et al.*, 2009).

Based on an economic study, biodiesel production using immobilized lipase was found to be more cost effective than using soluble lipase, but the immobilized lipase process was more costly than the alkali process and the enzyme must be reused more than five times to be industrially competitive (Jegannathan *et al.*, 2011). The benefits of immobilized enzymes over soluble enzymes include the enhanced ability for their recovery and reuse which decreases the effective cost of the enzyme, and the potential for improved activity and stability depending on the nature of the immobilization scheme (Fan, 2012).

By immobilizing lipase in a sol-gel, the thermal and chemical stability is known to be enhanced as well as the enzymatic activity (Aucoin *et al.*, 2004; Pirozzi *et al.*, 2009; Reetz *et al.*, 1996; Reetz, 1997). Many studies have focused on a secondary support material for the immobilization of lipase sol-gels to help overcome the potential for diffusion limitations, to make the immobilized lipase more practical for enzymatic reactors, and to further simplify the recovery and reuse of the enzyme (Brányik *et al.*, 2000; Meunier and Legge, 2010; Meunier and Legge, 2012; Orçaire *et al.*, 2006; Pogorilyi *et al.*, 2007).

Research on enzymatic biodiesel production can be classified based on whether the process is conducted using a solvent-based or solvent-free reaction media. Although solvent-free transesterification is complicated by high viscosity and an enhanced potential for inhibition, the use of organic solvents is undesirable due to the increased costs, environmental concerns, and the need for further downstream separation (Dossat *et al.*, 2002; Selmi and Thomas, 1998; Szczesna Antczak *et al.*,

2009; Tongboriboon *et al.*, 2010). A major concern for solvent-free biodiesel production is the increase in enzyme inhibition by the alcohol which exists as droplets in the organic phase due to its insolubility in the oil phase (Ognjanovic *et al.*, 2009).

Most enzymatically catalyzed biodiesel production plants operate with stirred tank batch reactors (Fjerbaek *et al.*, 2009). However, the agitation required for this type of reactor is one of the primary causes of enzyme deactivation, and by implementing a packed bed reactor without agitation, higher conversions can be achieved (Ognjanovic *et al.*, 2009). In addition, packed bed reactors have more industrial flexibility than batch stirred tank reactors. The commercially immobilized lipase, Novozym® 435, has been the subject of many packed bed reactor studies and is sufficiently stable and active for use for the continuous production of biodiesel (Chang *et al.*, 2009; Chen *et al.*, 2011; Halim *et al.*, 2009; Hama *et al.*, 2011a; Hama *et al.*, 2011b; Ognjanovic *et al.*, 2009; Royon *et al.*, 2007; Shaw *et al.*, 2008). Studies have also been conducted with other immobilized lipases (Lee *et al.*, 2010; Nie *et al.*, 2006; Wang *et al.*, 2011).

Enzymatic activity is known to be affected by a variety of chemicals as well as operating conditions. Lipase inhibition by the alcohol substrate in biodiesel production has been an extensive area for research with some alternatives for maintaining enzymatic activity including the pre-treatment of the lipase with organic solvents or the biodiesel reaction substrates or products (Chen and Wu, 2003; Samukawa *et al.*, 2000); the use of alternate acyl acceptors to alleviate the need for alcohol substrates (Du *et al.*, 2004; Ruzich and Bassi, 2011; Xu *et al.*, 2003); and the use of smaller than the required stoichiometric amounts of alcohol in the reaction medium (Shimada *et al.*, 1999; Shimada *et al.*, 2002; Watanabe *et al.*, 2000; Watanabe *et al.*, 2001; Watanabe *et al.*, 2002; Xu *et al.*, 2004).

In addition to inhibition by the alcohol substrate, the presence of the glycerol product is known to have an adverse effect on the enzymatic activity. To prevent undesirable reductions in enzymatic activity in continuous biodiesel production, glycerol is typically removed from the product stream via dialysis (Bélafi-Bakó *et al.*, 2002), adsorption on silica beds (Mazzieri *et al.*, 2008; Samukawa *et al.*, 2000; Yori *et al.*, 2007), or gravity-driven settling (Chen *et al.*, 2009; Hama *et al.*, 2011a; Hama *et al.*, 2011b). From an in-depth study of the influence of glycerol on immobilized lipase transesterification, Dossat *et al.* (1999) determined that the phenomena causing the decrease in the enzymatic activity involves the accumulation of a hydrophilic layer of glycerol around the immobilized enzyme which prevents access of the hydrophobic substrate (triglyceride) to the enzyme.

In this work, the initial reaction kinetics for Celite[®] supported lipase sol-gels and Novozym[®] 435 were determined using a batch stirred tank reactor at different methanol concentrations. Using the kinetic data from these studies along with the appropriate mass transfer equations, the concentration of the methyl oleate product with respect to time in a packed bed reactor was modelled, and the effect of flow rate on the conversion analyzed. The performance of the batch and continuous reactors with Celite[®] sol-gel immobilized lipase and Novozym[®] 435 were subsequently compared. Finally, the reusability of the Celite[®] sol-gel catalyst bed was evaluated.

8.2 Experimental

8.2.1 Materials

Two lipases were used in this study: Novozym[®] 435 (Novozymes North America Inc., Franklinton, NC) and Lipase PS “Amano” SD (Amano Enzyme USA Co., Elgin, IL). The biological source of lipase used for Novozym[®] 435 is *Candida antarctica*, the activity was 10 000 PLU/g, and it is reported to be immobilized on a macroporous acrylic resin. The biological source of the lipase for Lipase PS “Amano” SD is *Burkholderia cepacia* and the reported activity was 25 800 U/g. Lipase PS “Amano” SD was immobilized in a sol-gel composed of 80% trimethoxypropylsilane and 20% tetramethyl orthosilicate (Sigma-Aldrich Canada Ltd, Oakville, ON) and supported on Celite[®] R632 (World Minerals, Santa Barbara, CA). Ultrapure water was obtained from a Milli-Q water purification system (Millipore, Billerica, MA). All other chemicals used were of reagent grade.

8.2.2 Methods

8.2.2.1 Enzyme immobilization

Celite[®] R632 supported lipase sol-gels were produced as previously reported (Meunier and Legge, 2010). Trimethoxypropylsilane (14 mL), tetramethyl orthosilicate (2.95 mL), ultrapure water (17.4 mL), and 0.1 M HCl (200 μ L) were combined and sonicated for 1 h to allow hydrolysis of the precursors. The solution was rotary evaporated at 40°C for 30 min to remove any water or alcohol. 6.5 g of lipase PS “Amano” SD was dissolved in 18 mL of 50 mM phosphate buffer at pH 7.0, and 14 mL was added to the rotary evaporated precursor solution. The lipase sol-gel solution (27 mL) was then mixed thoroughly with the Celite[®] R632 support (18 g) and deposited into a Petri dish and sealed for 24 h at 4°C. Finally, the Celite[®] sol-gel was dried uncovered at 4°C until the drying rate slowed to less than 1 mg/hr. After the Celite[®] sol-gels were dried, they were washed twice with 50 mM pH=7.0 phosphate buffer (45 mL each wash) to

remove any free protein. The resulting gels were dried overnight at room temperature and stored in a sealed container at 4°C. This procedure produced approximately 25 g of Celite® supported sol-gel.

8.2.2.2 Protein content determination

The total protein content in the supported sol-gels was determined based on a mass balance approach. A BCA protein assay (Pierce Biotechnology Inc., Rockford, IL) with bovine serum albumin (BSA) as the standard over a concentration range of 25 to 2000 µg/mL was used. The absorbance was measured at 562 nm using a BioTek Synergy 4 Microplate Reader (BioTek US, Winooski, VT) according to the recommendations from Pierce Biotechnology Inc. for the microplate method. Samples of the stock enzyme solution were compared to samples of the wash solutions and a mass balance was performed to determine the amount of protein remaining in the supported sol-gel.

8.2.2.3 Batch stirred tank reactor operation

To determine the kinetic constants for transesterification, the immobilized lipase (1 g Celite® sol-gel or 50 mg Novozym® 435) and 6.5 mL triolein were combined with various concentrations of methanol in an agitated (500 rpm) batch reactor at 40°C for 6 h as previously described (Meunier and Legge, 2010). A 10 µL sample was taken every hour from the reaction vial for GC-MS quantification of the methyl oleate.

8.2.2.4 Packed bed reactor operation

Figure 8.1 is a schematic of the packed bed reactor apparatus which was fabricated in-house and consisted of a glass double walled reaction column of 1 cm diameter packed to approximately 17 cm high with immobilized lipase (6.00 g for the Novozym® 435 and 7.50 g for the Celite® supported lipase sol-gel). According to Thoenes (1994), the recommended particle diameter for packing materials is typically 3-10 mm and the reactor height should be 10 to a few hundred times the particle diameter. In this study, the particle diameter was 1 mm for Celite® sol-gel and 0.6 mm for Novozym® 435 and the reactor height was 170 times the particle diameter. The direction of the flow was downward due to the high substrate viscosity and the need to avoid any challenges associated with catalyst particle retention.

The reactor was maintained at a constant temperature (40°C) using a circulating water bath (NESLAB RTE-111, Neslab Instruments Inc., Portsmouth, NH, USA). The reaction mixture (1.95 mL methanol and 49.5 mL 97% triolein) was vigorously mixed and delivered to the top of the column at a constant flow rate using a peristaltic pump (Cole Parmer Masterflex Easyload L/S 7518-00, Montreal, QC, Canada). The reaction mixture was recycled through the packed bed until no further increase in conversion was observed. After each pass, a 10 µL sample was taken from the liquid phase for methyl oleate analysis.

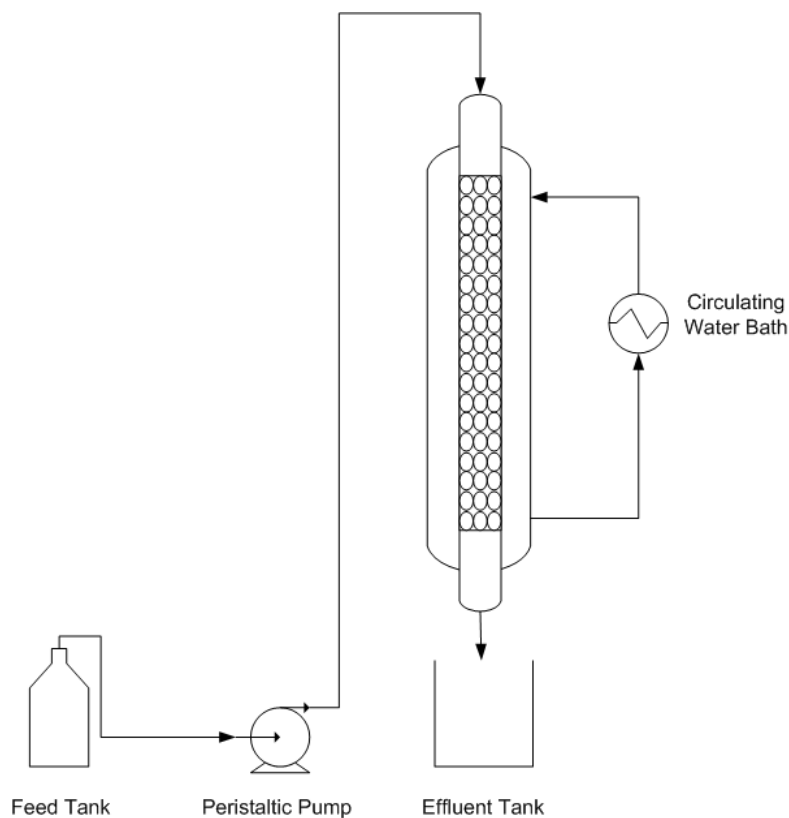


Figure 8.1: Schematic of the packed bed reactor apparatus.

8.2.2.5 Quantification of fatty acid methyl esters

The 10 μL samples from the batch stirred tank and packed bed reactors were diluted in 990 μL hexane and 100 μL of 320 μM heptadecanoic acid methyl ester (internal standard), and analyzed for methyl oleate content using a GC-MS (CP-3800 gas chromatograph, Saturn 2000 mass spectrometer/mass spectrometer, Varian Inc., Mississauga, ON) equipped with a CP-Wax 52 CB fused silica column (CP8513, Varian Inc., Mississauga, ON). The injector was set at 250°C with a split ratio of 50; the oven temperature was held at 170°C for 10 min, ramped 10°C/min to 250°C and held at 250°C for 2 min; helium was the carrier gas at a flow rate of 1 mL/min; and the injection volume was 1 μL . Only the methyl oleate concentration was measured using this method – the methanol and triolein concentrations were determined using a mass balance based on the reaction stoichiometry. No other components were observed in the GC-MS chromatograms.

8.3 Modelling

8.3.1 Kinetic model

The initial reaction rate for enzymatic biodiesel production with inhibition by the alcohol substrate can be described by Equation 8.1 for the reaction $T + A \leftrightarrow G + M$ where T is the triglyceride, A is the alcohol, G is the glycerol, and M is the methyl oleate (Al-Zuhair, 2005; Al-Zuhair *et al.*, 2007; Al-Zuhair *et al.*, 2009; Dossat *et al.*, 2002; Xu *et al.*, 2005).

$$\frac{dC_A}{dt} = -\frac{V_{max}[A][T]}{K_{mT}[A](1 + [A]/K_{IA}) + K_{mA}[T] + [A][T]} \quad (8.1)$$

where V_{max} is the maximum initial reaction velocity, $[A]$ and $[T]$ are the alcohol and triglyceride concentrations respectively, K_{mA} and K_{mT} are the apparent Michaelis constants for the alcohol and triglyceride respectively, and K_{IA} is the alcohol inhibition constant. The 4 kinetic constants (V_{max} , K_{mA} , K_{mT} , and K_{IA}) for Celite® lipase sol-gel (CSG) and Novozym® 435 (N435) catalysts were optimized using non-linear least squares fitting with the Trust-region algorithm conducted with MATLAB® software (Version 7, Mathworks) based on 13 data points for CSG and 17 data points for N435.

8.3.2 Packed bed reactor model

Considering the flow and reaction in a packed bed reactor, Equation 8.2 presents a differential equation to describe the substrate concentration with respect to the position along the height of the reactor (Fogler, 1999).

$$-U \frac{dC_A}{dz} = k_c S_B (C_A - C_A^S) \quad (8.2)$$

where U is the fluid linear velocity, k_c is the external mass transfer coefficient ($k_c = Sh \times D_{MT}/d_p$), S_B is the external surface area of the catalyst, C_A is the bulk concentration of the substrate, C_A^S is the concentration of the substrate at the catalyst surface, and z refers to the position along the reactor height. The steady state operation of an enzymatic packed bed reactor can also be described by Equation 8.3 (Dunn, 2003).

$$\frac{dC_A}{dz} = -\frac{1}{U} r_A \quad (8.3)$$

where r_A refers to the reaction rate with respect to the substrate. Considering a series of packed bed and fluidized bed studies, Equation 8.4 presents a general equation for the Sherwood number (Sh) that can be used to determine the mass transfer coefficient (k_c) in Equation 8.2 (Dwivedi and Upadhyay, 1977; Seguin *et al.*, 1996).

$$Sh = \frac{1.1}{\varepsilon} Re_p^{0.28} Sc^{\frac{1}{3}} \quad (8.4)$$

where ε is the void fraction in the reactor, Re_p is the Reynolds number for the particle and Sc is the Schmidt number.

8.3.3 Physical properties

The Wilke and Chang equation (Equation 8.5) was used to estimate the diffusivity, D_{MT} , of solute M in a very dilute solution in solvent T where M refers to the methanol and T to the triolein (Treybal, 1980).

$$D_{MT} = \frac{117.3 \times 10^{-18} \times (\varphi \times M_T)^{0.5} \times T}{\mu v_M^{0.6}} \quad (8.5)$$

where φ is the dissociation factor for the triolein, M_T is the molecular mass of the triolein, T is the temperature, μ is the triolein viscosity, and v_A is the molar volume of the methanol. Assuming uniform spherical particles, the void fraction (ε) can be calculated based on the particle diameter (d_p) and the reactor diameter (d_R) as shown in Equation 8.6 (Rase, 1990).

$$\varepsilon = 0.4 \left(1 + 0.42 \frac{d_p}{d_R} \right) \quad (8.6)$$

Since triolein consisted of approximately 97.6 % (v/v) of the liquid mixture, the density (ρ) and dynamic viscosity (μ) of pure triolein were used for the modelling. Equation 8.7 was used to determine the kinematic viscosity ($\nu = \mu/\rho$) with respect to temperature based on pure triolein where ν is cSt, μ is cP, ρ is g/cm³ and T is K (Valeri and Meirelles, 1997).

$$\ln \nu = 1.5554 - 2182.0021/T + 888879.2445/T^2 \quad (8.7)$$

The surface area and particle diameter for the Celite® R632 sol-gel were 1.49 m²/g and 1 mm, respectively (Meunier and Legge, 2010). For Novozym® 435 the surface area and particle diameter were 89 m²/g and 0.6 mm, respectively (Wiemann *et al.*, 2009).

8.3.4 Packed bed efficiency correlation

Despite mass transfer effects, the solvent-free packed bed reactor with Celite® supported sol-gel containing lipase achieved higher conversions more quickly than the stirred tank batch reactor that was used to develop the initial kinetic equations. Based on the effect of glycerol for continuous enzymatic transesterification described by Dossat *et al.* (1999), the presence of glycerol in the liquid phase is assumed to cause a diffusion limitation preventing the organic substrate from accessing the enzyme. Additionally, Dossat *et al.* (1999) found that increasing the amount of enzyme in the system caused a delay in the point at which the enzymatic activity begins to decrease. To accommodate this effect, an efficiency correlation, α , was developed that depends on both the Reynolds number for the reactor (Re) and the concentration of glycerol with respect to the weight of enzyme in the packed bed ($[G]/W_p$) as described by Equation 8.8.

$$\alpha = \frac{\alpha_1}{1 + \alpha_2 e^{\alpha_3 Re} + \left(\alpha_4 \frac{[G]}{W_p}\right)^{\alpha_5}} \quad (8.8)$$

From this correlation, as the Reynolds number increases the glycerol layer is removed thereby reducing the resistance layer resulting in an increase in the observed enzymatic activity. Conversely, as the glycerol concentration increases, so does the glycerol layer resulting in an increase in resistance resulting in a decrease in the observed activity. The constants of the model (α_1 , α_2 , α_3 , α_4 , and α_5) were obtained using an inverse parameter estimation approach. The experimental methyl oleate concentrations obtained at 1.4, 5 and 20 mL/min (29 data points) were used to calibrate the model by estimating the parameters of the efficiency equation (Equation 8.8). A genetic algorithm code available in the MATLAB® software was used for parameter estimation by minimizing the sum of squared error (SSE) between experimental and model estimation of the methyl oleate concentration. The model was validated against the experimental data obtained at 12.5 mL/min and a second set of data obtained at 20 mL/min (30 additional data points).

Table 8.1: Kinetic constants determined by fitting the results of the batch experiments to Equation 8.1 for the Celite® sol-gel (CSG) and the Novozym® 435 (N435) immobilized enzyme preparations. Ethanolysis kinetic constants from the literature using N435 are included for comparison (Chesterfield *et al.*, 2012).

| Kinetic coefficient | CSG | N435 | Chesterfield <i>et al.</i> (2012) |
|-----------------------|-------------------|----------------------|-----------------------------------|
| V_{max} (mol/L min) | 408.26 | 1.022 | 3.26 |
| K_{mT} (mol/L) | 1.2×10^4 | 0.132 | 0.029 |
| K_{mA} (mol/L) | 5.5×10^4 | 830 | 0.948 |
| K_{IA} (mol/L) | 0.137 | 4.2×10^{-5} | 0.083 |

8.4 Results and discussion

8.4.1 Batch kinetics

The kinetic constants determined for Celite® supported sol-gels and Novozym® 435 (Table 8.1) indicate that a faster reaction was observed for Celite® sol-gel ($V_{max,CSG} \gg V_{max,N435}$) and that alcohol inhibition was greater for Novozym® 435 ($K_{IA,CSG} \gg K_{IA,N435}$). These results show that the Celite® sol-gel has better kinetic performance in comparison to the commercially immobilized Novozym® 435. However, the Celite® sol-gels exhibit lower apparent affinities for both substrates in comparison Novozym® 435 ($K_{mT,CSG} \gg K_{mT,N435}$ and $K_{mA,CSG} \gg K_{mA,N435}$). The kinetic models developed for both enzyme preparations provide good fit with respect the experimental data ($SSE_{CSG}=0.219$, $R^2_{CSG}=0.888$, $SSE_{N435}=3.9 \times 10^{-9}$, $R^2_{N435}=0.895$).

A recent study by Chesterfield *et al.* (2012) considered the reaction kinetics for Novozym® 435 biodiesel production and found V_{max} and K_{IA} values between those found for CSG and N435 in this study (Table 8.1). A similar catalyst loading was used, however ethanol was used as the acyl acceptor, which is known to be less inhibitory to lipase (Hernández-Martín and Otero, 2008; Salis *et al.*, 2005). This effect is substantiated by the lower alcohol inhibition constant and higher apparent Michaelis constant observed in this study in comparison to the observations of Chesterfield *et al.* (2012).

8.4.2 Experimental and modelling results

To determine the constants for the correlation coefficient (Equation 8.8), Equations 8.1-8.8 were solved at a variety of flow rates to achieve the best fit for all conditions tested. Table 8.2 provides the data used for the immobilized enzyme including the catalyst density, surface area, particle size, porosity, efficiency correlation constants, diffusivity coefficient and viscosity while Table 8.3 provides the additional data necessary for the packed bed reactor model including the Reynolds number, Sherwood number, and mass transfer coefficient as described in Section 8.3.2.

The model developed showed very good agreement with the experimental data for all the flow rates examined (Figure 8.2). Increasing the flow rate from 1.4 mL/min to 5 mL/min and from 5 mL/min to 12.5 mL/min influenced the methyl oleate concentration profile, but a further increase in the flow rate from 12.5 mL/min to 20 mL/min had a minimal effect on the product concentration profile. A similar effect was observed by Hama *et al.* (2011) who observed that the glycerol removal efficiency increased with increasing flow rate until the optimal flow for glycerol removal was achieved. At the two highest flow rates (12.5 mL/min and 20 mL/min), the maximum conversion (90%) is reached within

approximately 10 minutes of contact time between the substrates and the enzyme. The inability to achieve 100% conversion is attributed to the high glycerol concentration which results in a hydrophilic layer around the enzyme and support preventing the triglyceride from reaching the enzyme's active site (Dossat *et al.*, 1999).

Table 8.2: Parameters used to model the experimental packed bed reactor results for each of the immobilized biocatalysts.

| Parameter | CSG | N435 |
|---|------------------------|--------------------|
| ρ_B (kg/m ³) | 562 | 449 |
| Su (m ² /kg) | 1490 | 82000 |
| S_B (m ² /m ³) | 8.37×10^5 | 3.69×10^7 |
| d_P (m) | 0.001 | 0.0006 |
| ϵ | 0.42 | 0.41 |
| α_1 | 23 | 8 |
| α_2 | 6 | 4 |
| α_3 | -14 | -14 |
| α_4 | 1×10^{-4} | 5×10^{-2} |
| α_5 | 4 | 4 |
| D_{MT} (m ² /s) | 2.11×10^{-10} | |
| μ (Pa s) | 0.0355 | |

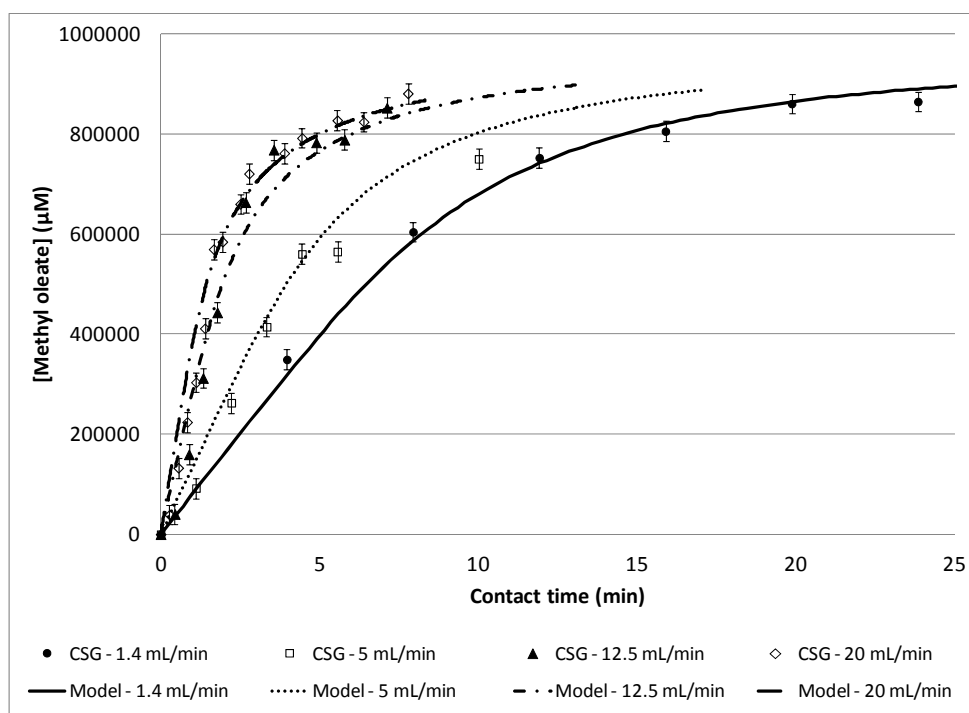


Figure 8.2: Packed bed results with the experimental (symbols) and model (lines) methyl oleate concentrations as a function of contact time in the reactor with Celite® supported sol-gels at 4 flow rates (1.4 mL/min, 5 mL/min, 12.5 mL/min and 20 mL/min). The confidence intervals shown are estimated from a pooled variance of 16 samples in triplicate.

Table 8.3: Summary of some of the parameters calculated from the modelling of the packed bed reactor experiments.

| Enzyme | CSG | CSG | CSG | CSG | N435 | N435 |
|----------------|--------|--------|--------|--------|--------|--------|
| Q (mL/min) | 1.4 | 5 | 12.5 | 20 | 5 | 20 |
| Re_p | 0.0075 | 0.0267 | 0.0669 | 0.1070 | 0.0160 | 0.0640 |
| Sh | 38.77 | 55.37 | 71.56 | 81.62 | 48.74 | 71.86 |
| k_c (cm/min) | 0.477 | 0.681 | 0.881 | 1.004 | 1.002 | 1.477 |

Table 8.4: Comparison of solvent-free biodiesel packed bed reactor performance using immobilized lipase.

| Reference | Catalyst | Reactor volume (cm ³) | Substrate volume (mL) | Flow rate (mL/min) | Reaction time (min) | Conversion (%) |
|--------------------------|----------|-----------------------------------|-----------------------|--------------------|---------------------|----------------|
| This work | CSG | 13.35 | 52 | 20 | 60 | 84 |
| This work | N435 | 13.35 | 52 | 20 | 60 | 63 |
| Chang et al. (2009) | N435 | 4.15 | 56 | 0.1 | 560 | 76 |
| Hama et al. (2011b) | N435 | 290 | 1020 | 4 | 255 | 75 |
| Hsu et al. (2004) | Sol-gel | 67 | 155 | 30 | 180 | 30 |
| Ognjanovic et al. (2009) | N435 | 10.68 | 110 | 16.6 | 60 | 25 |
| Xu et al. (2012) | NS8801 | 17 | 120 | 0.8 | 150 | 16 |

The observed effect of flow rate is consistent with what is described in the literature (Chang *et al.*, 2009, Hama *et al.*, 2011b; Lee *et al.*, 2010). Hama *et al.* (2011b) observed an optimal flow rate of approximately 9 mL/min based on the glycerol removal efficiency and the fatty acid methyl ester content of the product stream for a similarly sized reactor (15.7 mm internal diameter in comparison to the 10 mm internal diameter for this study). Table 8.4 presents a review of the literature for immobilized enzyme packed bed biodiesel reactors in solvent-free reaction media. The reaction time is presented in this table, different from the contact time in the figures in that the reaction time is the time required for the liquid to flow through the reactor (substrate volume / flow rate x number of passes) as opposed to the contact time between the liquid and the catalyst which accounts for the void fraction in the reactor and the reactor dimensions. The packed bed reactor results achieved in this study surpass the conversions reported in the literature.

8.4.3 Comparison of Celite® supported sol-gel to Novozym® 435

As a basis for comparison, a commercially available immobilized lipase, Novozym® 435, was tested in the same packed bed reactor at flow rates of 5 mL/min and 20 mL/min. The same model (with different efficiency correlation constants, Table 8.2) was used to predict the methyl oleate concentration profile and was found to be in good agreement with the experimental data (Figure 8.3). There was a significant improvement of the packed bed reactor performance using CSG in comparison to N435 (Figures 8.2 and 8.3).

Much higher methyl oleate concentrations were observed for the packed bed reactor with CSG than for N435. After 5 min of contact time at 5 mL/min the CSG had a conversion of 58% while N435 had a conversion of 42%, and at 20 mL/min the CSG had a conversion of 83% while N435 had 59% conversion. Since the maximum reaction rate is higher and the methanol inhibition effect is lower for CSG than for N435, an improvement in the performance of the batch stirred tank and packed bed reactors with CSG is expected. An internal diffusion limitation for many biocatalysts including N435 has been reported in the literature (Almeida *et al.*, 1998; Jung and Bauer, 1992; Xiao *et al.*, 2012; Xu and Chuang, 1997), which is a likely cause of the decrease in reactor performance using N435.

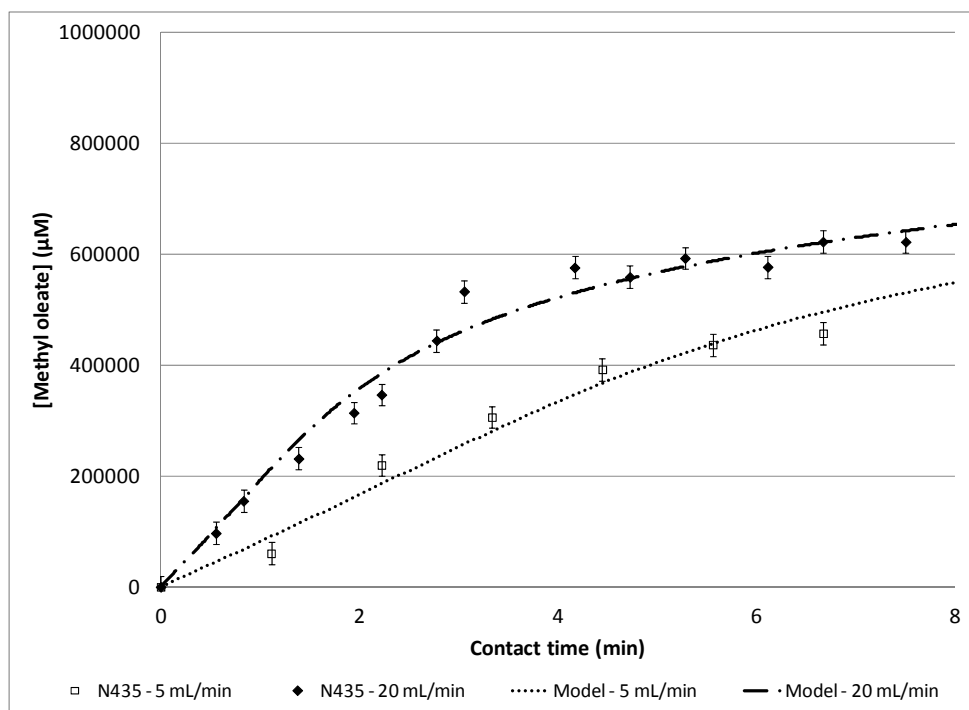


Figure 8.3: Packed bed results with the experimental (symbols) and modelling (lines) methyl oleate concentrations as a function of contact time in the reactor for Novozym® 435 at flow rates of 5 mL/min and 20 mL/min. The confidence intervals shown are estimated from a pooled variance of 16 samples in triplicate.

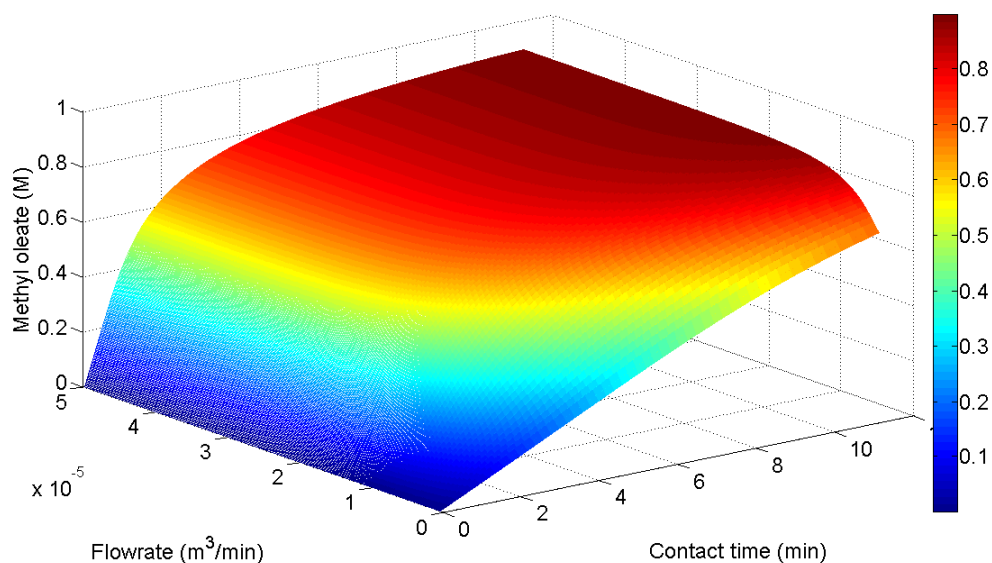


Figure 8.4: Contour map for model predictions for methyl oleate concentration with respect to the flow rate and contact time based on kinetics and mass transfer.

8.4.4 Model predictions

The predictions using the model developed support the experimental observations that increasing the flow rate and the contact time cause an increase in the methyl oleate concentration, but both variables have thresholds for which further increases in the flow rate do not substantially increase the final achievable concentration of methyl oleate (Figure 8.4). For example, a contact time of 5 min at a flow rate of 0.5 mL/min results in a methyl oleate concentration of 0.35 M, a flow rate of 16 mL/min results in a methyl oleate concentration of 0.79 M, and a flow rate of 50 mL/min results in a methyl oleate concentration of 0.81 M. A similar effect is observed with contact time. This is consistent with the literature which indicates that a hydrophilic glycerol layer hinders the enzymatic activity by limiting the access of the triglyceride to the enzyme – increasing the flow rate will remove the glycerol, but increasing the contact time (conversion) will increase the glycerol concentration (Bélafi-Bakó *et al.*, 2002; Dossat *et al.*, 1999; Hong *et al.*, 2011).

8.4.5 Catalyst reusability

The reusability of the Celite® sol-gel was considered over a five day period where each day new substrates were supplied to the existing catalyst bed in the reactor. From the experimental data (Figure 8.5), no significant activity loss was observed over the five day time span supporting the claim that the Celite® sol-gel is a promising immobilized lipase suitable for transesterification in a packed bed reactor.

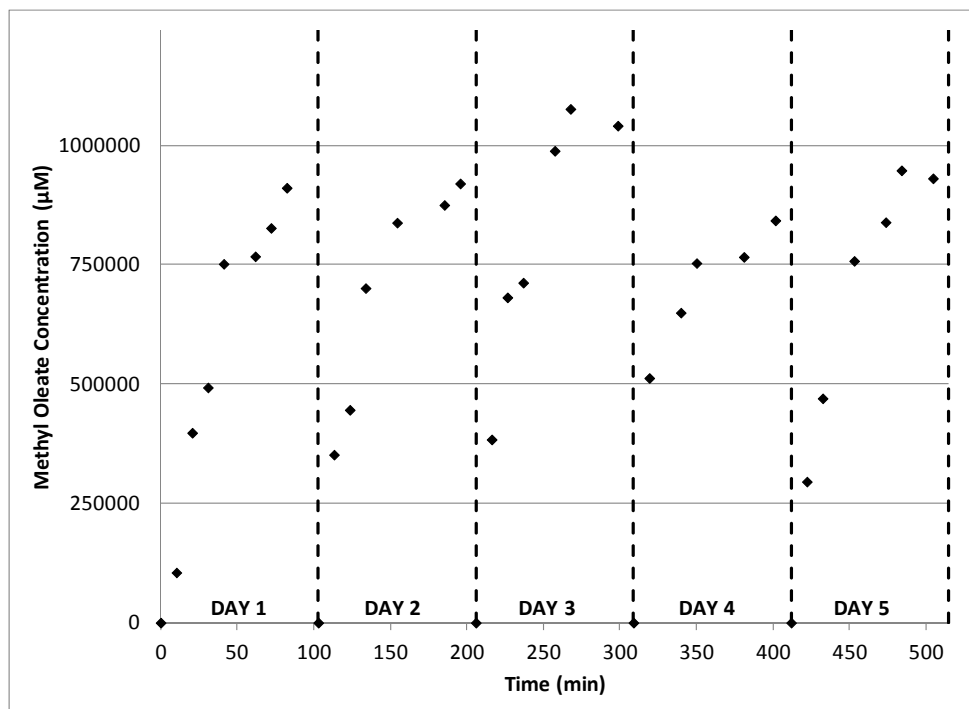


Figure 8.5: Reusability runs in the packed bed reactor over 5 days at $T = 40^{\circ}\text{C}$, substrate ratio 1:1, and flow rate = 5 mL/min. A new substrate mixture (triolein and methanol) was supplied to the existing CSG bed at the beginning of each day.

8.5 Conclusions

A packed bed reactor containing Celite® supported lipase sol-gel was developed and its performance was analyzed using a combination of reaction kinetics and mass transfer with the addition of a novel efficiency correlation to account for the effect of glycerol on the observed enzymatic activity. The reaction kinetics for Celite® supported sol-gels and Novozym® 435 were determined using an initial reaction rate model with alcohol inhibition. The CSG had a much faster maximum reaction velocity and alcohol was found to be less inhibitory. The reaction kinetics from the stirred batch reactor in combination with mass transfer correlations were insufficient to describe the performance of the packed bed reactor which is attributed to the presence of a glycerol layer which creates an additional mass transfer resistance. An efficiency correlation dependent on the Reynolds number and the concentration of glycerol with respect to the amount of enzyme in the packed-bed reactor was developed and used in the model. The efficiency correlation describes the relationship between the reduction of the glycerol layer with increasing flow rate and the increasing glycerol layer with increasing glycerol concentration. Combining the reaction kinetics, mass transfer, and efficiency correlation, the resulting model exhibited good agreement with the experimental data over a range of flow rates from

1.4 mL/min to 20 mL/min. Both the experimental results and the model predictions demonstrate the strong effect of flow rate on the methyl oleate concentration at low flow rates, but as the flow rate increases beyond 12.5 mL/min the activity enhancing effect is minimized. The results for the Celite® supported sol-gel system were compared to a commercially available immobilized lipase, N435, and showed that CSG system resulted in significantly higher final methyl oleate percent conversions (83% at 20 mL/min) in comparison to N435 (59% at 20 mL/min) supporting the inherent advantages of this enzyme-based system for the production of fatty acid methyl esters. Additionally, over five days no enzymatic activity loss was observed for the CSG further indicating its potential for use in a packed bed reactor configuration.

8.6 Acknowledgements

This work was supported by the Natural Sciences and Engineering Research Council (NSERC) in the form of a Postgraduate Scholarship to SMM and a Discovery Grant to RLL. We thank Amano Enzyme USA for supplying samples of the lipase formulation, World Minerals for the samples of the Celite® support materials and Novozymes North America Inc. for the samples of the Novozym® 435.

8.7 Nomenclature

| | |
|----------|--|
| [A] | Alcohol concentration (mol/m ³) |
| C_A | Concentration of substrate A (mol/m ³) |
| C_A^S | Concentration of substrate A at the catalyst surface (mol/m ³) |
| CSG | Celite® supported lipase sol-gel |
| D_{MT} | Diffusion of methanol in triolein (m ² /s) |
| d_P | Catalyst particle diameter (m) |
| d_R | Reactor diameter (m) |
| [G] | Glycerol concentration (mol/m ³) |
| k_C | Mass transfer coefficient (m/min) |

| | |
|------------|---|
| K_{IA} | Alcohol inhibition constant (mol/m ³) |
| K_{mA} | Apparent Michaelis constant for alcohol (mol/m ³) |
| K_{mT} | Apparent Michaelis constant for triglyceride (mol/m ³) |
| M_T | Molecular mass of the triolein (g/mol) |
| N435 | Novozym® 435 |
| Q | Flow rate (m ³ /min) |
| R^2 | Coefficient of determination |
| r_A | Reaction rate with respect substrate A (mol/m ³ min) |
| Re | Reynolds number for the reactor $Re = (\rho \times 10^3)(U/60)d_p/(\mu\varepsilon)$ (dimensionless) |
| Re_p | Reynolds number for the particle $Re_p = (\rho \times 10^3)(U/60)d_p/\mu$ (dimensionless) |
| S_B | External surface area of the catalyst (m ² /m ³) |
| Sc | Schmidt number (dimensionless) |
| Sh | Sherwood number (dimensionless) |
| SSE | Sum of squared errors |
| Su | Catalyst surface area (m ² /kg) |
| t | Time (min) |
| T | Temperature (K) |
| $[T]$ | Triglyceride concentration (mol/m ³) |
| U | Linear velocity (m/min) |
| v_M | Molar volume of the methanol (m ³ /mol) |
| V'_{max} | Apparent maximum initial reaction velocity (mol/m ³ min) |
| W_p | Protein weight in the reactor (kg) |

| | |
|---------------|--|
| z | Position along the reactor height (m) |
| α | Efficiency correlation (dimensionless) |
| α_X | Constants for the efficiency correlation ($X=1, 2, 3, 4$ or 5) |
| ε | Void fraction in the reactor (dimensionless) |
| μ | Oil dynamic viscosity (Pa s) |
| ν | Kinematic viscosity (cSt) |
| ρ | Density (g/cm^3) |
| ρ_B | Bulk catalyst density (kg/m^3) |
| φ | Dissociation factor for the oil (dimensionless) |

Chapter 9

Conclusions and Recommendations

9.1 Most significant contributions

The research conducted for this thesis focused on the development and characterization of a novel immobilized enzyme, Celite® supported lipase sol-gel, and the elucidation of its potential for the production of biodiesel in an enzymatic packed bed reactor. A series of lipase sol-gel support materials were evaluated based on their fatty acid methyl ester production capabilities in a stirred tank batch reactor; the support material with the most potential, diatomaceous earth Celite® R632, was chosen and further characterized to predict any challenges that may be associated with enzymatic transesterification; the reaction kinetics of the supported sol-gel for fatty acid methyl ester production was ascertained; and the performance of the immobilized enzyme was assessed using a packed bed reactor with kinetic and mass transfer modelling. The following sections describe the specific conclusions drawn from each of the chapters presented in this thesis.

9.1.1 Objective A – Experimental Background

Chapter 3 presents the preliminary results collected to determine the feasibility of formulating and evaluating lipase sol-gels for biodiesel production. Based on the research presented, lipase sol-gels were found to be very active enzymatically with high thermal stability and good potential for fatty acid methyl ester production when high hydrophobicity sol-gels (80% PTMS) are used. Additionally, using the commercially immobilized lipase, Novozym® 435, the presence of methanol in the reaction mixture was found to have a strong effect on the achievable conversion, the effects of the presence of a hexane solvent and temperature were only evident at high temperatures (above 60°C), and water had a minimal effect on conversion. This information was used as a basis for the developing a supported lipase sol-gel for the production of fatty acid methyl esters.

9.1.2 Objective B – Study of Support Materials for Sol-gel Immobilized Lipase

In Chapter 4, a series of support materials were examined and used to formulate supported lipase sol-gels which were evaluated based on their ability to retain sol-gel, load protein, and remain catalytically active for the production of methyl oleate. The goal in selecting a support material was its potential for use as a biocatalyst preparation practical for use in a packed bed reactor for biodiesel production. Six

support materials were considered: silica gel, three types of diatomaceous earth (Celite® R633, Celite® R632, and Celite® R647), an anion exchange resin, and Quartzel® felt. Each supported sol-gel had unique advantages for this application, but Celite® R632 was chosen as the support material with the most potential for biodiesel production due to its observed high transesterification conversion ability, activity and reaction rate, as well as its high thermal stability and sol-gel adhesion levels in comparison to the other supports considered.

9.1.3 Objective C – Evaluation of Diatomaceous Earth as a Support for Sol-gel Immobilized Lipase for Transesterification

Chapter 5 is a study of the diatomaceous supported sol-gels in more depth by looking at their surface morphology, physical properties, and enzymatic properties. The main differences between the three Celite® materials used is with respect to their particle size, pore diameter, and surface area: R633 has a small particle size and large pore diameter, R632 has a large particle size and large pore diameter, and R647 has large particle size, small pore diameter and very large surface area. The sol-gel adhesion and protein loading were comparable for all three types of Celite® considered. Celite® R632 exhibited good initial activity and methyl oleate conversion in comparison to the other supported sol-gels and the unsupported sol-gel validating the potential of Celite® R632 supported lipase sol-gels for biodiesel production.

9.1.4 Objective D – Evaluation of Diatomaceous Earth Supported Sol-gels as a Medium for Enzymatic Transesterification to Produce Biodiesel

In Chapter 6, the Celite® R632 supported lipase sol-gels were further investigated for biodiesel production potential based on their protein content, methyl oleate conversion, enzymatic activity, stability, and glycerol-water adsorption. Unsupported and Celite® supported lipase sol-gels with different protein loading levels were compared. Based on the results obtained, the Celite® R632 supported sol-gel with the highest protein content achieved the best conversion over the 6 h reaction period (80%), a drying step prior to reaction was found to improve the conversion, and the adsorption of glycerol was only found to be significant at high concentrations of glycerol (75% by volume). The unsupported and Celite® supported lipase sol-gels were found to be catalytically stable upon storage at 4°C over a 1.5 yr period. These results demonstrate that Celite® R632 supported lipase sol-gels show promise as a novel biocatalyst for biodiesel production.

9.1.5 Objective E – Kinetic Modelling of the Production of Methyl Oleate by Celite® Supported Lipase Sol-gels

Chapter 7 presents a kinetic study based on a ping-pong bi-bi mechanism for methyl oleate production using Celite® R632 supported lipase sol-gels. A kinetic model was developed to include inhibition by methanol and glycerol, the effect of temperature, the presence of products, and the reverse reaction and was shown to be consistent with the experimental data. An optimal methanol concentration range (1.3 – 2.0 M) that was increased with increasing reaction temperature was identified. Glycerol inhibition was found to have a more significant effect on the kinetics than methanol inhibition, indicating the importance of considering the reaction kinetics beyond the initial conditions. The model developed in this study can be considered valuable for understanding and identifying the combined effects of methanol inhibition, glycerol inhibition, and temperature on the production of methyl oleate by enzymatic transesterification.

9.1.6 Objective F – Kinetic and Mass Transfer Modelling of Methyl Oleate Production in an Immobilized Lipase Packed Bed Reactor

Chapter 8 provides the results for a modeling study based on kinetics and mass transfer for a packed bed reactor with Celite® supported lipase sol-gels and Novozym® 435. Comparing the methyl oleate production capabilities of the Celite® supported sol-gel with Novozym® 435 under both batch and packed bed reactor conditions, the Celite® supported sol-gel had superior performance indicating the potential of this novel biocatalyst for transesterification. To model the reactor performance, reaction kinetics and mass transfer equations were used in combination with a novel efficiency correlation to account for the effect of glycerol. The model developed was consistent with the experimental data over a range of flow rates from 1.4 mL/min to 20 mL/min. The presence of glycerol had a dominant effect on the methyl oleate concentration profile and increasing the flow rate, presumably reducing the glycerol layer surrounding the biocatalyst, resulted in improved apparent enzymatic activity.

9.2 Recommendations for Future Work

Based on the research conducted in this study, several recommendations for further work are provided:

- **Fundamentals:** Quantification of glycerol and the reaction intermediates (diglycerides and monoglycerides) in the product stream would be useful for gaining a better understanding of the reaction mechanism. This could be accomplished using HPLC with a refractive index detector or a GC with FID detection and a temperature programmable injector.
- **Process optimization:** There are several variables that should be studied to complete the process optimization for the Celite® supported packed bed reactor such as the lipase source, sol-gel composition, acyl acceptor, water content, and temperature. Each of these variables is crucial for the performance and stability of the reactor. Ideally, these variables should be considered simultaneously to evaluate any interaction effects.
- **Applicability for biodiesel production:** To determine the industrial applicability of this Celite® supported packed bed reactor for biodiesel production, the reactor should be considered with alternative feed-stocks such as waste, vegetable, and non-edible oils.
- **Operational stability:** The long term conversion capabilities and mechanical stability of the immobilized enzyme should be studied as well as the catalyst lifetime. This information is essential in evaluating the practicality of large scale biodiesel production using the proposed enzymatic reactor.
- **Glycerol separation:** Given the effects of glycerol revealed in Chapters 6, 7, and 8, the continuous removal of glycerol from the packed bed operation could significantly benefit the achievable conversion. Although there are a variety of options for glycerol removal, implementation of a packed bed reactor with membrane-based separation for glycerol may be of value for industrial applications.

References

- Abbaszaadeh A, Ghobadian B, Omidkhah MR, Najafi G. 2012. Current biodiesel production technologies: A comparative review. *Energy Convers Manage* 63:138-148.
- Akoh CC, Chang S-W, Lee G-C, Shaw J-F. 2007. Enzymatic approach to biodiesel production. *J Agric Food Chem* 55:8995-9005.
- Almeida MC, Ruivo R, Maia C, Freire L, Corrêa De Sampaio T, Barreiros S. 1998. Novozym 435 activity in compressed gases. Water activity and temperature effects. *Enzyme Microb Technol* 22:494-499.
- Al-Zuhair S. 2007. Production of biodiesel: Possibilities and challenges. *Biofuel Bioprod Bior* 1:57-66.
- Al-Zuhair S. 2005. Production of biodiesel by lipase-catalyzed transesterification of vegetable oils: A kinetics study. *Biotechnol Progr* 21:1442-1448.
- Al-Zuhair S, Almenhali A, Hamad I, Alshehhi M, Alsuwaidi N, Mohamed S. 2011. Enzymatic production of biodiesel from used/waste vegetable oils: Design of a pilot plant. *Renewable Energy* 36:2605-2614.
- Al-Zuhair S, Dowaidar A, Kamal H. 2009. Dynamic modeling of biodiesel production from simulated waste cooking oil using immobilized lipase. *Biochem Eng J* 44:256-262.
- Al-Zuhair S, Ling FW, Jun LS. 2007. Proposed kinetic mechanism of the production of biodiesel from palm oil using lipase. *Process Biochem* 42:951-960.
- Atadashi IM, Aroua MK, Abdul Aziz AR, Sulaiman NMN. 2012. The effects of catalysts in biodiesel production: A review. *J Ind Eng Chem* In press.
- Aucoin MG, Erhardt FA, Legge RL. 2004. Hyperactivation of *Rhizomucor miehei* lipase by hydrophobic xerogels. *Biotechnol Bioeng* 85:647-655.
- Avnir D, Braun S, Lev O, Ottolenghi M. 1994. Enzymes and other proteins entrapped in sol-gel materials. *Chem Mater* 6:1605-1614.
- Azócar L, Ciudad G, Heipieper HJ, Muñoz R, Navia R. 2010. Improving fatty acid methyl ester production yield in a lipase-catalyzed process using waste frying oils as feedstock. *J Biosci Bioeng* 109:609-614.

- Bajaj A, Lohan P, Jha PN, Mehrotra R. 2010. Biodiesel production through lipase catalyzed transesterification: An overview. *J Mol Catal B: Enzym* 62:9-14.
- Balasubramaniam B, Sudalaiyadum Perumal A, Jayaraman J, Mani J, Ramanujam P. 2012. Comparative analysis for the production of fatty acid alkyl esterase using whole cell biocatalyst and purified enzyme from *Rhizopus oryzae* on waste cooking oil (sunflower oil). *Waste Manage* 32:1539-1547.
- Bastida A, Sabuquillo P, Armisen P, Fernández-Lafuente R, Huguet J, Guisán JM. 1998. A single step purification, immobilization, and hyperactivation of lipases via interfacial adsorption on strongly hydrophobic supports. *Biotechnol Bioeng* 58:486-493.
- Bélafi-Bakó K, Kovács F, Gubicza L, Hancsók J. 2002. Enzymatic biodiesel production from sunflower oil by *Candida antarctica* lipase in a solvent-free system. *Biocatal Biotransform* 20:437-439.
- Bendikiene V, Kiriliauskaite V, Juodka B. 2011. Production of environmentally friendly biodiesel by enzymatic oil transesterification. *J Environ Eng Landsc* 19:123-129.
- Brányik T, Kuncová G, Páca J. 2000. The use of silica gel prepared by sol-gel method and polyurethane foam as microbial carriers in the continuous degradation of phenol. *Appl Microbiol Biotechnol* 54:168-172.
- Chang C, Chen J-H, Chang C-mJ, Wu T-T, Shieh C-J. 2009. Optimization of lipase-catalyzed biodiesel by isopropanolysis in a continuous packed-bed reactor using response surface methodology. *New Biotechnol* 26:187-192.
- Chang H-M, Liao H-F, Lee C-C, Shieh C-J. 2005. Optimized synthesis of lipase-catalyzed biodiesel by Novozym 435. *J Chem Technol Biotechnol* 80:307-312.
- Cheirsilp B, H-Kittikun A, Limkatanyu S. 2008. Impact of transesterification mechanisms on the kinetic modeling of biodiesel production by immobilized lipase. *Biochem Eng J* 42:261-269.
- Chen H-C, Ju H-Y, Wu T-T, Liu Y-C, Lee C-C, Chang C, Chung Y-L, Shieh C-J. 2011. Continuous production of lipase-catalyzed biodiesel in a packed-bed reactor: Optimization and enzyme reuse study. *J Biomed Biotechnol* 2011 Article ID 950725 6 pages doi:10.1155/2011/950725
- Chen J-W, Wu W-T. 2003. Regeneration of immobilized *Candida antarctica* lipase for transesterification. *J Biosci Bioeng* 95:466-469.

- Chen Y, Xiao B, Chang J, Fu Y, Lv P, Wang X. 2009. Synthesis of biodiesel from waste cooking oil using immobilized lipase in fixed bed reactor. *Energy Convers Manage* 50:668-673.
- Chesterfield DM, Rogers PL, Al-Zaini EO, Adesina AA. 2012. Production of biodiesel via ethanolysis of waste cooking oil using immobilised lipase. *Chem Eng J* 207–208:701-710.
- Chew YH, Lee CT, Sarmidi MR, Aziz RA, Razali F. 2008. External mass transfer model for the hydrolysis of palm olein using immobilized lipase. *Food Bioprod Process* 86:276-282.
- Chouhan APS, Sarma AK. 2011. Modern heterogeneous catalysts for biodiesel production: A comprehensive review. *Renewable Sustainable Energy Rev* 15:4378-4399.
- Cleland WW. 1963a. The kinetics of enzyme-catalyzed reactions with two or more substrates or products. I. Nomenclature and rate equations. *Biochim Biophys Acta* 67:104-137.
- Cleland WW. 1963b. The kinetics of enzyme-catalyzed reactions with two or more substrates or products. II. Inhibition: Nomenclature and theory. *Biochim Biophys Acta* 67:173-187.
- Cleland WW. 1963c. The kinetics of enzyme-catalyzed reactions with two or more substrates or products. III. Prediction of initial velocity and inhibition patterns by inspection. *Biochim Biophys Acta* 67:188-196.
- Clifford JS, Legge RL. 2005. Use of water to evaluate hydrophobicity of organically-modified xerogel enzyme supports. *Biotechnol Bioeng* 92:231-237.
- Dossat V, Combes D, Marty A. 2002. Lipase-catalysed transesterification of high oleic sunflower oil. *Enzyme Microb Technol* 30:90-94.
- Dossat V, Combes D, Marty A. 1999. Continuous enzymatic transesterification of high oleic sunflower oil in a packed bed reactor: Influence of the glycerol production. *Enzyme Microb Technol* 25:194-200.
- Du W, Xu Y, Liu D, Zeng J. 2004. Comparative study on lipase-catalyzed transformation of soybean oil for biodiesel production with different acyl acceptors. *J Mol Catal B: Enzym* 30:125-129.
- Dunn IJ. 2003. *Biological reaction engineering: dynamic modelling fundamentals with simulation examples*. Weinheim, Germany: VCH p 272.

- Dwivedi PN, Upadhyay SN. 1977. Particle-fluid mass transfer in fixed and fluidized beds. *Ind Eng Chem Proc DD* 16:157-165.
- Fan X. 2012. Enzymatic biodiesel production - the way of the future. *Lipid Technol* 24:31-32.
- Fan X, Niehus X, Sandoval G. 2012. Lipases as biocatalyst for biodiesel production. *Methods Mol Biol* 861:471-483.
- Fjerbaek L, Christensen KV, Norddahl B. 2009. A review of the current state of biodiesel production using enzymatic transesterification. *Biotechnol Bioeng* 102:1298-1315.
- Fogler HS. *Elements of chemical reaction engineering* 3rd ed. Upper Saddle River, N.J.: Prentice Hall PTR c1999.
- Fukuda H, Kondo A, Noda H. 2001. Biodiesel fuel production by transesterification of oils. *J Biosci Bioeng* 92:405-416.
- Furukawa S-Y, Ono T, Ijima H, Kawakami K. 2002a. Activation of protease by sol-gel entrapment into organically modified hybrid silicates. *Biotechnol Lett* 24:13-16.
- Furukawa S-Y, Ono T, Ijima H, Kawakami K. 2002b. Effect of imprinting sol-gel immobilized lipase with chiral template substrates in esterification of (R)-(+)- and (S)-(-)-glycidol. *J Mol Catal B: Enzym* 17:23-28.
- Furukawa S-Y, Ono T, Ijima H, Kawakami K. 2000. Catalytic capabilities of lipase immobilized into organically modified silicates by sol-gel method. *Kagaku Kogaku Ronbunshu* 26:885-886.
- Furukawa S-YA, Kawakami K. 1998. Characterization of *Candida rugosa* lipase entrapped into organically modified silicates in esterification of menthol with butyric acid. *J Ferment Bioeng* 85:240-242.
- Gagnon MD, Vasudevan PT. 2011. Effects of solvent and enzyme source on transesterification activity. *Energy Fuels* 25:4669-4674.
- Galarneau A, Mureseanu M, Atger S, Renard G, Fajula F. 2006. Immobilization of lipase on silicas. Relevance of textural and interfacial properties on activity and selectivity. *New J Chem* 30:562-571.

- Ganesan D, Rajendran A, Thangavelu V. 2009. An overview on the recent advances in the transesterification of vegetable oils for biodiesel production using chemical and biocatalysts. *Rev Environ Sci Biotechnol* 8:367-394.
- Gill I, Ballesteros A. 2000. Bioencapsulation within synthetic polymers (Part 1): Sol-gel encapsulated biologicals. *Trends Biotechnol* 18:282-296.
- Gog A, Roman M, Toşa M, Paizs C, Irimie FD. 2012. Biodiesel production using enzymatic transesterification - Current state and perspectives. *Renewable Energy* 39:10-16.
- Gupta MN. *Thermostability of Enzymes*. Berlin: Springer-Verlag c1993
- Halim SFA, Kamaruddin AH, Fernando WJN. 2009. Continuous biosynthesis of biodiesel from waste cooking palm oil in a packed bed reactor: Optimization using response surface methodology (RSM) and mass transfer studies. *Bioresour Technol* 100:710-716.
- Hama S, Tamalampudi S, Yoshida A, Tamadani N, Kuratani N, Noda H, Fukuda H, Kondo A. 2011a. Enzymatic packed-bed reactor integrated with glycerol-separating system for solvent-free production of biodiesel fuel. *Biochem Eng J* 55:66-71.
- Hama S, Tamalampudi S, Yoshida A, Tamadani N, Kuratani N, Noda H, Fukuda H, Kondo A. 2011b. Process engineering and optimization of glycerol separation in a packed-bed reactor for enzymatic biodiesel production. *Bioresour Technol* 102:10419-10424.
- Hartmeier W. *Immobilized biocatalysts: an introduction*. Berlin: Springer-Verlag c1988.
- Hasan F, Shah AA, Hameed A. 2006. Industrial applications of microbial lipases. *Enzyme Microb Technol* 39:235-251.
- Hernández-Martín E, Otero C. 2008. Different enzyme requirements for the synthesis of biodiesel: Novozym® 435 and Lipozyme® TL IM. *Bioresour Technol* 99:277-286.
- Hong WP, Park JY, Min K, Ko MJ, Park K, Yoo YJ. 2011. Kinetics of glycerol effect on biodiesel production for optimal feeding of methanol. *Korean J Chem Eng* 28:1908-1912.
- Hsu A-F, Foglia TA, Jones K, Shen S. 2001a. Phyllosilicate sol-gel immobilized enzymes: Their use as packed bed column bioreactors. *ACS Symp Ser* 776:155-164.

- Hsu A-F, Jones K, Marmer WN, Foglia TA. 2001b. Production of alkyl esters from tallow and grease using lipase immobilized in a phyllosilicate sol-gel. *J Am Oil Chem Soc* 78:585-588.
- Hsu A-F, Jones KC, Foglia TA, Marmer WN. 2004. Continuous production of ethyl esters of grease using an immobilized lipase. *J Am Oil Chem Soc* 81:749-752.
- Hsu A-F, Jones KC, Foglia TA, Marmer WN. 2003. Optimization of alkyl ester production from grease using a phyllosilicate sol-gel immobilized lipase. *Biotechnol Lett* 25:1713-1716.
- Huang Y, Zheng H, Yan Y. 2010. Optimization of lipase-catalyzed transesterification of lard for biodiesel production using response surface methodology. *Appl Biochem Biotechnol* 160:504-515.
- Iso M, Chen B, Eguchi M, Kudo T, Shrestha S. 2001. Production of biodiesel fuel from triglycerides and alcohol using immobilized lipase. *J Mol Catal B: Enzym* 16:53-58.
- Jaeger K-E, Eggert T. 2002. Lipases for biotechnology. *Curr Opin Biotechnol* 13:390-397.
- Jegannathan KR, Eng-Seng C, Ravindra P. 2011. Economic assessment of biodiesel production: Comparison of alkali and biocatalyst processes. *Renewable Sustainable Energy Rev* 15:745-751.
- Jin W, Brennan JD. 2002. Properties and applications of proteins encapsulated within sol-gel derived materials. *Anal Chimica Acta* 461:1-36.
- Jung HJ, Bauer W. 1992. Determination of process parameters and modelling of lipase-catalyzed transesterification in a fixed bed reactor. *Chem Eng Technol* 15:341-348.
- Kaieda M, Samukawa T, Kondo A, Fukuda H. 2001. Effect of methanol and water contents on production of biodiesel fuel from plant oil catalyzed by various lipases in a solvent-free system. *J Biosci Bioeng* 91:12-15.
- Kaieda M, Samukawa T, Matsumoto T, Ban K, Kondo A, Shimada Y, Noda H, Nomoto F, Ohtsuka K, Izumoto E, Fukuda H. 1999. Biodiesel fuel production from plant oil catalyzed by *Rhizopus oryzae* lipase in a water-containing system without an organic solvent. *J Biosci Bioeng* 88:627-631.
- Kargi F, Shuler ML. 2001. *Bioprocess Engineering: Basic Concepts*. United States: Prentice Hall PTR. p. 576.

- Kawakami K. 1996. Enhancement of thermostability of lipase by the sol-gel entrapment into methyl-substituted organic silicates formed on diatomaceous earth. *Biotechnol Tech* 10:491-494.
- Kawakami K, Matsui Y, Ono T, Ijima H. 2003. Enhancement of protease activity in transesterification of glycidol with vinyl n-butyrate by entrapment into alkyl-substituted silicates and pretreatment with a substrate. *Biocatal Biotransform* 21:49-52.
- Kawakami K, Yoshida S. 1996. Thermal stabilization of lipase by sol-gel entrapment in organically modified silicates formed on Kieselguhr. *J Ferment Bioeng* 82:239-245.
- Köse O, Tüter M, Aksoy HA. 2002. Immobilized *Candida antarctica* lipase-catalyzed alcoholysis of cotton seed oil in a solvent-free medium. *Bioresour Technol* 83:125-129.
- Koszelewski D, Muller N, Schrittwieser JH, Faber K, Kroutil W. 2010. Immobilization of omega-transaminases by encapsulation in a sol-gel/celite matrix. *J Mol Catal B: Enzym* 63:39-44.
- Krebs WG, Gerstein M. 2000. The morph server: A standardized system for analyzing and visualizing macromolecular motions in a database framework. *Nucleic Acids Res* 28:1665-1675.
- Kumari V, Shah S, Gupta MN. 2007. Preparation of biodiesel by lipase-catalyzed transesterification of high free fatty acid containing oil from *Madhuca indica*. *Energy Fuels* 21:368-372.
- Lai C-C, Zullaikah S, Vali SR, Ju Y-H. 2005. Lipase-catalyzed production of biodiesel from rice bran oil. *J Chem Technol Biotechnol* 80:331-337.
- Lee JH, Kim SB, Park C, Tae B, Han SO, Kim SW. 2010. Development of batch and continuous processes on biodiesel production in a packed-bed reactor by a mixture of immobilized *Candida rugosa* and *Rhizopus oryzae* lipases. *Appl Biochem Biotechnol* 161:365-371.
- Lee M, Lee J, Lee D, Cho J, Kim S, Park C. 2011. Improvement of enzymatic biodiesel production by controlled substrate feeding using silica gel in solvent free system. *Enzyme Microb Technol* 49:402-406.
- Li F-Y, Xing Y-J, Ding X. 2007. Immobilization of papain on cotton fabric by sol-gel method. *Enzyme Microb Technol* 40:1692-1697.
- Livage J, Coradin T, Roux C. 2001. Encapsulation of biomolecules in silica gels. *J Phys Condens Matter* 13:R673-R691.

- Macario A, Giordano G, Moliner M, Corma A. 2009. Increasing stability and productivity of lipase enzyme by encapsulation in a porous organic-inorganic system. *Microporous Mesoporous Mater* 118:334-340.
- Marchetti JM, Miguel VU, Errazu AF. 2007. Possible methods for biodiesel production. *Renewable Sustainable Energy Rev* 11:1300-1311.
- Mazzieri VA, Vera CR, Yori JC. 2008. Adsorptive properties of silica gel for biodiesel refining. *Energy Fuels* 22:4281-4284.
- McDuffie NG. *Bioreactor design fundamentals*. Massachusetts: Butterworth-Heinemann c1991.
- Meher LC, Sagar DV, Naik SN. 2006. Technical aspects of biodiesel production by transesterification – A review. *Renewable Sustainable Energy Rev* 10:248-268.
- Messing RA, ed. *Immobilized enzymes for industrial reactors*. New York:Academic Press. 1975.
- Meunier SM, Legge RL. 2012. Evaluation of diatomaceous earth supported lipase sol-gels as a medium for enzymatic transesterification of biodiesel. *J Mol Catal B: Enzym* 77:92-97.
- Meunier SM, Legge RL. 2010. Evaluation of diatomaceous earth as a support for sol-gel immobilized lipase for transesterification. *J Mol Catal B: Enzym* 62:53-57.
- Moreira ABR, Perez VH, Zanin GM, de Castro HF. 2007. Biodiesel synthesis by enzymatic transesterification of palm oil with ethanol using lipases from several sources immobilized on silica-PVA composite. *Energy Fuels* 21:3689-3694.
- Mukesh D, Banerji AA, Newadkar R, Bevinakatti HS. 1993. Lipase catalysed transesterification of vegetable oils - A comparative study in batch and tubular reactors. *Biotechnol Lett* 15:77-82.
- Nassreddine S, Karout A, Christ ML, Pierre AC. 2008. Transesterification of a vegetal oil with methanol catalyzed by a silica fibre reinforced aerogel encapsulated lipase. *Appl Catal, A* 344:70-77.
- Nie K, Xie F, Wang F, Tan T. 2006. Lipase catalyzed methanolysis to produce biodiesel: Optimization of the biodiesel production. *J Mol Catal B: Enzym* 43:142-147.

- Noel M, Combes D. 2003. *Rhizomucor miehei* lipase: Differential scanning calorimetry and pressure/temperature stability studies in presence of soluble additives. *Enzyme Microb Technol* 33:299-308.
- Noureddini H, Gao X, Joshi S. 2003. Immobilization of *Candida rugosa* Lipase by Sol-Gel Entrapment and Its Application in the Hydrolysis of Soybean Oil. *J Am Oil Chem Soc* 80:1077-1083.
- Noureddini H, Gao X, Joshi S, Wagner PR. 2002. Immobilization of *Pseudomonas cepacia* lipase by sol-gel entrapment and its application in the hydrolysis of soybean oil. *J Am Oil Chem Soc* 79:33-40.
- Noureddini H, Gao X, Philkana RS. 2005. Immobilized *Pseudomonas cepacia* lipase for biodiesel fuel production from soybean oil. *Bioresour Technol* 96:769-777.
- Ognjanovic N, Bezbradica D, Knezevic-Jugovic Z. 2009. Enzymatic conversion of sunflower oil to biodiesel in a solvent-free system: Process optimization and the immobilized system stability. *Bioresour Technol* 100:5146-5154.
- Orçaire O, Buisson P, Pierre AC. 2006. Application of silica aerogel encapsulated lipases in the synthesis of biodiesel by transesterification reactions. *J Mol Catal B: Enzym* 42:106-113.
- Pierre AC. 2004. The sol-gel encapsulation of enzymes. *Biocatal Biotransform* 22:145-170.
- Pirozzi D, Fanelli E, Aronne A, Pernice P, Mingione A. 2009. Lipase entrapment in a zirconia matrix: Sol-gel synthesis and catalytic properties. *J Mol Catal B: Enzym* 59:116-120.
- Pogorilyi RP, Siletskaya EY, Goncharik VP, Kozhara LI, Zub YL. 2007. Immobilization of urease on the silica gel surface by sol-gel method. *Russ J Appl Chem* 80:330-334.
- Rahman NK, Kamaruddin AH, Uzir MH. 2011. Enzymatic synthesis of farnesyl laurate in organic solvent: Initial water activity, kinetics mechanism, optimization of continuous operation using packed bed reactor and mass transfer studies. *Bioprocess Biosyst Eng* 34:687-699.
- Ranganathan SV, Narasimhan SL, Muthukumar K. 2008. An overview of enzymatic production of biodiesel. *Bioresour Technol* 99:3975-3981.
- Rase HF. *Fixed-bed reactor design and diagnostics: gas-phase reactions*. Boston: Butterworths c1990.

- Reetz MT. 1997. Entrapment of biocatalysts in hydrophobic sol-gel materials for use in organic chemistry. *Adv Mater* 9:943-954.
- Reetz MT, Zonta A, Simpelkamp J. 1996. Efficient immobilization of lipases by entrapment in hydrophobic sol-gel materials. *Biotechnol Bioeng* 49:527-534.
- Rizzi M, Stylos P, Riek A, Reuss M. 1992. A kinetic study of immobilized lipase catalysing the synthesis of isoamyl acetate by transesterification in *n*-hexane. *Enzyme Microb Technol* 14:709-714.
- Robles-Medina A, González-Moreno PA, Esteban-Cerdán L, Molina-Grima E. 2009. Biocatalysis: Towards ever greener biodiesel production. *Biotechnol Adv* 27:398-408.
- Royon D, Daz M, Ellenrieder G, Locatelli S. 2007. Enzymatic production of biodiesel from cotton seed oil using *t*-butanol as a solvent. *Bioresour Technol* 98:648-653.
- Ruzich NI, Bassi AS. 2011. Proposed kinetic mechanism of biodiesel production through lipase catalysed interesterification with a methyl acetate acyl acceptor and ionic liquid [BMIM][PF₆] co-solvent. *Can J Chem Eng* 89:166-170.
- Ruzich NI, Bassi AS. 2010a. Investigation of enzymatic biodiesel production using ionic liquid as a co-solvent. *Can J Chem Eng* 88:277-282.
- Ruzich NI, Bassi AS. 2010b. Investigation of lipase-catalyzed biodiesel production using ionic liquid [BMIM][PF₆] as a co-solvent in 500 mL jacketed conical and shake flask reactors using triolein or waste canola oil as substrates. *Energy Fuels* 24:3214-3222.
- Sağiroğlu A. 2008. Conversion of sunflower oil to biodiesel by alcoholysis using immobilized lipase. *Artificial Cells, Blood Substitutes, and Biotechnology* 36:138-149.
- Sağiroğlu A, Kiliç A, Telefoncu A. 2004. Preparation and properties of lipases immobilized on different supports. *Artif Cells Blood Substitutes Immobilization Biotechnol* 32:625-636.
- Sağiroğlu A, Telefoncu A. 2004. Immobilization of lipases on different carriers and their use in synthesis of pentyl isovalerates. *Prep Biochem Biotechnol* 34:169-178.
- Salis A, Pinna M, Monduzzi M, Solinas V. 2005. Biodiesel production from triolein and short chain alcohols through biocatalysis. *J Biotechnol* 119:291-299.

- Samukawa T, Kaieda M, Matsumoto T, Ban K, Kondo A, Shimada Y, Noda H, Fukuda H. 2000. Pretreatment of immobilized *Candida antarctica* lipase for biodiesel fuel production from plant oil. J Biosci Bioeng 90:180-183.
- Santacesaria E, Tesser R, Di Serio M, Guida M, Gaetano D, Garcia Agreda A. 2007. Kinetics and mass transfer of free fatty acids esterification with methanol in a tubular packed bed reactor: A key pretreatment in biodiesel production. Ind Eng Chem Res 46:5113-5121.
- Sarda L, Desnuelle P. 1958. Action de la lipase pancréatique sur les esters en émulsion. Biochim Biophys Acta 30:513-521.
- Seguin D, Montillet A, Brunjail D, Comiti J. 1996. Liquid-solid mass transfer in packed beds of variously shaped particles at low Reynolds numbers: Experiments and model. Chem Eng J 63:1-9.
- Selmi B, Thomas D. 1998. Immobilized lipase-catalyzed ethanolysis of sunflower oil in a solvent-free medium. J Am Oil Chem Soc 75:691-695.
- Semwal S, Arora AK, Badoni RP, Tuli DK. 2011. Biodiesel production using heterogeneous catalysts. Bioresour Technol 102:2151-2161.
- Shah S, Sharma S, Gupta MN. 2004. Biodiesel preparation by lipase-catalyzed transesterification of Jatropha oil. Energy Fuels 18:154-159.
- Shahid EM, Jamal Y. 2011. Production of biodiesel: A technical review. Renewable Sustainable Energy Rev 15:4732-4745.
- Shaw J-F, Chang S-W, Lin S-C, Wu T-T, Ju H-Y, Akoh CC, Chang R-H, Shieh C-J. 2008. Continuous enzymatic synthesis of biodiesel with Novozym 435. Energy Fuels 22:840-844.
- Shimada Y, Watanabe Y, Samukawa T, Sugihara A, Noda H, Fukuda H, Tominaga Y. 1999. Conversion of vegetable oil to biodiesel using immobilized *Candida antarctica* lipase. J Am Oil Chem Soc 76:789-793.
- Shimada Y, Watanabe Y, Sugihara A, Tominaga Y. 2002. Enzymatic alcoholysis for biodiesel fuel production and application of the reaction to oil processing. J Mol Catal B: Enzym 17:133-142.
- Soares CMF, dos Santos OA, de Castro HF, de Moraes FF, Zanin GM. 2006. Characterization of sol-gel encapsulated lipase using tetraethoxysilane as precursor. J Mol Catal B: Enzym 39:69-76.

- Soumanou MM, Bornscheuer UT. 2003a. Improvement in lipase-catalyzed synthesis of fatty acid methyl esters from sunflower oil. *Enzyme Microb Technol* 33:97-103.
- Soumanou MM, Bornscheuer UT. 2003b. Lipase-catalyzed alcoholysis of vegetable oils. *Eur J Lipid Sci Technol* 105:656-660.
- Szczesna Antczak M, Kubiak A, Antczak T, Bielecki S. 2009. Enzymatic biodiesel synthesis - Key factors affecting efficiency of the process. *Renewable Energy* 34:1185-1194.
- Tan T, Lu J, Nie K, Deng L, Wang F. 2010. Biodiesel production with immobilized lipase: A review. *Biotechnol Adv* 28:628-634.
- Tesser R, Di Serio M, Guida M, Nastasi M, Santacesaria E. 2005. Kinetics of oleic acid esterification with methanol in the presence of triglycerides. *Ind Eng Chem Res* 44:7978-7982.
- Thoenes D. *Chemical reactor development: from laboratory synthesis to industrial production*. Dordrecht: Kluwer Academic Publishers c1994.
- Tongboriboon K, Cheirsilp B, H-Kittikun A. 2010. Mixed lipases for efficient enzymatic synthesis of biodiesel from used palm oil and ethanol in a solvent-free system. *J Mol Catal B: Enzym* 67:52-59.
- Treybal RE. *Mass-transfer operations*. New York: McGraw-Hill c1980.
- Valeri D, Meirelles AJA. 1997. Viscosities of fatty acids, triglycerides, and their binary mixtures. *J Am Oil Chem Soc* 74:1221-1226.
- Vasudevan PT, Briggs M. 2008. Biodiesel production-current state of the art and challenges. *J Ind Microbiol Biotechnol* 35:421-430.
- Vieira APDA, da Silva MAP, Langone MAP. 2006. Biodiesel production via esterification reactions catalyzed by lipase. *Lat Am Appl Res* 36:283-288.
- Wang L, Du W, Liu D, Li L, Dai N. 2006. Lipase-catalyzed biodiesel production from soybean oil deodorizer distillate with absorbent present in *tert*-butanol system. *J Mol Catal B: Enzym* 43:29-32.
- Wang X, Liu X, Zhao C, Ding Y, Xu P. 2011. Biodiesel production in packed-bed reactors using lipase-nanoparticle biocomposite. *Bioresour Technol* 102:6352-6355.

- Wang Y-D, Shen X-Y, Li Z-L, Li X, Wang F, Nie X-A, Jiang J-C. 2010. Immobilized recombinant *Rhizopus oryzae* lipase for the production of biodiesel in solvent free system. *J Mol Catal B: Enzym* 67:45-51.
- Watanabe Y, Shimada Y, Sugihara A, Noda H, Fukuda H, Tominaga Y. 2000. Continuous production of biodiesel fuel from vegetable oil using immobilized *Candida antarctica* lipase. *J Am Oil Chem Soc* 77:355-360.
- Watanabe Y, Shimada Y, Sugihara A, Tominaga Y. 2002. Conversion of degummed soybean oil to biodiesel fuel with immobilized *Candida antarctica* lipase. *J Mol Catal B: Enzym* 17:151-155.
- Watanabe Y, Shimada Y, Sugihara A, Tominaga Y. 2001. Enzymatic conversion of waste edible oil to biodiesel fuel in a fixed-bed bioreactor. *J Am Oil Chem Soc* 78:703-707.
- Wiemann L, Nieguth R, Eckstein M, Naumann M, Thum O, Ansorge-Schumacher M. 2009. Composite particles of Novozyme 435 and silicone: Advancing technical applicability of macroporous enzyme carriers. *ChemCatChem* 1:455-462.
- Xiao Y, Gao L, Xiao G, Fu B, Niu L. 2012. Experimental and modeling study of continuous catalytic transesterification to biodiesel in a bench-scale fixed-bed reactor. *Ind Eng Chem Res* 51:11860-11865.
- Xu Y, Du W, Liu D. 2005. Study on the kinetics of enzymatic interesterification of triglycerides for biodiesel production with methyl acetate as the acyl acceptor. *J Mol Catal B: Enzym* 32:241-245.
- Xu Y, Du W, Liu D, Zeng J. 2003. A novel enzymatic route for biodiesel production from renewable oils in a solvent-free medium. *Biotechnol Lett* 25:1239-1241.
- Xu Y, Du W, Zeng J, Liu D. 2004. Conversion of soybean oil to biodiesel fuel using lipozyme TL IM in a solvent-free medium. *Biocatal Biotransform* 22:45-48.
- Xu Y, Nordblad M, Woodley JM. 2012. A two-stage enzymatic ethanol-based biodiesel production in a packed bed reactor. *J Biotechnol*. Article in Press:
<http://dx.doi.org.proxy.lib.uwaterloo.ca/10.1016/j.bbr.2011.03.031>
- Xu ZP, Chuang KT. 1997. Effect of internal diffusion on heterogeneous catalytic esterification of acetic acid. *Chem Eng Sci* 52:3011-3017.

- Yadav GD, Devi KM. 2004. Immobilized lipase-catalysed esterification and transesterification reactions in non-aqueous media for the synthesis of tetrahydrofurfuryl butyrate: Comparison and kinetic modeling. *Chem Eng Sci* 59:373-383.
- Yori JC, D'Ippolito SA, Pieck CL. 2007. Deglycerolization of biodiesel streams by adsorption over silica beds. *Energy Fuels* 21:347-353.
- Yücel Y, Demir C. 2012. The optimization of immobilized lipase-catalyzed transesterification of canola oil by response surface methodology and mixture design. *Energy Sources Part A* 34:2031-2040.
- Yusuf NNAN, Kamarudin SK, Yaakub Z. 2011. Overview on the current trends in biodiesel production. *Energy Convers Manage* 52:2741-2751.
- Zhang B, Weng Y, Xu H, Mao Z. 2012. Enzyme immobilization for biodiesel production. *Appl Microbiol Biotechnol* 93:61-70.

Appendix A

List of Publications

Peer-Reviewed Publications

Study of Support Materials for Sol-gel Immobilized Lipase, S.M. Meunier and R.L. Legge, Biocatal. Biotransform., submitted July 2012. Manuscript ID GBAB-12-404.R1.

Evaluation of Diatomaceous Earth Supported Lipase Sol-gels as a Medium for Enzymatic Transesterification of Biodiesel, S.M. Meunier and R.L. Legge, J. Mol. Catal. B: Enzym., vol. 77, pp. 92-97, 2012.

Evaluation of Diatomaceous Earth as a Support for Sol-gel Immobilized Lipase for Transesterification, S.M. Meunier and R.L. Legge, J. Mol. Catal. B: Enzym., vol. 62, no. 1, pp. 53-57, 2010.

Conference Presentations

Biodiesel Production Potential via Supported Lipase Sol-gels, S.M. Meunier and R.L. Legge, 14th Annual CSChE Ontario-Québec Biotechnology Meeting, May 2012.

Biodiesel Production Catalyzed by Celite® Supported Lipase Sol-gels, S.M. Meunier and R.L. Legge, Current Research in Engineering, Science, & Technology (CREST) Meeting, March 2012.

Sol-gel Immobilized Lipase Supported on Diatomaceous Earth for Lipid Transesterification, S.M. Meunier and R.L. Legge, 11th Annual CSChE Ontario-Quebec Biotechnology Meeting, June 2009.

Supported Sol-gel Immobilized Enzymes for Lipid Transesterification, S. M. Meunier and R. L. Legge, WISE Initiative 2009 International Women's Day Conference, March 2009.

Appendix B

Lipase Source Change

The experimental work described in Chapters 3 through 6 was completed using lipase NS44035 provided by Novozymes North America Inc. This lipase was used since the sol-gel immobilization procedure and linoleic acid assay methodologies were well established based on earlier experiments. Since all the initial experiments were conducted using the Novozymes lipase, the supported sol-gels studied for methyl oleate production were produced using the same methodology.

One of the concerns identified regarding the results obtained was that the Novozymes lipase is not a common lipase and the supplier will not disclose the source of the enzyme. A review of the literature on enzymatic biodiesel production revealed that Lipase PS “Amano” SD from Amano Enzyme USA Co. was a very active lipase for this application. The enzyme source for the Celite® supported lipase sol-gels formulated for Chapters 7 and 8 is therefore from Amano rather than Novozymes.

The basic information regarding the two types of lipase used in this thesis is provided in Table B.1. Experimentally, the main difference between the two lipases is that the Novozymes lipase was supplied as a liquid and Amano lipase as a powder, resulting in a slight change in the sol-gel formulation procedure to ensure that the Amano lipase was well dissolved in the phosphate buffer prior to use. The protein content of the Amano lipase was unknown, so the amount of lipase used was chosen so that the activity of the protein loaded would be comparable between the two enzyme sources.

Table B.1: Information from Novozymes North America Inc. and Amano Enzyme USA Co. for the two types of lipase used in the experiments performed for this research.

| Lipase (Supplier) | Source | Form | Activity (U/g) | Optimal conditions |
|--|--------------------------------|--------|----------------|--------------------------------|
| NS44035 (Novozymes) | Unknown 1,3-specific lipase | Liquid | 20 000 | pH = 7.5 Temperature = 40°C |
| Lipase PS “Amano” SD (Amano Enzyme) | <i>Burkholderia cepacia</i> | Powder | 23 000 | pH = 7 Temperature = 50°C |

A series of experiments were conducted with the Amano lipase to ensure that similar levels of performance could be obtained using the new source of lipase (Table B.2). Based on the results obtained, the unsupported sol-gel and the Celite® supported sol-gel with Amano lipase had slightly higher protein content compared to the Novozymes lipase. However, the degree of immobilization that could be achieved using the Novozymes lipase sol-gels was much higher for both the unsupported and Celite® supported sol-gels than that with the Amano lipase. This could be due to the need to dissolve the Amano lipase powder in phosphate buffer prior to its addition to the sol-gel precursor solution. For the free lipase, unsupported sol-gel, and Celite® supported sol-gel, the Amano lipase exhibited higher methyl oleate conversion after the 6 h reaction than the Novozymes lipase. In each case, the 6 h methyl oleate concentration for the Amano lipase was close to double that of the Novozymes lipase. Considering the initial activity of the lipase, both the unsupported sol-gel and the Celite® supported sol-gel had approximately double the initial activity using the Amano enzyme, but the free lipase exhibited only half the initial activity of the Novozymes lipase. Therefore, immobilizing the Amano lipase in the sol-gel (unsupported or supported) dramatically increased the enzymatic activity for methyl oleate production. Based on these results, the Amano lipase was found to be a good choice of lipase for the subsequent Celite® supported lipase sol-gel methyl oleate production studies.

For the sol-gels produced using the Amano lipase, the HPLC procedure for protein content identification was found to be unreliable. Although, the composition for the Amano lipase from the supplier indicated that the powder provided was 90% dextrin and 10% lipase, HPLC analysis indicated many peaks (10 or more) which is likely due to the mixture of carbohydrates in the dextrin that was used. The resolution of the peaks was very poor, and identification of a lipase peak was not possible. Therefore, a BCA assay was used to determine the protein content of the Amano lipase supported sol-gels.

Table B.2: Protein content, degree of immobilization (DOI), methyl oleate concentration after 6 h (6 h [MO]) and initial activity for the Novozymes and Amano lipases for free lipase, sol-gel immobilized lipase, and Celite® supported lipase sol-gel.

| Support | Lipase | Protein content (mg/g) | DOI (%) | 6 h [MO] (μM/g) | Initial activity (U/g) |
|------------------------|---------------|-------------------------------|----------------|------------------------|-------------------------------|
| Free | Novozymes | NA | NA | 1.05 | 59.78 |
| | Amano | NA | NA | 1.65 | 29.74 |
| Sol-gel | Novozymes | 4.86 | 80.11 | 178480 | 6077 |
| | Amano | 5.60 | 26.54 | 396382 | 10128 |
| Celite® Sol-gel | Novozymes | 1.45 | 85.88 | 203513 | 4676 |
| | Amano | 2.21 | 72.52 | 440473 | 10503 |

The unsupported sol-gel and the Celite® supported sol-gel containing both types of lipase were studied using SEM to determine if there were any structural differences in the nature of the sol-gel material (Figure B.1). The most notable difference observed was with the unsupported lipase sol-gels where the Novozymes unsupported sol-gel resulted in an irregularly shaped surface, but the Amano unsupported sol-gel produced defined particles possessing a globular structure, even after sol-gel immobilization. This is likely due to the differences in other components in the Amano lipase preparation. For the Celite® sol-gel with the Amano lipase, the sol-gel on the Celite® support was very spherical with no air bubbles, but for the Celite® sol-gel with the Novozymes lipase, the sol-gel was non-spherical with many air bubbles.

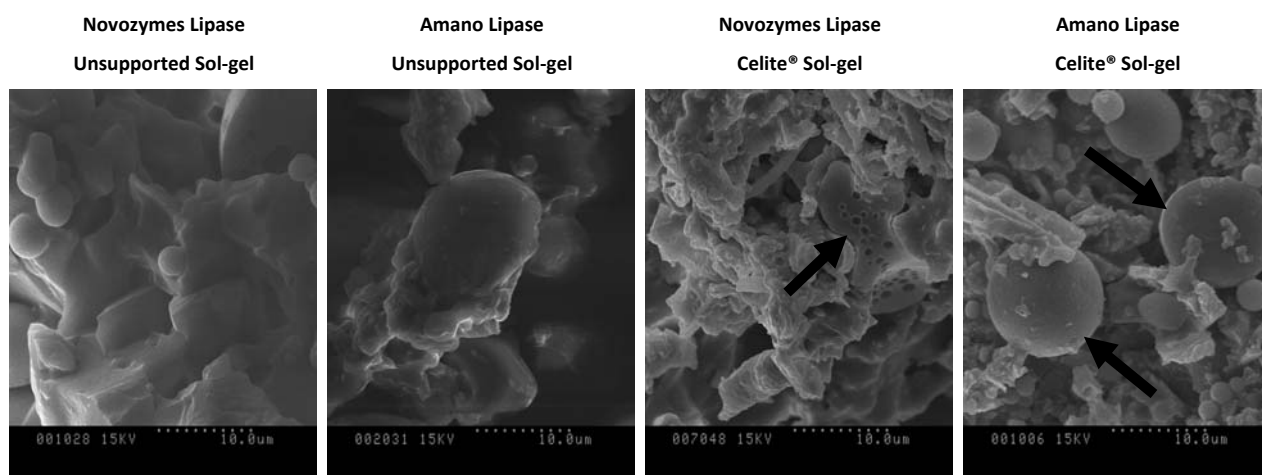


Figure B.1: SEM images at 3000x magnification of the unsupported lipase sol-gel and the Celite® lipase sol-gel with the Novozymes and Amano lipases. Arrows on the Celite® sol-gels images indicate the presence of sol-gel on the Celite®.

Appendix C

Sample Calculations

GC-MS – Enzymatic Properties

The GC-MS method used to follow the enzymatic production of methyl oleate (MO) with time is described in Sections 4.2.2.6, 5.2.2.5, 6.2.2.3, 7.2.2.3, and 8.2.2.5. Heptadecanoic acid methyl ester (HDA-ME) was used as an internal standard and a plot of the peak area of MO/HDA-ME vs. the known concentration of MO/HDA-ME is a calibration curve used to determine the MO concentration from the peak areas obtained using the GC-MS Varian ProStar software (Figure C.1).

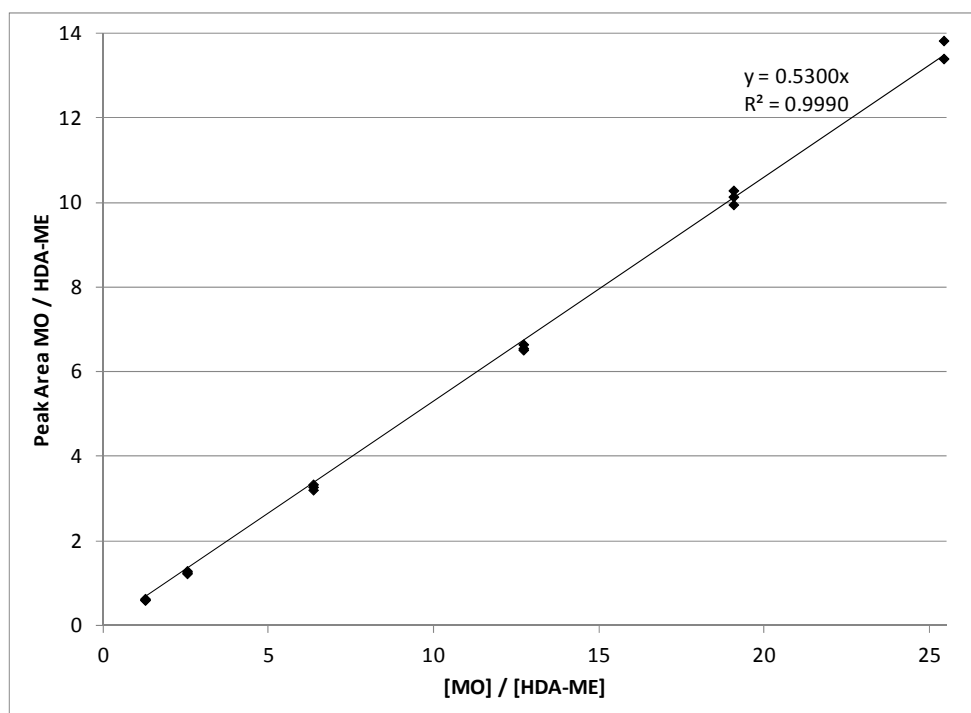


Figure C.2: Sample calibration curve for the GC-MS calibration used to determine the concentration of methyl oleate, [MO], based on the peak areas. The internal standard is heptadecanoic acid methyl ester (HDA-ME).

Chromatogram Plots

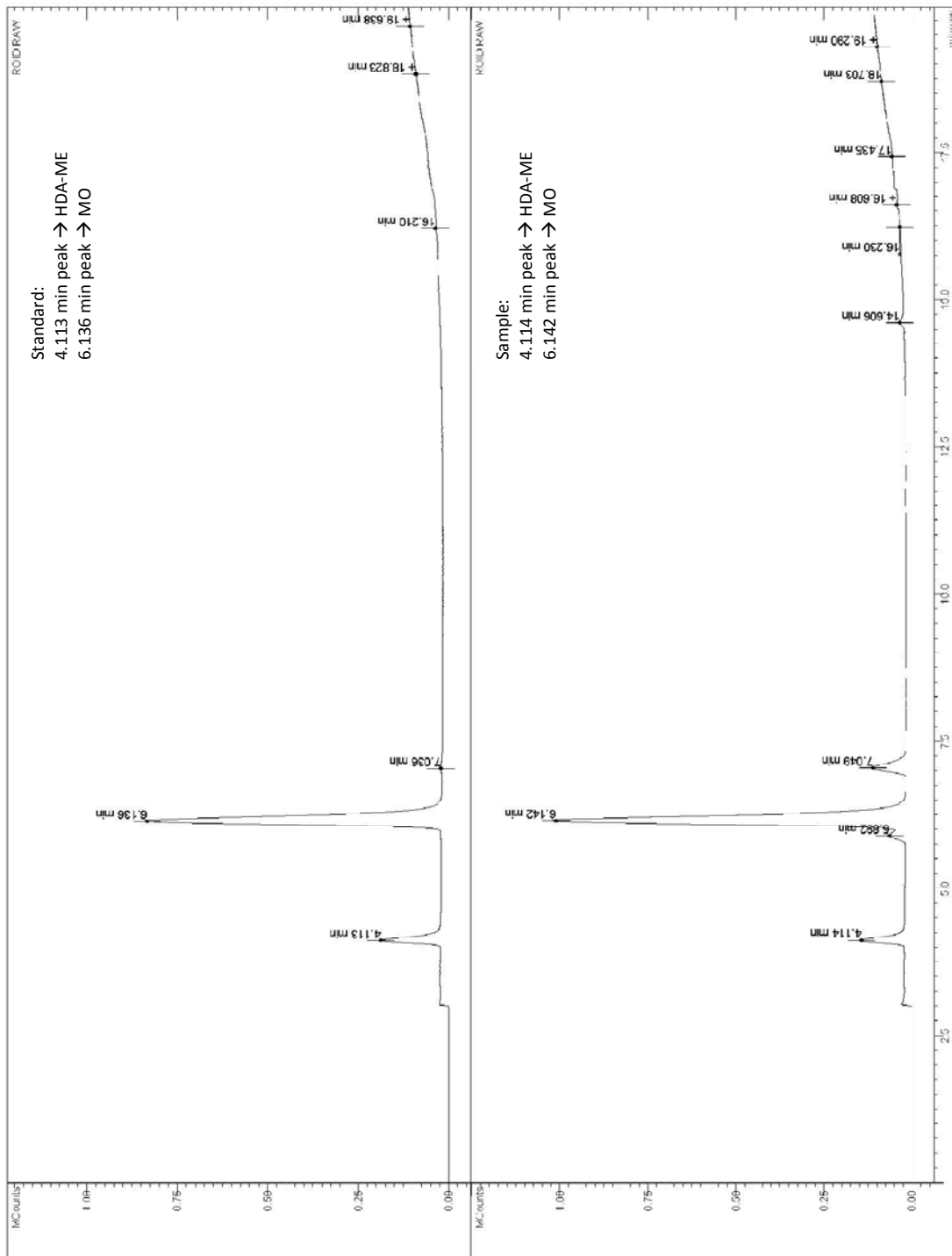


Figure C.2: Sample chromatograms obtained from GC-MS where the top chromatogram is a standard solution and the bottom chromatogram is a sample solution. The peak at 4.11 min is HDA-ME and at 6.14 min is MO.

To calculate the enzymatic properties for any given run, a plot of MO concentration vs. time (Figure C.3) was created based on the chromatogram and calibration curve obtained from the GC-MS. The initial reaction rate, initial activity, and 6 h percent conversion were calculated based on the equations provided. Further description of these parameters and calculations can be found in section 4.3.3.

$$\text{Initial reaction rate} = \text{Slope of initial line (mM/hr)}$$

$$\text{Initial activity} \left(\frac{\mu\text{mol}}{\text{min g}} \right) = \frac{\text{Initial reaction rate } (\mu\text{M/min}) \times \text{Total reaction volume (mL)}}{\text{CSG mass (g)} \times \text{Protein loading (mg/g)}}$$

$$\text{Max [MO]} = \frac{\text{Initial MeOH volume (mL)} \times \text{MeOH density (g/mL)}}{\text{MeOH MW (g/mol)} \times \text{Total reaction volume (mL)}}$$

$$6 \text{ hour \% conversion} = \frac{6 \text{ hr [MO]}}{\text{Max [MO]}} \times 100$$

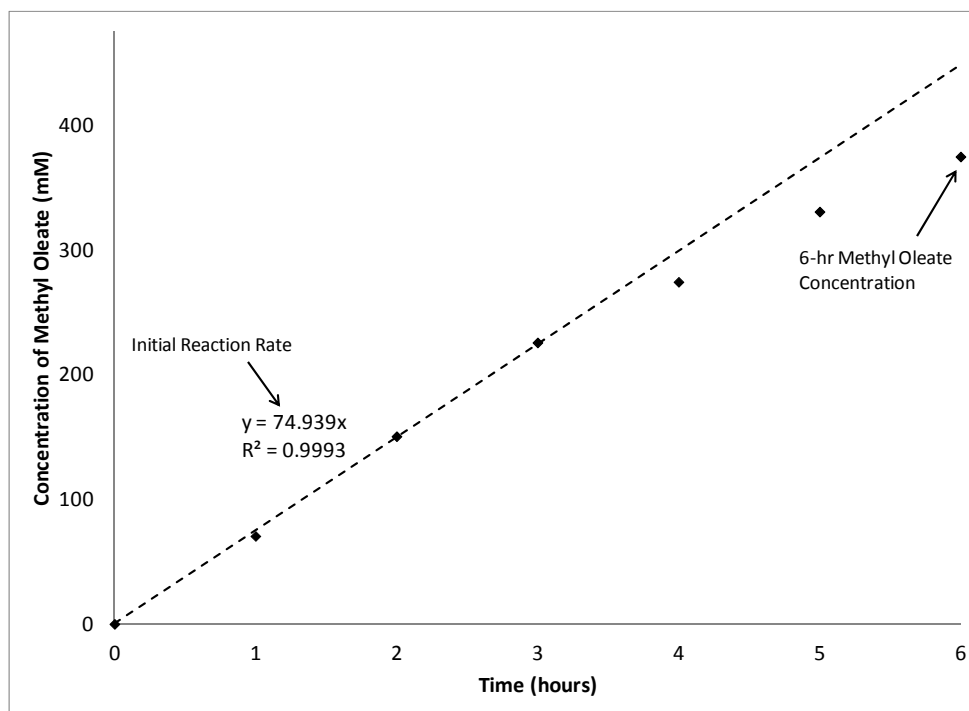


Figure C.3: Sample methyl oleate concentration vs. time plot used to determine the enzymatic properties (initial reaction rate and 6 h methyl oleate concentration) based on a 6 h batch reaction.

HPLC – Protein Content

To determine the protein content of the sol-gels, the HPLC method described in sections 3.1, 4.2.2.3, 5.2.2.4, and 6.2.2.2 was used and a calibration curve for a BSA standard was developed (Figure C.4).

To determine the protein content of the sol-gels, a mass balance was used based on the amount of protein loaded to the sol-gel from the immobilization procedure and the amount of protein present in the sol-gel phosphate buffer washes. Chromatograms were obtained from the HPLC method (Figure C.5) where the upper chromatogram represents the lipase solution loaded to the sol-gel and the lower chromatogram represents the phosphate buffer wash. Based on activity assays, the lipase peak is known to elute after approximately 10 minutes. The 15 minute peak is an additive in the protein solution obtained from the supplier. The peak height was used in the analysis.

Other data necessary for the calculations were obtained from the sol-gel preparation, such as the volume of lipase solution loaded to the sol-gels, the volume of lipase solution in the buffer washes, the mass of support material used in the supported sol-gels, and the total mass of material produced for both the supported and unsupported sol-gel formulations.

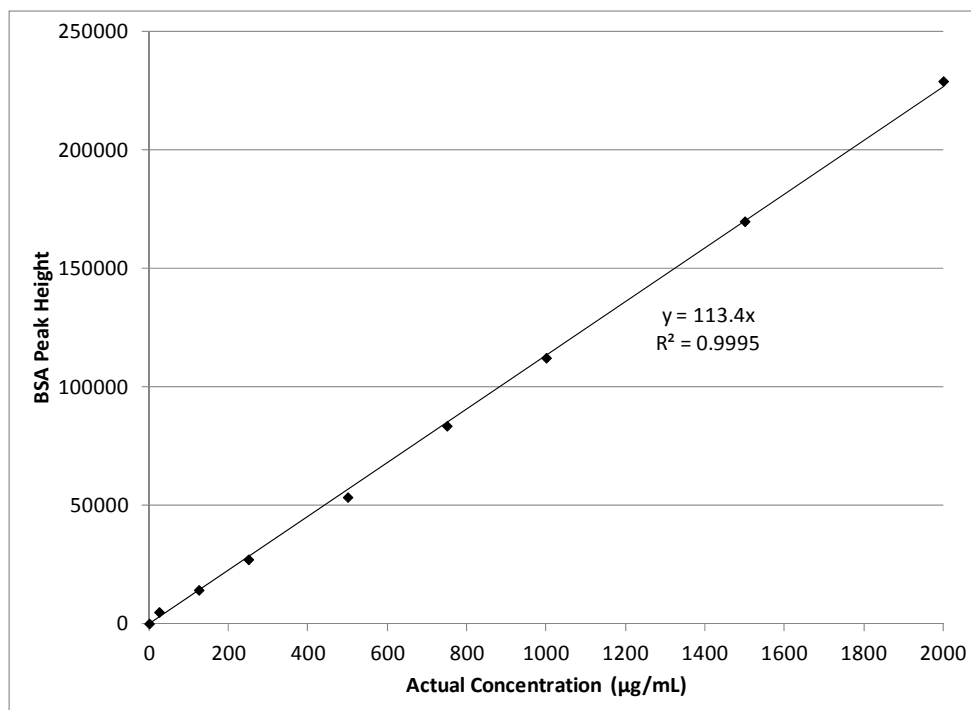


Figure C.4: Sample calibration curve for the HPLC calibration based on a BSA standard and used to determine the total protein content of the sol-gels.

Based on this data, the protein loading, degree of immobilization, and sol-gel adhesion of the supported and unsupported sol-gels were obtained from the following equations.

$$\text{Mass lipase} = \text{Concentration lipase solution} \times \text{Volume lipase solution}$$

$$\text{Protein loading (mg lipase/g material)} = \frac{\text{Mass lipase loaded (mg)} - \text{Mass lipase wash (mg)}}{\text{Mass material made (g)}}$$

$$\text{Protein loading (mg lipase/g sol gel)} = \frac{\text{Mass lipase loaded (mg)} - \text{Mass lipase wash (mg)}}{\text{Mass material made (g)} - \text{Mass of support used (g)}}$$

$$\text{Degree of immobilization (\%)} = \frac{\text{Mass lipase loaded (mg)} - \text{Mass lipase wash (mg)}}{\text{Mass lipase loaded (mg)}} \times 100$$

$$\text{Sol gel adhesion} = \frac{\text{Mass supported sol gel made (g)} - \text{Mass support used (g)}}{\text{Mass supported solgel made (g)}}$$

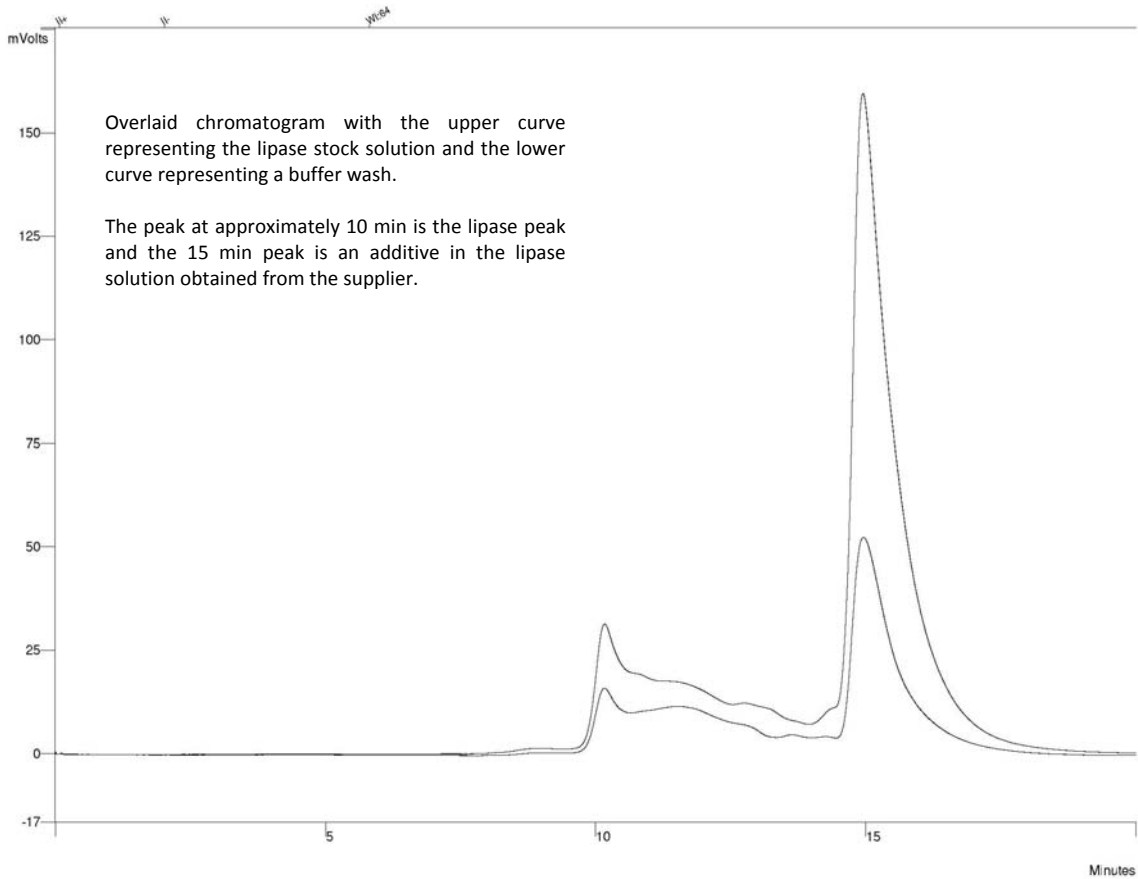


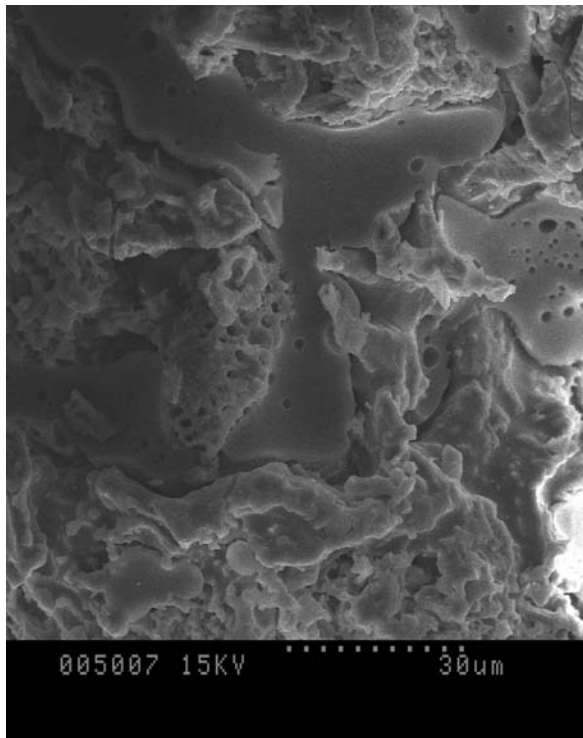
Figure C.5: Sample chromatograms for the HPLC protein content determination where the upper curve is the protein solution loaded to the sol-gels and the lower curve is a buffer wash. The peak at 10 minutes is the lipase peak.

SEM – Coating Analysis

To quantify the amount of sol-gel coating present on Celite® sol-gels as described in sections 5.2.2.3, 5.3.1, and 5.3.2 a series of 45 SEM images were taken for each supported sol-gel and the sol-gel clusters on the surface of the Celite® were identified visually. Figure C.6 is an example of two SEM images to demonstrate this process where a) is a sample SEM image and b) shows 6 sol-gel clusters that were identified on the original image.

A MatLab program was developed to calculate the area of each sol-gel cluster identified in the images. Based on the collection of images, the percent coverage of sol-gel on the surface of the Celite® and the average cluster size were determined and compared between the three different types of Celite® considered as sol-gel support materials.

a)



b)

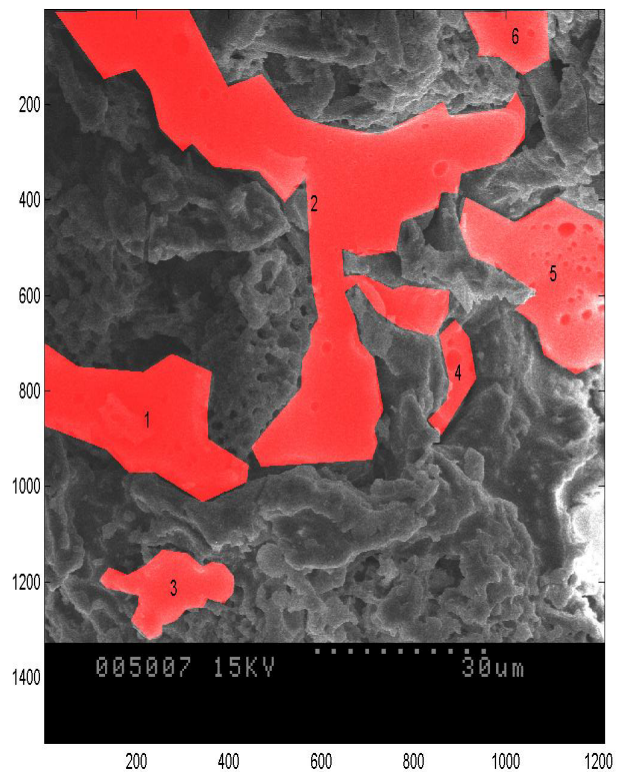


Figure C.6: SEM images demonstrating the surface area coverage procedure developed where a) is a sample image and b) shows the same image with 6 sol-gel clusters identified for analysis.

TGA – Water Content and Thermostability

A variety of properties of the supported sol-gels were determined based on plots of the weight vs. temperature and the derivative weight vs. temperature obtained via TGA (Figure C.7).

As described in section 4.2.2.6, the water content and thermal stability of the supported sol-gels was determined via TGA. For this procedure, the supported sol-gels were analyzed without pre-treatment, and the total mass loss, which occurred at approximately 100°C, was assumed to be solely due to the presence of water. In addition, from these thermograms the thermal stability of the supported sol-gel was evaluated based on whether the weight stabilized after the water was removed (stable) or the weight continued to decrease as the temperature increased (unstable).

Section 6.2.2.4 describes the methodology for an alternative use of TGA to measure glycerol and water desorption from the Celite® sol-gels. For this analysis, the sol-gels were immersed in solutions of varying concentrations of glycerol for 24 hrs, rinsed to remove excess glycerol, and air dried overnight. Subsequent to this treatment, the Celite® sol-gels were analyzed via TGA and the thermograms were used to determine the peak desorption rate, peak desorption temperature, total mass loss, and onset of desorption.

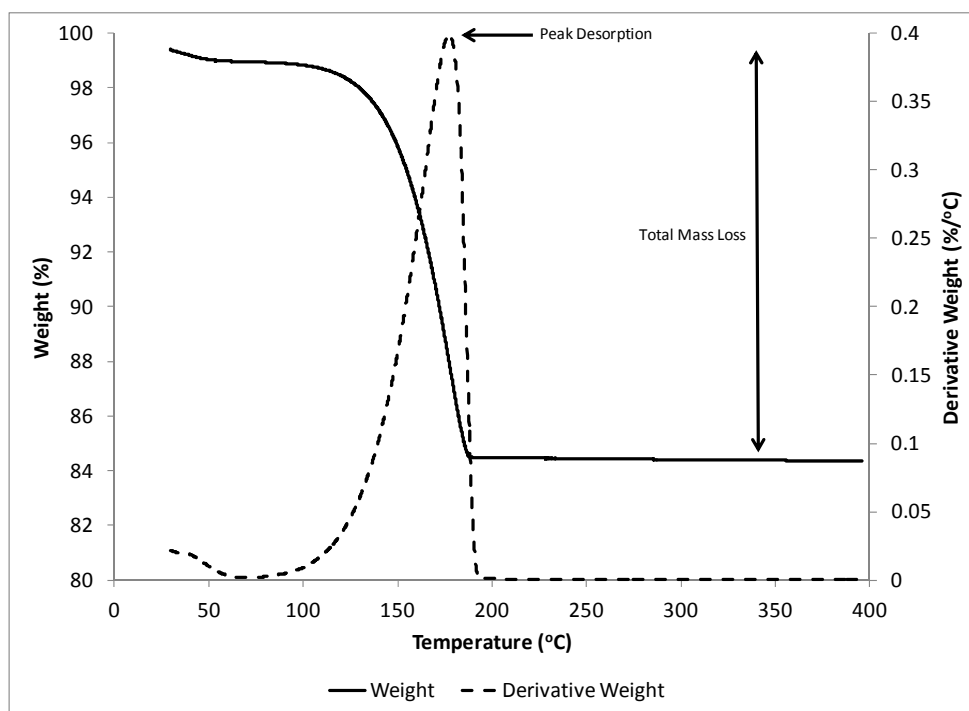


Figure C.7: Sample thermogram showing the weight percent and derivative weight percent as a function of temperature.